Studies on Characterization Methods

of Model Biomembranes

Modified with Cholesterol and Its Derivatives

THAM THI BUI

OCTOBER 2019

Studies on Characterization Methods

of Model Biomembranes

Modified with Cholesterol and Its Derivatives

A dissertation submitted to

THE GRADUATE SCHOOL OF ENGINEERING SCIENCE

OSAKA UNIVERSITY

in partial fulfillment of the requirements for the degree of

DOCTOR OF PHILOSOPHY IN ENGINERRING

BY

THAM THI BUI

OCTOBER 2019

PREFACE

This dissertation work was conducted under the supervision of Professor Hiroshi Umakoshi at Division of Chemical Engineering, Graduate School of Engineering Science, Osaka University from 2014 to 2019.

The objective of this thesis is to establish the characterization methods to investigate the interaction mechanism of steroid molecules at the lipid membranes. Especially, from the aspects of the localized interaction behaviors of sterols from the surface to inner membrane regions of phospholipid membranes, the roles of sterols in biosynthesis pathway and the regulation functions of physicochemical membrane properties by sterol molecules were studied by employing Cholesterol and its derivatives such as Lanosterol and Ergosterol. As model biomembranes, the sterol-modified membranes were systematically characterized using Langmuir monolayers and liposomal bilayer systems with the presence of variety of phospholipid types. Furthermore, the diagram of sterol in membranes were constructed, and the characterization methods were applied for bio-inspired membrane systems such as the liposomes reconstructed by the lipid extracted from bacterial membranes.

The author hopes that this research would contribute to evaluation of the properties of biomembranes, and to well-designed characteristic functional membranes and to apply for drug carrier materials that enable the selective interaction with target molecules. The insights obtained in this study are expected to contribute to the regulation mechanism of biological membrane properties from the surface to inner membranes.

Tham Thi Bui

Division of Chemical Engineering

Graduate School of Engineering Science

Osaka University

Toyonaka, Osaka, 560-8531, Japan

Abstract

As one of the most abundant membrane components, phospholipids and sterols have been studied for better understanding of their self-assembly behaviors and functions in biological membranes. The functions of membranes, such as molecular recognition and transportation, can be controlled by the physicochemical membrane properties that are regulated by the presence of sterols, while the details of the sterol-incorporated membrane properties should be furthermore investigated. The objective of this thesis is to establish the characterization methods to investigate the interaction mechanism of sterol molecules at the lipid membranes.

In chapter II, the sterol-modified liposome membranes were systematically characterized using multiple fluorescent probes. Herein, the localized membrane properties were estimated by comparing the fluorescence emission properties of TMA-DPH, Prodan, ANS, Laurdan, and DPH. Cholesterol (Chol) showed significant ordering effects in unsaturated 1,2-dioleoyl-*sn*-glycero-3-phosphocholine (DOPC) membranes, whereas those effects of Lanosterol (Lan), a precursor of all sterols, were less especially at the membrane surface regions.

In chapter III, the potential interaction behaviors between unsaturated phospholipids and Chol and Lan were extendedly estimated using Langmuir monolayer systems by comparing with Chol. The interpreted data from surface pressure-area isotherms were utilized to analyze the ordering effect of each sterol. Particularly, the results of DOPC/Chol systems revealed a stronger condensing effect of Chol even though at low concentration, while the condensing effect of Lan became significantly at higher Lan content. The findings using monolayer membrane systems could be responsible to weak but sure ordering effect of Lan in unsaturated lipid bilayers.

In chapter IV, the sterol Ergosterol (Erg) known to regulate membrane properties in lower eukaryotes was studied based on the method described in above. Compared to Chol that orders both saturated and unsaturated phospholipid membranes, Erg only preferentially ordered saturated lipids such as 1,2-dipalmitoyl-*sn*-glycero-3-phosphocholine (DPPC) above their melting temperature (T_m). The results from both monolayer and bilayer studies indicated the formation of a liquid-ordered phase with saturated acyl tail lipids above T_m and the interaction of Erg in different membrane phase states to modulate membrane fluidity and polarity. Presumably, Erg preferentially interacts with saturated PC in the melted state, which stabilizes membranes at high temperature.

In chapter V, the ordering effects of Chol and Erg in ternary lipid mixture systems composed of unsaturated DOPC, saturated DPPC, and sterol were studied. The presence of ≥ 30 mol% of Erg exhibited a significant ordering effect and stabilized membrane properties when temperatures increased, similarly to Chol. Based on the dependence of membrane fluidity and polarity on environmental temperatures, the coexisting phase states in ternary lipid mixture systems could be estimated and phase diagram was constructed. It should be emphasized that Erg had higher efficiency for ordering membranes enriched in saturated DPPC at high temperatures (> Tm of DPPC). Estimated phase diagrams of membrane containing Chol and Erg contribute to modeling the mammalian and lower eukaryote membranes, respectively.

In chapter VI, a strategy to characterize the physicochemical membrane properties had been suggested, which efficiently provided insights into the ordering effects of sterol derivatives in biomembranes. Deeper understandings in the membrane properties are expected to contribute to the regulation mechanism of biological membrane properties, and to the design of functional membranes that enable the selective interaction with target molecules.

CONTENTS

CHAPTER I

General Introduction

1. Biological membrane and phospholipid membranes

Biological membranes play important roles in cell life and performs a variety of cell functions. The plasma membrane of

living species is consisted of a double sheet of lipid molecules and its functions as barriers which separate the inner and outer compartments, protect inner contents from external stimuli, recognize the signal transduction, and as a selective interaction with micro- and macromolecules. In general, the membranes are composed of lipids, sterols, proteins and sugars, and the compositions vary between types of cells (**Fig. 1-1**).

Lipid, one of essential components of biomembranes, is water-insoluble biomolecule that is highly soluble in organic solvents. Lipid itself has a variety of biological roles such as cell protection, cell-to-cell communication, control of micro-environments, and metabolism. In which, lipids as membrane constituents have been mainly focused with the three major kinds of membrane lipids as phospholipids, glycolipids, and sterols (**Fig. 1-2**).

All membrane lipids are amphipathic molecules which contain both hydrophobic and hydrophilic regions. The amphipathic nature of membrane lipids that they can self-assemble to make the membrane in polarizing environment with distinctive structures as micelle, bicelle or vesicle (Shimizu et al., 2005). Whereas, vesicle of lipid bilayer has common structure to biological membranes. The ability of lipid molecules such as differences in the acyl chain

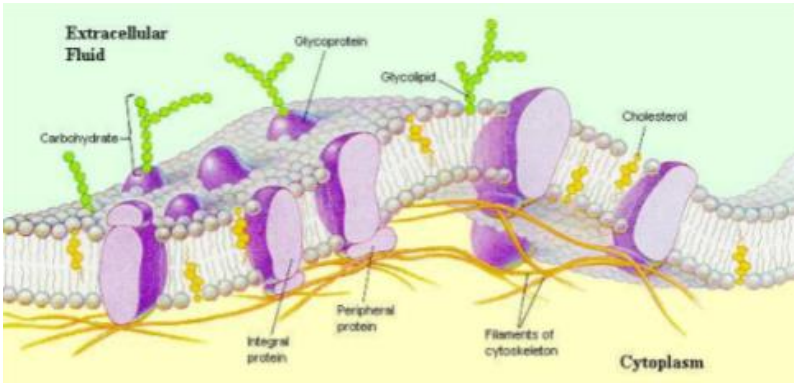

Fig. 1-1 A schematic presentation of a biomembrane.

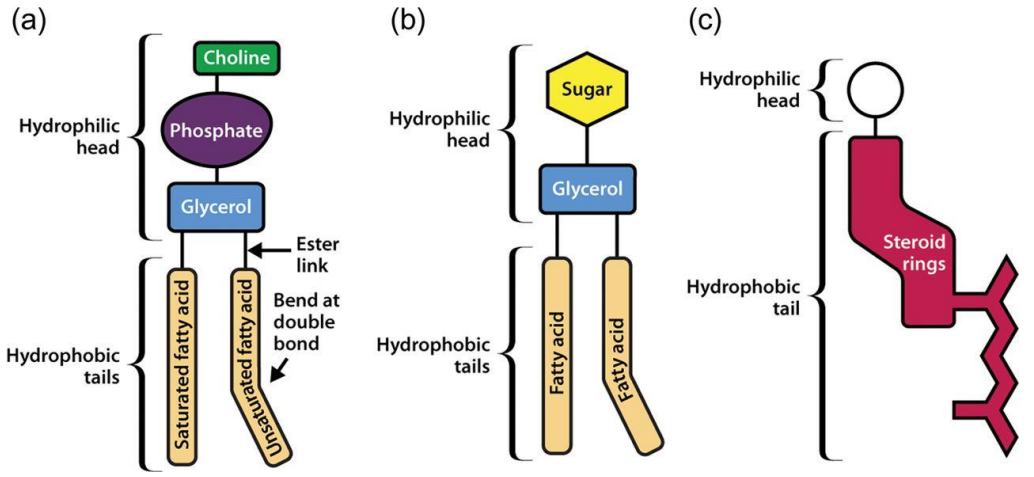

Fig. 1-2 Chemical structure of phospholipids, glycolipids and sterols (Helen et al., 2015).

length or the number of double bonds in the fatty acid tails are important to influence the packing of membrane that influences the fluidity of the bilayer. The presence of sterol is well-known as thermodynamically unfavorable for lipid motions and changes the membrane phase behaviors.

2. The applications, applicability and trends of the lipid membrane systems

Table 1-1 Applications of the lipid self-assembly systems

Research Tools	Target	System	Reference
Biosensor	Cholesterol	Cholesterol oxidase/ polymerized membranes	Nikolei *et al.*, 2013
	Enzyme activity	Langmuir-Blodgett membrane	Graca *et al.*, 2014
	Dopamine	Peroxidase/Dithiotreitol supported membranes	Fritzen-Garcia *et al.*, 2013
	Vanillin in alcoholic beverages and wine	Polymerized membranes	Nikolelis *et al.*, 2002
Drug delivery	Quinolones	Langmuir-Blodgett membranes	Bensikaddour *et al.*, 2008
	Chitosan/ Dextran	Langmuir-Blodgett membranes	Pavinatto *et al.*, 2007
	Haloperidol	Liposomes	Rodrigues *et al.*, 2001
	Azithromycin	Liposomes	Fa *et al.*, 2006

The lipid self-assembly systems are considered as the potential research tools to elucidate physiological responses, interaction behaviors between molecules, and biosynthesis pathway of sterols or any molecule. These systems have been applied in vaious fields such as the development of biosensors for environmental monitoring, clinical diagnostics and drug delivery systems, which have been reported and summarized in **Table 1-1** (Siontorou et al., 2017).

The lipid membrane can also maintain lots of membrane associating candidates, i.e., enzymes, antibodies, receptors, transporters in the preserved physiological conditions to mimic cell conditions. The formation of lipid membranes immobilized with these biomolecules changes the electrical characteristics of the membrane which are readily recorded by electrochemistry. In a broad sense, a biosensor detector can select and optimize any artificial lipid systems incorporated various bio-elements. Specifically, Langmuir-based technology was utilized to monitor enzyme activity using electrochemiluminescence. This technology facilitated the introduction of different lipid groups and conjugates in each monolayer to yield membranes with entirely new properties (Jiao et al., 2010). As another example of biosensors, a novel potentiometric Chol biosensor has been fabricated through the immobilization of the stabilized polymeric lipid membrane onto graphene electrode. Consequently, the Chol biosensor revealed a high sensing, capability and good selectivity (Nikoleli et al., 2013).

Due to the various forms of lipid self-assembly systems, these structures can deliver both hydrophilic and hydrophobic drugs for cancer, antibacterial, antifungal, diagnostics and etc. For example, the development of liposomal amphotericin B using liposome is a novel and successful drug to improve the potential antifungal activity and reduce the cytotoxic effect. However, drugs usually target intracellular reaction sites. Thus, drug-lipid membrane interactions occur at some points and result in drug pharmacokinetics and efficacy (Peetla et al., 2009). Moreover, the different intracellular accumulation rates of drugs, four structurally similar quinolones as ciprofloxacin, levofloxacin, garenoxacin and moxifloxacin were recorded (Michot et al., 2005) and studied with Langmuir-Blodgett model membranes. The data shown that quinolones exerted a condensing effect on the membrane and the efficiency differed between the quinolones and its derivatives,

as even small differences in their molecular structures alter the lipophilicity of each compound (Bensikaddour et al., 2008).

3. Sterol and its biosynthesis pathways

It is widely recognized that sterols play important roles in regulating biological processes and stabilize membrane structures. The roles of sterol in physicochemical

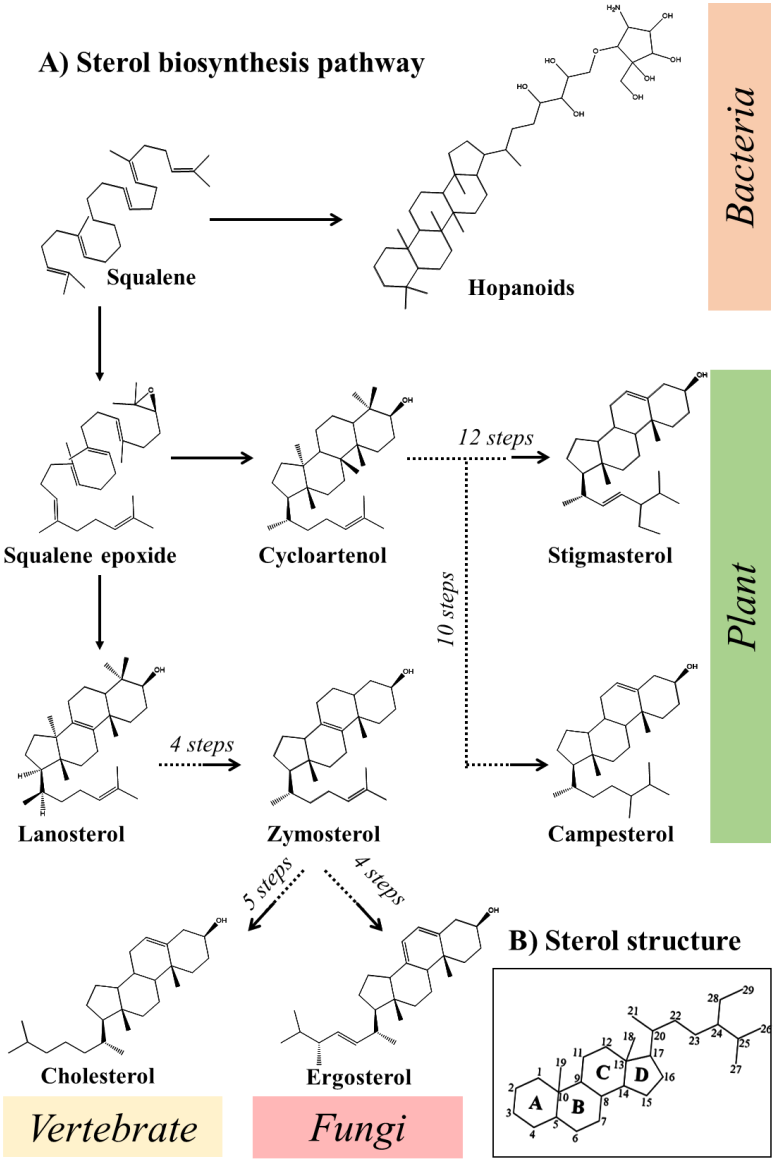

Fig. 1-3 The biosynthesis pathway of sterols leading to bacteria, fungi, plant and vertebrate sterols (**A**) and numbering of carbons and cycles of steroids (**B**) (Desmond and Gribaldo, 2009).

properties of the lipid self-assembly systems have been elucidated. However, how sterol synthesis based on lipid membrane still need studying.

In sterol synthesis pathway, squalene is convert to hopanoids in bacteria membrane in the presence of a squalene-hopene cyclase enzyme, while by several steps and specific enzymes squalene itself also can altered to ergosterol (Erg) in lower eukaryote membranes, to stigmasterol or campesterol in plant cells or to cholesterol (Chol) in

Table 1-2 Roles of sterols in membrane dynamics

Species	Systems	Sterol	Method	Membrane dynamic	Reference
Mammals	DMPC	Chol	Solid state NMR	Thickening membrane	Gamier *et al.*, 1991
	DPPC	Chol	NMR	Orientperpendicular the membrane surface Membrane fluidity stabilization	James *et al.*, 2008
	DPPC	Cho	Neuron diffraction, NMR	Increase the ordered membrane	Leonard *et al.*, 2001
	DPPC	Chol sulphate	NMR	Less ordering membranes	Faure *et al.*, 1996
Plants	DMPC DPPC	Cycloartenol	Solid-state NMR	Effect on the membrane order	Beck *et al.*, 2007 Leonard *et al.*, 1993
	DPPC	Stigmasterol Sitosterol	NMR	Increase the membrane order	Mehran *et al.*, 2016
Fungi	POPC	Erg	NMR	Disordering and ordering effect in unsaturated and saturated lipid membranes, respectively	Huesh *et al.*, 2007
Bacteria	DMPC	Hopanoids	NMR	Ordering effect Inhibit proton leakage through membrane rein force membrane cohension	Haines *et al.*, 2001 Ribeiro *et al.*, 2007 Leonard et al., 2001

vertebrates (**Fig. 1-3**) (Desmond and Gribaldo, 2009). Whereas, sterols in bacteria, plant and animal were well-studied as the roles in membrane properties, but the roles and mechanism of Erg regulating membranes were still need further studies.

For examples, the hopanoids are studied well and are found in diverse bacteria with special structures as compared to sterols in other species. Particularly, hopanoids is a planar, polycyclic hydrocarbon containing five rings compared with four rings in sterols, and it has a variety of polar and nonpolar side chains (Sessions et al., 2013; Talbot et al., 2001). Owing to their chemical structures, hopanoids can intercalate into lipid bilayers and interact with lipids to alter the biophysical properties of membranes, as they have a condensing effect and decrease the permeability of membranes (Kannenberg et al., 1983; Poralla et al., 1980; Belin et al., 2018; Nagumo et al., 1991; Chen et al., 1995), promote the formation of raft domains in bacteria and eukaryotic membranes (Saenz et al., 2012; Sáenz, 2010; Sáenz et al., 2015; Pike, 2009; Gumí-Audenis et al., 2016; Brown and London, 2000).

Similarly, there are variety of researches about plant sterols which are synthesized via the mevalonate pathway of isoprenoid metabolism. Stigmasterol and sitosterol are typical plant sterols among phytosterols, they have a strong ordering effect on model membranes above the phase transition temperature and the disordering effect at temperatures below the phase transition (Beck et al., 2007; Hodzic et al., 2008; Nikolelis and Theoharis, 2002; Halling and Slotte, 2004; Roche et al., 2008).

Furthermore, in vertebrates, Chol has been the most studied both in model and natural membranes and lots of experimental and theoretical efforts have provides evidence that Chol is able to increase the order of membrane packing (Mouritsen and Zuckermann, 2004; Simons, 2000; MacDermaid et al., 2015; Yuan and Johnston, 2002), lower permeability (Jurak, 2013; Szabo, 1974), maintain the fluidity and fusion rate (Mouritsen and Zuckermann, 2004; Simons, 2000; Yuan and Johnston, 2002). On the other hand, phase behavior studies of Chol/phospholipid mixtures show that Chol can induce the formation of a liquid-ordered phase (L_o). Which is responsible for the seemingly contradictory coexistence of tight packing and high fluidity in both monolayer and bilayer membranes (Yuan and Johnston, 2002; de Meyer and Smit, 2009). The small, dynamic, tightly bundled Chol–lipid assemblies, known as lipid rafts in the L_o phase, are considered

to be the microscopic mechanism for Chol's unique functions in bilayers and monolayers (Ando et al., 2015; Lingwood and Simons, 2010; Simons, 2000).

In higher eukaryotes, Chol is abundant, whereas Erg is found in lower eukaryotes such as protozoa, yeast, fungi and insects (Arora et al., 2004; Henriksen et al., 2006). Despite numerous studies focusing on Chol's impact on membrane properties, Erg and other sterols have not been studied nearly as extensively. The effects of sterols in model membrane were summarized in **Table 1-2**. Particularly, Erg has an additional double bond in the steroid ring in comparison to Chol, as well as a double bond and an extra methyl group in the alkyl tail (**Fig. 1-3**). These structural differences enable Erg to exhibit distinctive effects in membranes (Hung et al., 2016). However, it is still unclear exactly how Erg behaves and alters membrane properties, as well as why Erg is the primary sterol in lower eukaryotes.

More recently, Erg is reported as a target of antifungal agents such as polyene, azole, allylamine, thiocarbamate, morpholine (**Table 1-2**), in which agents act by forming a complex with Erg or deplete from the plasma membrane, causing the membrane disruption, increasing the leakage of cytoplasmic contents and ultimately cell death (**Fig. 1-4**) (Bellmann, 2013; Cheah et al., 2014; Francis et al., 1994; Gallis et al., 1990; Mazu

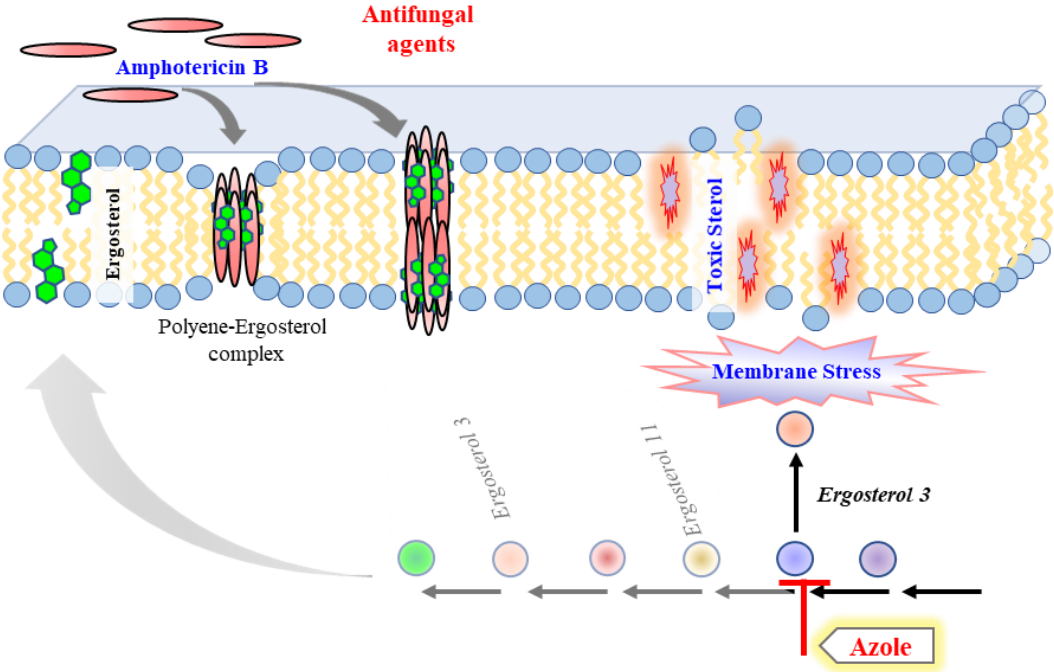

Fig. 1-4 The schematic of antifungal agents interfering membrane stuctures

et al., 2016; Bolard, 1986). Almost antifungal drugs have a higher affinity for Erg than Chol and less toxic in mammal cells, although there is a little difference between Erg and Chol (Warnock, 1991). Liposomes have been designed to incorporate antifungal drug to reduce the side effects of drugs (Francis et al., 1994; Moen et al., 2009). Upon the binding to the cell wall, the liposomes were disrupted and drugs were released and bound to Erg to kill fungal cells (Adler-Moore and Proffitt, 2002). The questions raised from this issue are why Erg and Chol had such as differences and how their membrane properties control sterol activity and how membrane properties alter during the applications of antifungal.

4. Membrane characterization methods

To investigate the role of sterols in membranes, especially Chol and its derivatives such as Erg and Lanosterol (Lan), the properties of membranes modified with sterols should be studied due to the biological functions of cell membranes strongly coupled with their fundamental physicochemical properties. In which, the phase state, hydration, and dynamics of the constituting molecules determine the membrane structure and regulate the binding and transport of molecular. Thus, monitoring these properties *in situ* is an important task in membrane biophysics. The unique features of fluorescence techniques in comparison with other methods that are capable of evaluating membrane properties (notably NMR, FTIR, EPR, etc.) and their ultimate sensitivity up to a single-molecule level and their ability to operate in biological systems of varying complexity, up to the level of living cells and tissues (Demchenko et al., 2009).

Additionally, as they present half of a membranes, phospholipid monolayers have also been considered as good models of biomembranes. The early work employing monolayer system was largely hampered by the absence of tools to investigate liquid-liquid interfaces with molecular resolution, which has not been revealed by the studies of fluorescent probes in bilayer membranes yet. Since many of interface-sensitive techniques have become applicable to fluid interfaces, for examples fluorescence, reflection–absorption FTIR-spectroscopy (Dluhy et al., 1983), X-ray (Kjaer et al., 1987; Dutta et al., 1987), neutron scattering (Penfold and Thomas, 1990; Vaknin et al., 1991), ellipsometry (Reiter et al., 1992), and Brewster angle microscopy (Hénon and Meunier,

1991; Reiter et al., 1992), and nonlinear optical spectroscopy (Vogel and Shen, 1991). Therefore, studies of Langmuir monolayers and fluorescent probes in bilayers are suitable for investigating the physicochemical properties of lipid membranes.

4.1. Multi-focal properties of lipid bilayer systems

A particularly popular approach to study the structure and dynamics of lipid membranes and the effects of molecules embedded in lipid bilayers is based on the use of fluorescent probes (Abrams and London, 1993; Chattopadhyay and London, 1987; Epand et al., 1996; Lentz, 1989; Lentz, 1993; Maier et al., 2002; Somerharju, 2002).

Firstly, the fluidity (micro-viscosity) is the measure of frictional resistance to rotational and translational motion of molecules that can estimated by the fluorescence anisotropy of 1,6-diphenyl-1,3,5-hexatriene and its trimethylamino-derivative (DPH and TMA-DPH, respectively). The quantum yield and fluorescence intensity decays show little sensitivity to the phase state of lipid membranes, unlike the fluorescence anisotropy, which decreases threefold upon melting of the lipid acyl chains. Consequently, both DPH and TMA-DPH have been commonly used as probes of membrane fluidity (Lentz, 1989; Lentz, 1993). Whereas, DPH is mostly utilized as a reporter of the highly disordered hydrophobic core, and TMA-DPH is dominant in shallow regions of the bilayer (glycerol backbone and upper segments of the phospholipid acyl chains) because of its cationic group acting as an anchor to the water/bilayer interface.

Secondly, lots of fluorescent probes are sensitive to membrane polarity with fluorescent decay kinetics depending on the dielectric constant of membrane environments (Stubbs et al., 1995; Macgregor and Weber, 1981). 6-Propionyl- and 6-lauroyl-2-dimethylaminonaphthalene (Prodan and Laurdan, respectively) are those with environmentally sensitive steady-state fluorescence parameters, in which a noticeable red-shift of their emission is observed with increasing solvent polarity due to the dipolar relaxation phenomenon (Parasassi et al., 1994; Parasassi and Gratton, 1995; Macgregor and Weber, 1981). The generalized polarization (*GP*) method was developed by Parasassi *et al.* to quantitatively analyze the differences in the emission spectra, and to exploit a possible selective excitation of two probe populations in different environments. The advantages of the *GP* method reside in its sensitivity to the properties of the membrane

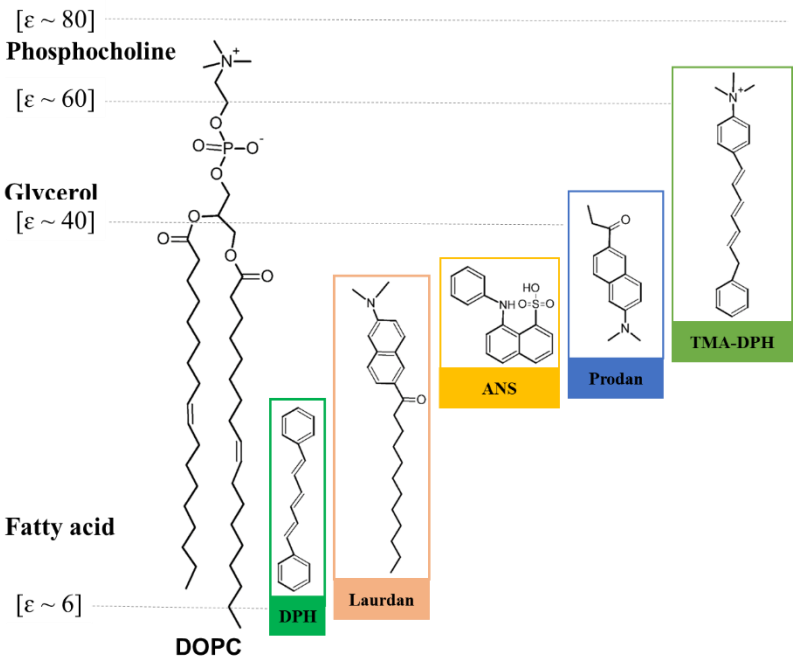

Fig. 1-5 Multiple fluorescent probes utilized for membrane characterization.

Table 1-3 The fluorescent probes utilized in investigation of membrane properties

Fluorescent probes	Detecting regions	Excited wavelengths (nm)	Emission wavelength (nm)
TMA-DPH	Interfacial fluidity	360	410
DPH	Inner fluidity	360	430
Prodan	Interfacial polarity	340	400 – 600
Laurdan	Inner polarity	340	400 – 600
ANS	Membrane hydrophobicity	350	375 – 600

and in the possibility of determining and quantifying the phase state of the membrane. Because of the different lengths of their acyl residues, the two probes locate differently in the bilayer depth, while Laurdan burdens in a deeper region as compared to Prodan.

Thirdly, a fluorescent probe of 1-anilino-8-naphthalene sulfonate (ANS) is an extensively utilized probe for characterization of protein binding sites of the hydrophobicity of membranes. ANS binds preferentially to hydrophobic cavities resulting in a low fluorescent intensity, and the quantum yield of ANS also depends on the physicochemical property of the membrane (Schonbrunn et al., 2000). Therefore, ANS is employed to demonstrate the membrane characteristic. Fluorescent probes used in this study were summary in **Table 1-3** and **Fig. 1-5**.

4.2. Monolayer at air-water interface

A singer layer formed at the air-water (A-W) interface by insoluble amphiphilic is called a Langmuir monolayer. An amphiphilic molecule generally comprises of two parts: hydrophilic (polar) head part and hydrophobic (non-polar) tail part. Their hydrophilic parts can be -COOH, -OH, -CN and $-NH_2$ which can easily form hydrogen bond with water and hence it can stay with water molecules without any appreciable change in the entropy. While the hydrophobic part can be aliphatic chains, aromatic ring systems or the combination of two and increase the membrane order. The ordering membrane decreases the overall entropy of the system and hence the hydrophobic tail group favors to stay away from the water (Findenegg, 1986). In Langmuir monolayer, the assemble of

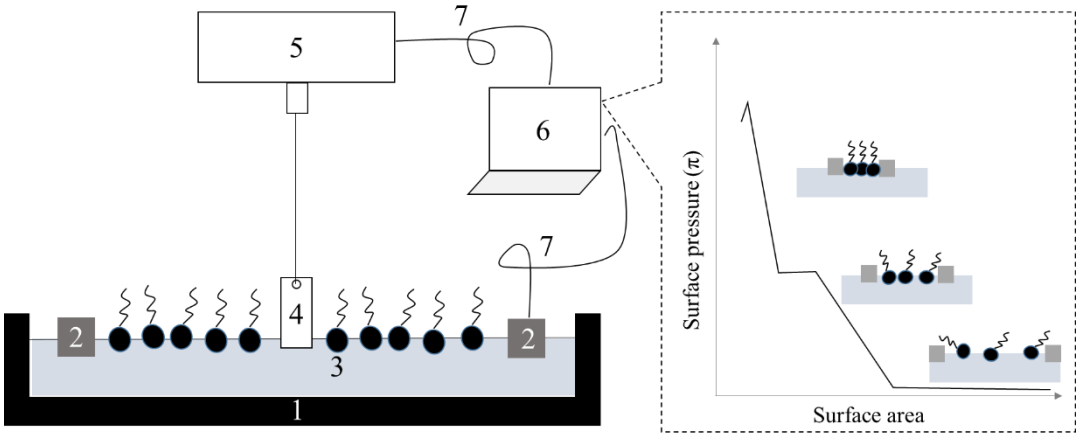

Fig. 1-6 A schematic diagram showing the experimental set up for the measurement of surface pressure – area isotherms. The basic part of the set up are as follows: (1) Teflon trough, (2) Teflon barriers, (3) subphase, (4) Wilhelmy plate, (5) surface pressure sensor, (6) computer, (7) connecting wires.

hydrophilic and hydrophobic parts form a monolayer at the A-W interface which provides an ideal two-dimensional (2D) system to study the surface thermodynamics where the 2D plane is provided by the smooth water surface. The surface density of the molecules in the monolayer is varied by changing the area available for the molecules by moving the barriers laterally. The surface pressure (π-A) was measured using a Wilhelmy plate method. The experimental set up for measurement of surface pressure-area isotherms was shown in **Fig. 1-6**.

A typical π-A isotherm was shown in **Fig. 1-6** with a plateau in the isotherms representing the coexisting of two phases. A plateau in the isotherm indicates a phase transition from gas phase, very large area and molecules to be far apart and not exert any force on each other. On compression, the molecules condense to a low-density liquid state. On further compression, the membrane phase transforms to a high-density liquid state. Therefore, the phase state of monolayers can be easily triggered at constant temperature by increasing the packing density of the lipids by compression. The interaction can be directly determined by the observed structure changes. The yield of enzymatic reaction, secondary structures of peptides or proteins can be measured by monolayer studies. Therefore, the relevance and utility of Langmuir monolayers are the suitable models to study physical state and chemical interaction at membrane surfaces.

5. Overview of this study

The final purpose of this thesis is to characterize properties of membranes modified with Chol and its derivatives by monolayer and bilayer studies. Then, the mechanism of interaction of between sterol molecules and membrane components will be clarified and the roles of sterol in regulating membrane properties could be investigated. Finally, these characterizations can be applied for the model and living cell membranes. The framework and the flow chart of the present study are shown in **Fig. 1-7** and **1-8**, respectively.

In Chapter II, the biosynthesis pathway and diversity of Chol from Lan were investigated based on membrane physicochemical properties, with the respect to the regulation of self-assembly via sterol insertion. The behavior of sterol molecules investigated in the mixture of unsaturated phospholipids as 1,2-doleoyl-*sn*-glycero-3-

phosphocholine (DOPC) were revealed by the influence in membrane properties from the surface to inner membrane leaflets by using multiple fluorescent probes. Given the different binding positions of the probes in the membranes, the differences in membrane properties reflected the degree of interactions between Chol and (or Lan) and DOPC at different locations in the membrane. The surface membrane fluidity, hydrophobicity, surface membrane polarity and inner membrane polarity, and inner membrane fluidity were indicated by several fluorescent probes, including TMA-DPH, ANS, Prodan, Laurdan, and DPH, respectively. The results clarified that both sterols could regulate membrane in distinctive ways. Particularly, Chol had strong ordering efficiency in unsaturated phospholipid membrane from surface to inner membrane even at low concentration. However, Lan with little difference in chemical structures, it showed weaker ordering effect as compared to Chol in ordering the unsaturated membrane in hydrophobic region at high concentration. It is proposed that Chol is suitable, dominant and plays important roles in regulate membrane properties of vertebrate membranes which are enriched in unsaturated phospholipids.

In Chapters III, the interaction behaviors of Lan and Chol was continued to investigate by monolayer studies to clarify and compare the potential interaction of sterols with unsaturated lipids as DOPC. The membranes modified with sterols at difference ratios were prepared at the air/water interface to obtain the Langmuir isotherms. The alteration phospholipid membrane areas at a specific surface pressure resulted in the negative or positive excessed area. Whereas, the negative values of excesses area indicated the attractive interaction of Lan and Chol with unsaturated phospholipid molecules and positive values shown the unattractive between molecules. Additionally, the increase of compression modulus for Chol mixed membranes was higher than that of Lan which had the highest values at high concentration, and indirectly reflect the ordering effect efficiency of sterols in mixed membranes. Finally, a favorable interaction between DOPC and Chol were emphasized by the negative excessed Gibbs free energy as explain why Chol is more suitable for animal membranes. Results from Langmuir monolayer surely confirmed that Lan had an interaction with membrane although it has insignificant effect in each membrane regions proved by fluorescent probes in bilayer systems.

In Chapter IV, both Langmuir monolayer and multiple fluorescent probes analysis were applied to determine the interaction behavior of Chol's derivative, Erg, in different membrane types. Erg is an ubiquitous constituent sterol in the membrane of lower eukaryote and had a small difference in chemical structures compared to Chol. The binary lipid membranes composed of Erg and diacylglycerophosphocholine (PC) with unsaturated acyl chains as DOPC, and saturated acyl chains be different in tail length as 1,2-dilauroyl-*sn*-glycero-3-phosphocholine (DLPC), 1,2-dimyristoyl-*sn*-glycero-3-phosphatidylcholine (DMPC) and 1,2-dipalmitoyl-*sn*-glycero-3-phosphocholine (DPPC) were studied in Langmuir monolayer and bilayer vesicle systems. From the excess area measured in π-A isotherms, the attractive interaction between Erg and saturated PC were significant above the melting temperature (T_m) of PC. Conversely, repulsive interactions were observed at temperature below T_m. From the analyses of membrane fluidity and polarity using fluorescent probes, similar trends were obtained in the bilayer systems where Erg had an ordering effect on saturated PC vesicles. In contrast, in unsaturated PC systems, Erg did not alter membrane ordering. These finding demonstrated that the interaction of Erg with fluid state PC lipid will maintain the lower eukaryote membranes in a more ordered state, similarly to the effect of Chol in higher eukaryote.

In Chapter V, the phase behaviors of Erg and phospholipid mixtures were investigated and phase diagram was constructed and compared to the effect of Chol in similar lipid systems. The effect of Erg in saturated DPPC and unsaturated DOPC bilayer membrane fluidity and polarity were systematically analyzed using fluorescent probes. The presence of Erg with ≥ 30mol% showed a significant ordering effect and stabilized membrane properties when temperatures increased, suggesting a similar function of Chol in same lipid systems that makes L_o phase. In addition, the interaction behavior and condensing effect of Erg in respective membrane systems were determined using Langmuir monolayer via the surface pressure-area isotherms. The results clarified that Erg in DOPC/DPPC=75/25 resulted in expending membranes, while Erg in DOPC/DPPC=50/50 and 25/75 were condensing. Based on the behaviors of Erg in membrane monolayer and bilayer systems, the phase diagram of DOPC/DPPC/Erg was constructed. These new findings suggest that, which are rich in saturated lipids, contain

Erg to stabilize membrane homeostasis. While, Chol has more influence in phase states of the membranes enriched both in unsaturated and saturated lipids.

In Chapter VI, the results obtained in this work are summarized in General Conclusion, and Suggestions for Future Works are described as extension of the present thesis.

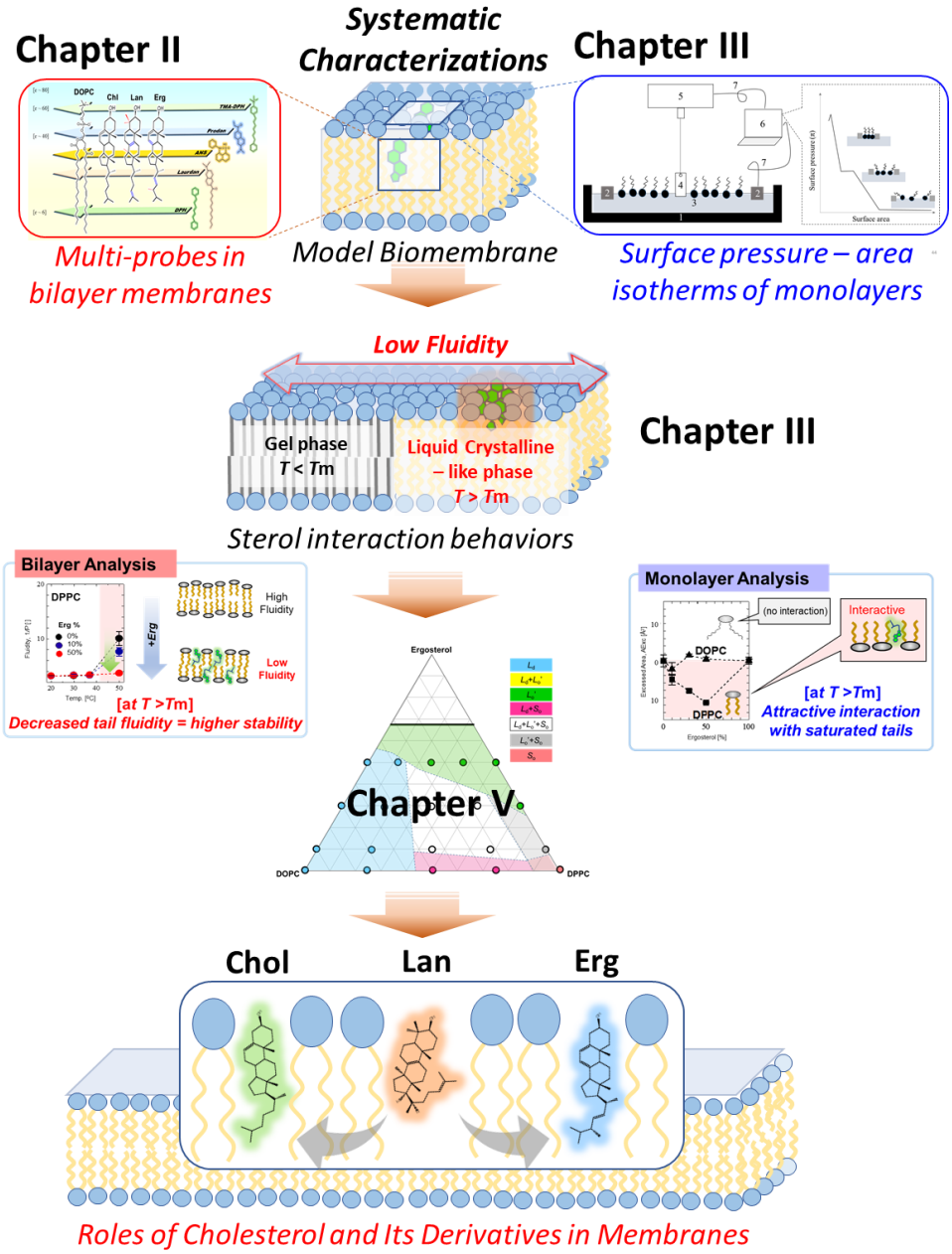

Fig. 1-7 Studies on characterization methods of model biomembranes modified with Cholesterol and its derivatives.

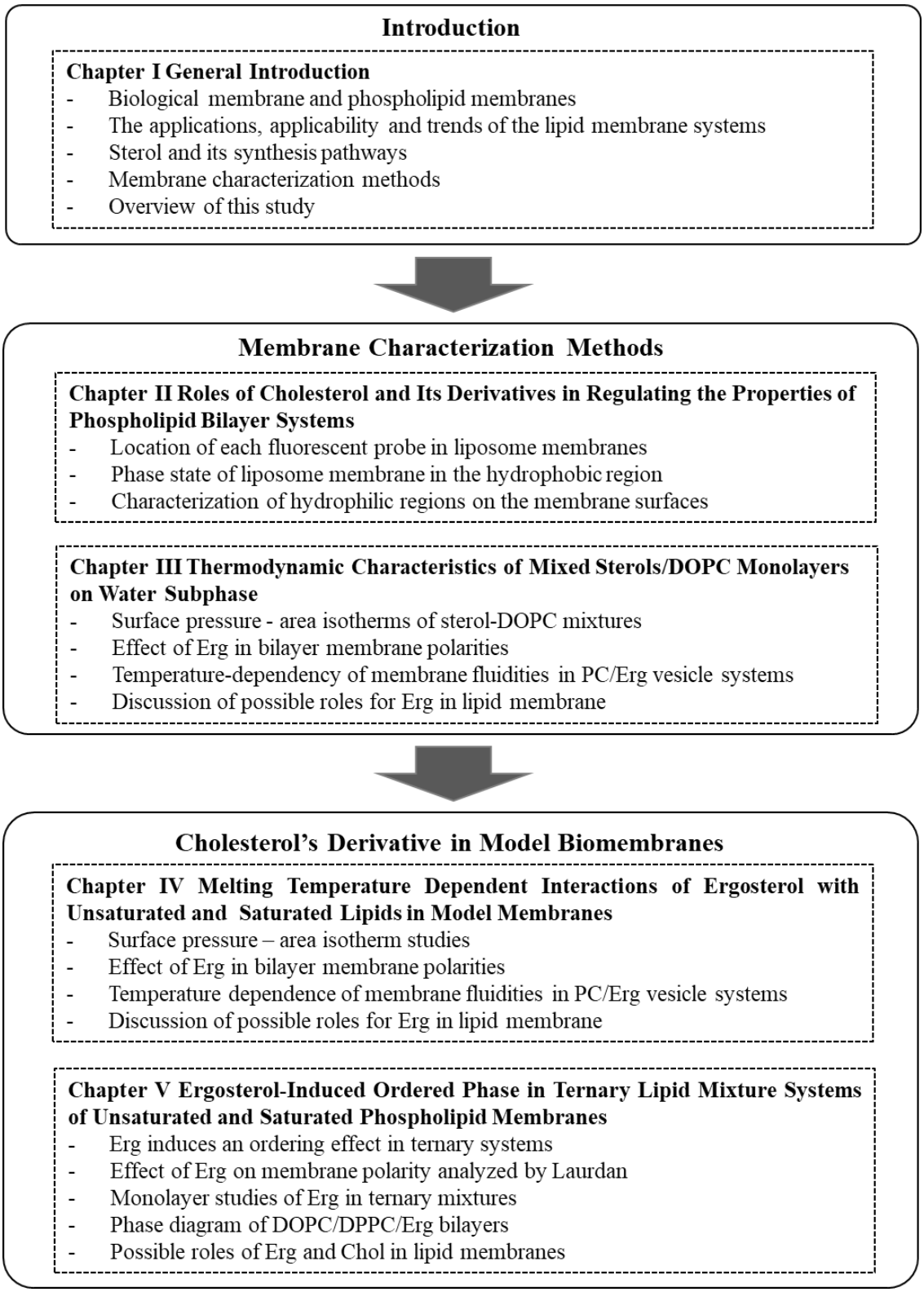

Fig. 1-8 Framework of present study.

Chapter II

Roles of Cholesterol and Its Derivatives in Regulating the Properties of Phospholipid Bilayer Systems

1. Introduction

Considering the roles of the sterol molecule in lipid bilayer membranes, such a diversity in the chemical structure of sterols could be reasonable to regulate the membrane properties depending on species. In artificial membranes, Cholesterol (Chol) inserts into and interacts with the plane of the bilayer, with its hydroxyl group near the ester carbonyl of phospholipid molecules and the hydrocarbon tails extending toward the bilayer center (Bittman, 1997; Yeagle, 1985; You et al., 2003; Worcester and Franks, 1976; Dufourc et al., 1984). In general, Chol is distributed in parallel to the phospholipid hydrocarbon chain, and its tetracyclic ring structure lies near the phospholipid hydrocarbon tail at positions 2–10 (Morrow et al., 1995; Stockton and Smith, 1976; Davies et al., 1990). Because of the closely proximity of the planar sterol ring system, the hydrocarbon chains are ordered in the inner membrane. Chol interacts with the phospholipid membrane in the headgroup region through hydrogen bonds and with the hydrocarbon chains through van der Waals forces and hydrophobic forces (Yeagle, 1985; Slotte, 1999; Yeagle et al., 1977; McMullen and McElhaney, 1996).

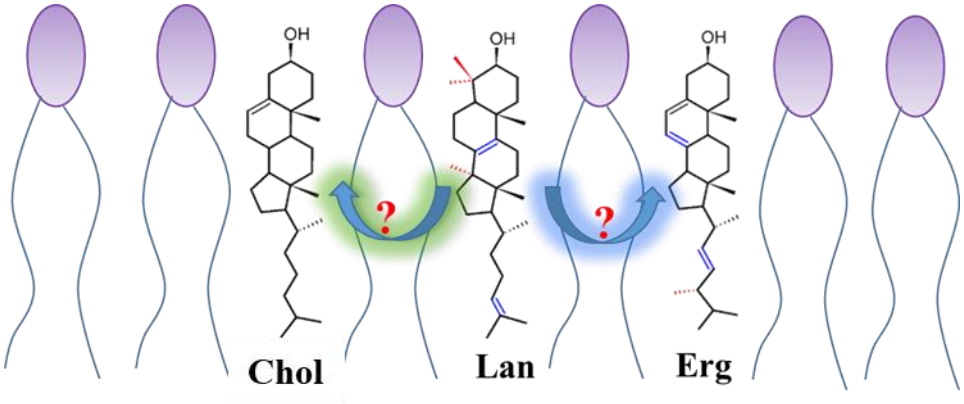

Fig. 2-1 Chemical structure of three sterols.

It is indicated that sterols influence the membrane permeability (Miao et al., 2002) and the conformational order of the lipid acyl chains (Bernsdorff and Winter, 2003; Pencer et al., 2005; (Dahl et al., 1980). Further, sterols also control the membrane lateral organization (Pencer et al., 2005; Xu et al., 2001) and the membrane hydrophobic thickness that is responsible in part for the regulation of lipid-protein interactions (Pencer et al., 2005; Ipsen et al., 1990; Ali et al., 2007). Specific sterols, in particular Chol, has cohesive interactions with saturated lipids (Bernsdorff and Winter, 2003; Xu et al., 2001). Chol and Lanosterol (Lan) (**Fig. 2-1**) have similar dimensions such as the length of the rigid ring and the total length of the molecule (Pencer et al., 2005), and they own common features like a planar cyclopentane-phenantrene ring, a 3β-OH group, and a hydrophobic side chain linked (Urbina et al., 1995). Thus, the other lipids and modulation of membrane properties(Urbina et al., 1995; Bernsdorff and Winter, 2003; Henriksen et al., 2004; Endress et al., 2002; Xu et al., 2001).

With two β-oriented methyl groups at 10C and 13C and a branched hydrocarbon tail at 17C, Chol orients with its 3β-OH group in proximity to the phospholipid ester carbonyl oxygen, within the hydrophobic-hydrophilic interface, and aligns its long molecular axis parallel with the acyl chains of membrane phospholipids. Thus, the interaction between the rigid and smooth hydrophobic part of Chol, as well as its side chain and other lipid species, is due to van der Waals forces and is inherent to the Chol structure itself. Lan has three additional methyl groups compared to Chol, two of which are attached to 4C (α- and β-faces) and the third attached to 14C (α-face), thus making the α-face asymmetric. Moreover, Lan contains two double bonds, one at position 8C and the second at position 24C. Because of the three additional methyl groups, Lan is bulkier than Chol, and its structure does not facilitate strong interactions with lipids. The amphiphilic nature of these molecules orient with their hydrophobic part between the lipid acyl chains and with the hydroxyl group close to the phospholipid ester carbonyl oxygen.

The cooperation and interaction of sterols in natural membranes comprise a topic of current research. However, because of the complexity of experimental method and the results obtained, such an approach is not frequently reported, as compared to bilayer lipid membranes (Miñones et al., 2009). The bilayer lipid membrane formed in the aqueous environment has advantages over other methods because it allows for control of the

composition, molecular packing, and physical states. The study of mixed lipid systems has been focused to investigate the nature of biological membranes, which contain high amounts of saturated and unsaturated phosphatidylcholines (PC) such as 1,2-dipalmitoyl-*sn*-glycero-3-phosphocholine (DPPC) and 1,2-dioleoyl-*sn*-glycero-3-phosphocholine (DOPC), respectively (Svetlovics et al., 2012). Recently, the effects of sterols (e.g. Chol and Lan) on the properties of DPPC membranes were compared on the basis of thermal phase behavior NMR (Mannock et al., 2006; Miao et al., 2002), and fluorescence anisotropy measurements (Bernsdorff and Winter, 2003). It was found that the interaction of these lipids depends on the structure of the sterol side chain and the tetracyclic nucleus. In particularly, they form the liquid ordered phase (L_o) in membranes and have a condensing effect of different scales. Nevertheless, the effect of these sterols on changing the characteristics of unsaturated phospholipids (i.e., DOPC) membranes has still not been clarified because of its complexity in contrast to that of saturated phospholipids (i.e., DPPC).

Therefore, in this study, the influences of Chol and Lan on the alterations in membranes was investigated, from the surface to interior of DOPC membranes. To understand the mechanism underlying the interaction between phospholipids and steroids in the membrane, the basic membrane properties were analyzed using multiple

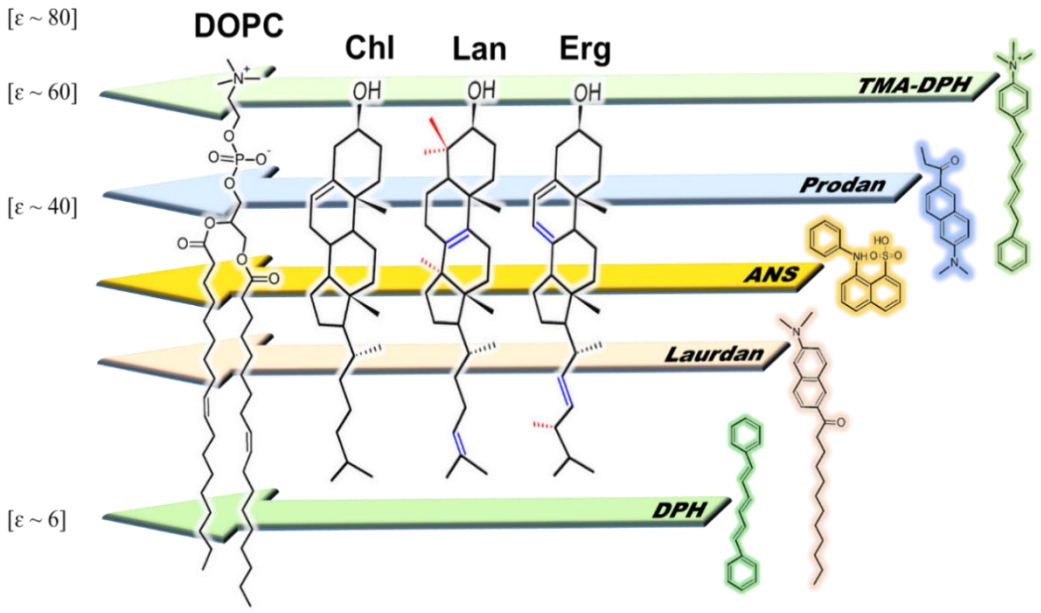

Fig. 2-2 Conceptual illustration of chapter II.

fluorescent probes with different binding depths within the membrane and each part of the membrane from the exterior to the interior of the membrane was analyzed. By analyzing the binding depth (ε) of each fluorescent probe, e.g., 1-[4-(Trimethylamino)phenyl]-6-phenylhexa-1,3,5-triene (TMA-DPH), 8-anilino-1-naphthalenesulfonic acid (ANS), 6-propionyl-2-dimethylaminonaphthalene (Prodan), 6-dodecanoyl-2-dimethylaminonaphthalene (Laurdan), and 1,6-Diphenyl-1,3,5-hexatriene (DPH), the experimental fluidity and polarity of full-part membranes and the affinity and location of sterols in the membrane could be determined. Thus, the roles of steroids in the membrane were clarified based on qualitative analysis (**Fig.2-2**).

2. Materials and methods

2.1 Materials

1,2-Dioleoyl-s*n*-glycero-3-phosphocholine (DOPC) and 1,2-dipalmitoyl-s*n*-glycero-3-phosphocholine (DPPC) were purchased from Avanti Polar Lipids (Alabaster, AL). Chol and Lan were purchased from Sigma-Aldrich (St. Louis, MO, USA). Other chemicals were purchased from Wako Pure Chemical Industry Ltd. (Osaka, Japan) and were used without further purification.

2.2 Liposome preparation

A chloroform solution of DPPC and DOPC with Chol and Lan in 10 mol%, 30 mol% and 50 mol% of each sterol in chloroform was dried in a round-bottom flask by rotary evaporation under a vacuum. The lipid films obtained were dissolved in chloroform twice, and the solvent was evaporated. The lipid thin films were kept under a high vacuum at least 3 h and then hydrated at room temperature with 3 mL phosphate-buffered saline (PBS). The vesicle suspension was frozen at -80 °C and thawed at 50 °C to enhance the transformation of small vesicles into larger multi lamellar vesicles (MLVs). This freeze and thaw cycle were repeated five times. MLVs were used to prepare the large unilamellar

vesicles (LUVs) by extruding the MLV suspension 11 times through two layers of polycarbonate membranes with mean pore diameters of 100nm using an extruding device (Liposofast; Avestin Inc,. Ottawa, ON, Canada).

2.3 Evaluation of the membrane fluidity in the surface and inner membrane

10 μL of fluorescent probes (100 μM of TMA-DPH or DPH, dissolved in ethanol) were added to 12.5 μL liposome solution (total lipid concentration: 20 mM) in 977.5 μL PBS buffer (molar ratio: total lipid/probe=250/1). The fluorescence polarizations of DPH and TMA-DPH (E_x = 360 nm, E_m = 430 nm) were measured after 1 h incubation at 37 °C, by using the fluorescence spectrophotometer (FP-6500; JASCO, Tokyo, Japan). The samples were incubated at least 30 min in the dark. The samples were excited with vertically polarized light (360 nm), and emission intensities both perpendicular (I⊥) (0 °, 0 °) and parallel (I∥) (0 °, 90 °) to the excited light were recorded at 430 nm. The polarization (P) of DPH was then calculated by using the following equations:

$$P = \frac{(I_{/\!/} - GI_{\perp})}{(I_{/\!/} + GI_{\perp})} \quad \textbf{(2-1)}$$

$$G = \frac{I_{\perp}}{I_{/\!/}} \quad \textbf{(2-2)}$$

where I⊥ and I∥ are the emission intensities perpendicular to the horizontally polarized light (90 °, 0 °) and parallel to the horizontally polarized light (90 °, 90 °), respectively, and G is the correction factor. The membrane fluidity was evaluated by the reciprocal of polarization (1/P). The total concentrations of lipid and DPH or TMA-DPH were 100 and 0.4 μM, and the final volume for each sample was 1 mL.

2.4 Identification of membrane hydrophobicity by using ANS

With the suitable excited wavelength at 350 nm, the fluorescent spectra for ANS were recorded at emission wavelengths from 375 nm to 600 nm for each kind of liposome.

The hydrophobicity of membrane was reflected by comparing the intensity values at 484 nm (I_{484}).

2.5 Characterization of membrane polarity by using Prodan and Laurdan

10 μL of fluorescent probes (100 μM of Laurdan or Prodan, dissolved in ethanol) were added to 12.5 μL liposome solution (total lipid concentration: 20 mM) in 977.5 μL PBS buffer (molar ratio: lipid/probe=100/1). The sample solutions were incubated for 2 h at 37 °C, then the fluorescence spectrum of Laurdan or Prodan for each liposome was recorded at appropriate emission wavelengths from 380 nm to 600 nm at 37 °C, with the excitation wavelength of 340 nm. For Laurdan, the membrane polarity ($GP_{340,\mathrm{Laurdan}}$) was estimated based on the following equation:

$$GP_{340Laurdan} = \frac{(I_{440} - I_{490})}{(I_{440} + I_{490})} \quad \textbf{(2-3)}$$

here I_{440} and I_{490} are the emission intensities of Laurdan at 440 nm and 490 nm, respectively.

For Prodan, the membrane polarity ($GP_{340,\mathrm{Prodan}}$) was estimated based on the following equation:

$$GP_{340Prodan} = \frac{(I_{437} - I_{510})}{(I_{437} + I_{510})} \quad \textbf{(2-4)}$$

where I_{437} and I_{510} are the emission intensities of Prodan at 437 nm and 510 nm, respectively. The total concentrations of lipid and Laurdan or Prodan were 100 and 1 μM, and the total volume for each sample was 1 mL.

2.6 Normalization of fluidity, hydrophobicity and polarity membrane

To understand and evaluate the effect of each sterol in phospholipid membranes, the raw data were normalized as the following equation (**2-5**). The normalized values *z*' for membrane fluidity (measured by TMA-DPH or DPH), hydrophobicity (measured by

ANS) and membrane polarity (measured by Prodan or Laurdan) were calculated by using $1/P$, I_{484}, and $-GP_{340}$, respectively.

$$z' = \frac{z-y}{x-y} \quad \textbf{(2-5)}$$

where x, y, z are the maximum, minimum and other values, respectively, among the liposomes tested in this study. Herein, the maximum ($z = x$, thus $z' = 1$) and minimum ($z = y$, thus $z' = 0$) values were regarded as most-disordered membrane and most-ordered membrane, in order. Finally, these normalized values could be used to construct the membrane properties chart for each liposome to indicate the distinction of each liposome membrane properties from the outer to inner membrane.

3. Results and Discussion

3.1 Location of Each Fluorescent Probe in Liposome Membrane

Fluorescent probes such as TMA-DPH, ANS, Prodan, Laurdan, and DPH are sensitive to their surrounding environments, and are used as the probes for liposome membranes properties. Liposome membranes have a hydrophobicity gradient in the vertical direction of membrane (Cevc, 1990), which is reflected by binding depths of fluorescent probes. In 1,4-dioxane/water systems, each probe showed different emission wavelength and fluorescent intensity (Ishigami et al., 2015; Suga and Umakoshi, 2013; Suga et al., 2011). Thus, the emission wavelength and intensity in liposome membranes were also depended on the surrounding environment. By analyzing the emission property of each probe in 1,4-dioxane/water systems, the location of probe in the liposome was estimated in the basis of (i) emission wavelength and (ii) intensity and shown in **Fig. 2-3**.

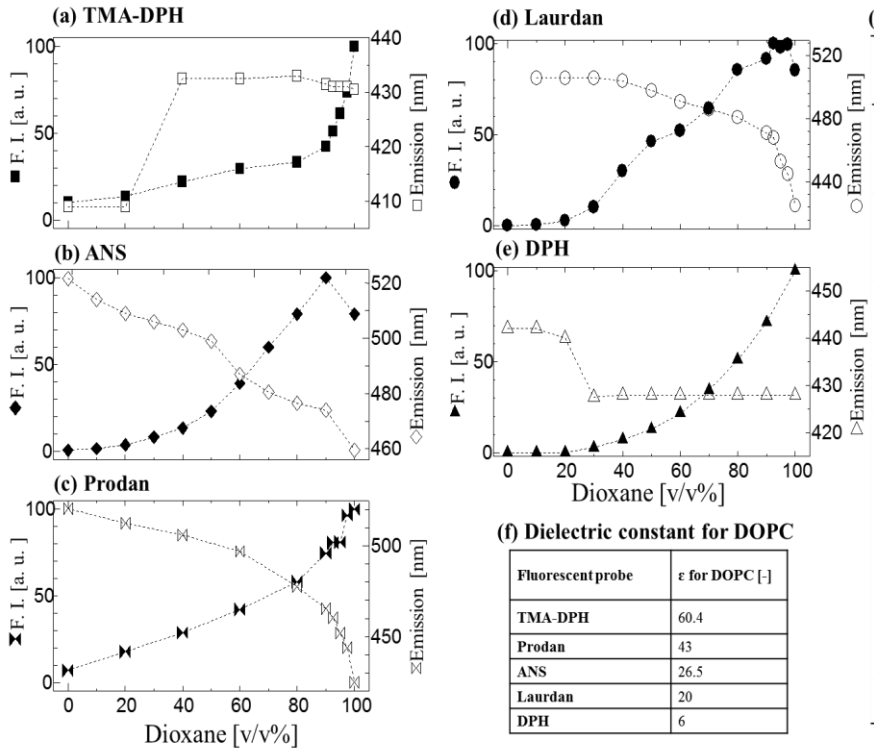

(f) Dielectric constant for DOPC

Fluorescent probe	ε for DOPC [-]
TMA-DPH	60.4
Prodan	43
ANS	26.5
Laurdan	20
DPH	6

(g) Dielectric constant

Dioxane [v/v%]	ε [-]
0	76.72
10	68.74
20	60.38
30	51.91
40	43.33
50	34.81
60	26.45
70	18.58
80	11.58
90	5.96
92.5	5.40
95	4.24
97.5	3.06
100	2.20

Fig. 2-3 Characterization of fluorescent probes in 1,4-dioxan/water systems: (**a**) TMA-DPH, (**b**) ANS, (**c**) Prodan, (**d**) Laurdan and (**e**) DPH. The estimated dielectric environment around each probe in DOPC liposome is summarized in Table (**f**). The dielectric constants of solvents were controlled by mixing 1,4-dioxane and water with different volume ratio (**g**).

(i) Laurdan, ANS, Prodan: These probes showed the emission peak shifts depending on the solvent hydrophobicity. Thus, their locations can be estimated by analyzing the emission peak wavelength in liposomes. For ANS, only one emission peak could be seen at 484 nm, which means that ANS bound to the similar location in membrane regardless of phase state, thus the surface hydrophobicity (i.e. the exposure of hydrophobic core to water) can be investigated by I_{484}. For Laurdan and Prodan, the appearance of two peaks indicate that the location of probe altered up on the membrane properties. The GP_{340} values can be used to understand the polarity of the membrane (**Fig. 2-4**).

In 1,4-dioxane/water systems, the $GP_{340,Laurdan}$ and $GP_{340,Prodan}$ values were monotonically decreased by increasing ε values. Thus, the GP_{340} value analysis can be applied to monitor the surrounding of Laurdan or Prodan depending on the polar

environments in the membrane. Considering the peak shift of Laurdan or Prodan, its actual location is flexible and depends on the membrane phase state, while it surely settles down in the inner membrane because it showed much higher intensity as compared to water system.

(ii) DPH, TMA-DPH: These probes have the emission peaks at 430 nm, independent to the surrounding hydrophobicity. In the liposome systems, both DPH and TMA-DPH showed similar emission peak wavelength a 430 nm, indicating that DPH and TMA-DPH located at $\varepsilon<43$ and $\varepsilon<60$, respectively. The fluorescence intensity increased in proportion to the hydrophobicity of solvent. In the case of DPH inserted into liposome membranes, the emission peak at 428 nm and its fluorescence intensity is ca. 70% as compared to 1,4-dioxane 100% as solvent, indicating that DPH is inserted into hydrophobic regions ($\varepsilon\sim6$). In the same manner, TMA-DPH can be located at $\varepsilon\sim60$.

Considering our experimental results (Suga and Umakoshi, 2013; Suga et al., 2011; Ishigami et al., 2015) and literatures (Parasassi and Gratton, 1995; Dhanikula and Panchagnula, 2008; Krasnowska et al., 1998; Cwiklik et al., 2011) the location of each probe in DOPC liposome can be estimated (**Fig. 2-3f**). No peak shifts of ANS or TMA-DPH were observed in DOPC/sterol liposomes, it was assumed that the binding location of probes did not change, and that the *in situ* environment around probes could be altered

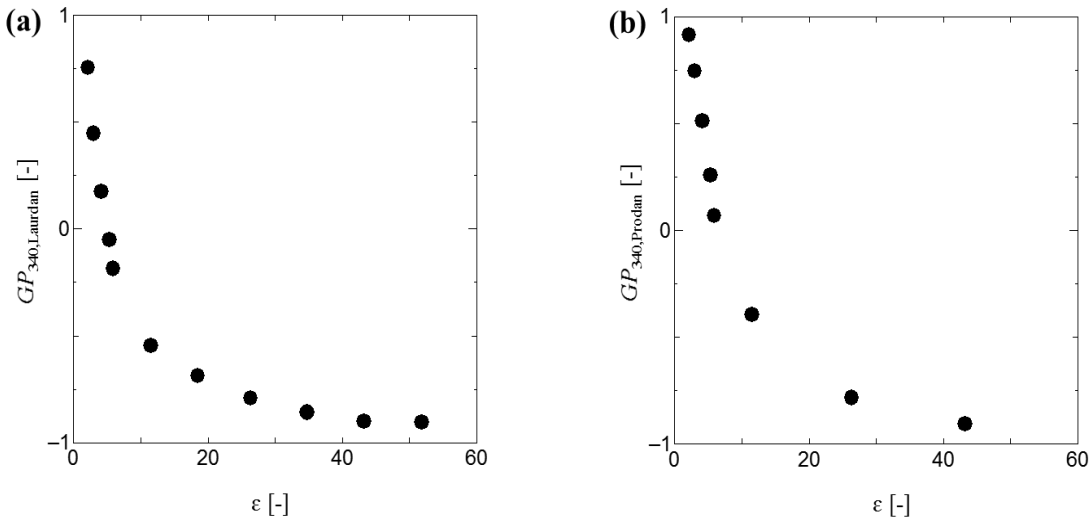

Fig. 2-4 $GP_{340,Laurdan}$ (**a**) and $GP_{340,Prodan}$ (**b**) values for 1,4-dioxane/water systems, as function of ε values.

depending on the type and amount of sterols. Hence, the variation in the membrane properties could be provided by the different interaction between DOPC and sterols. The location of Chol and Lan might be similar. The hydration in the membrane surface would be sensitive to the chemical structure of sterol and its interaction with DOPC.

3.2 Polar Environment of Liposome Membrane at the Hydrophobicity Region

Liposome membranes own a hydrophobic gradient in the vertical direction of membrane from the surface into inner membrane (Cevc, 1990), where the emission property of the fluorescent probe depends on the binding location in the membrane due to different surrounding environment. We have reported the binding location of DPH, Laurdan (Suga and Umakoshi, 2013; Hayashi et al., 2011) and ANS (Ishigami et al., 2015).

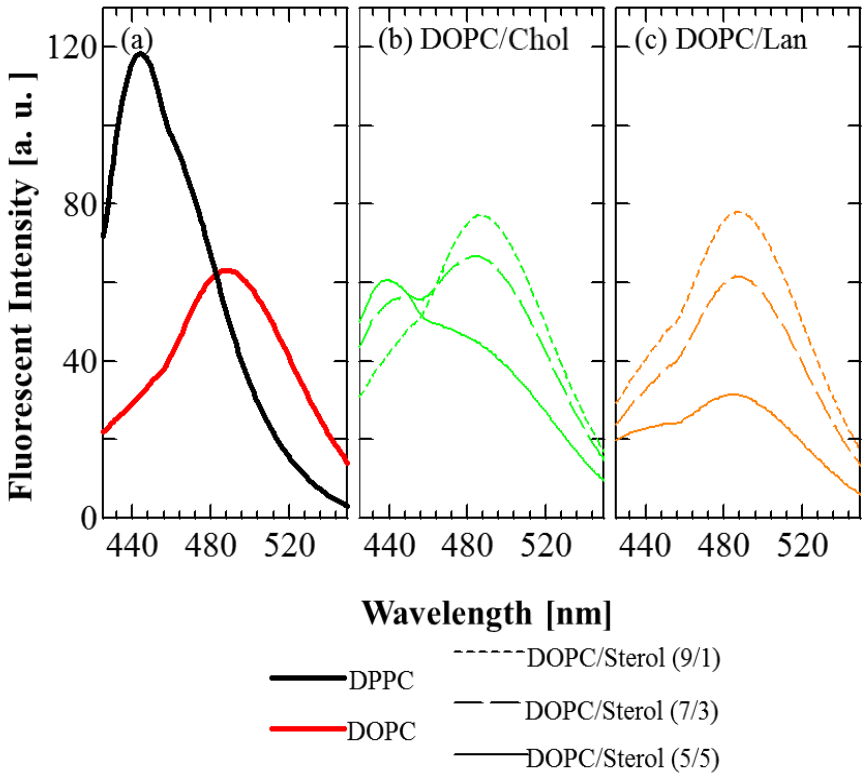

Fig. 2-5 Fluorescent spectra of Laurdan for DOPC and DPPC liposomes (**a**), for DOPC/Chol liposomes (**b**) and DOPC/Lan liposomes (**c**).

At first, Laurdan was used as a molecular probe to monitor liposome heterogeneity (Parasassi and Gratton, 1995; Suga and Umakoshi, 2013). Fluorescent spectra of Laurdan for liposomes were evaluated in **Fig. 2-5**. In the absence of sterols (**Fig. 2-5a**), DPPC showed the emission peak at 440 nm indicating the solid ordered phase (S_o), while the liquid disordered phase (L_d) membranes had peak intensity at 490 nm. Additionally, the membrane polarity ($GP_{340,Laurdan}$) was identified and shown in **Fig. 2-6 (a and b)**. The ordered phase, which was estimated by the Laurdan emission peak at 440 nm, was

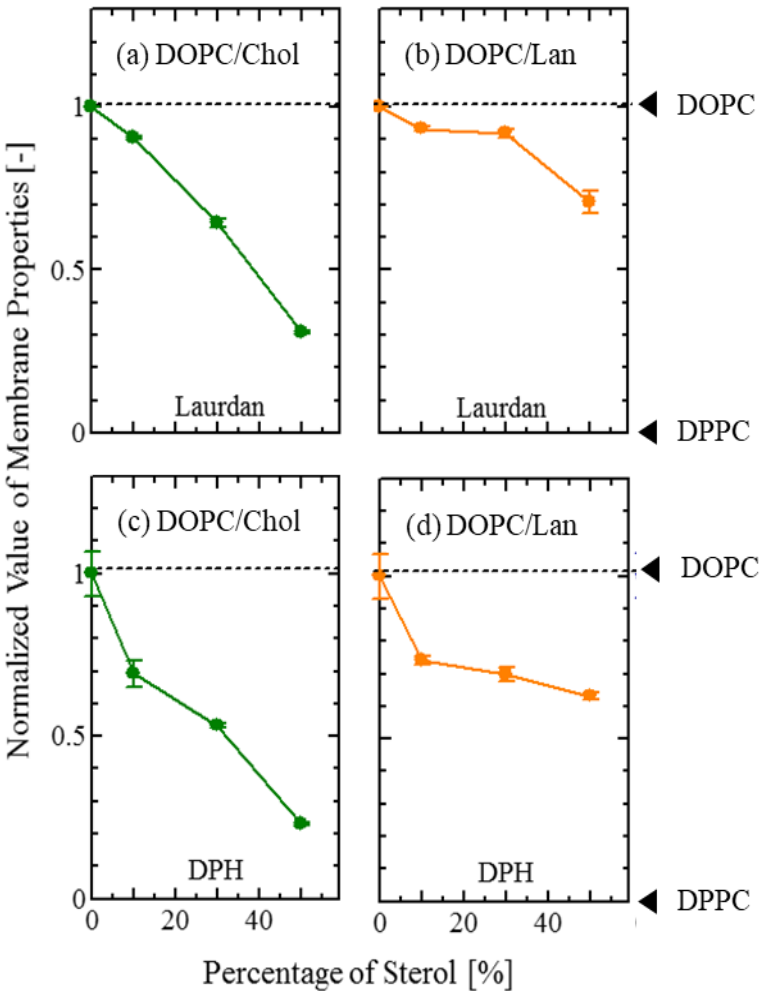

Fig. 2-6 Membrane polarity and fluidity at 37 °C investigated by Laurdan and DPH, respectively. Nomalized $GP_{340,Laurdan}$ values for (**a**) DOPC/Chol, (**b**) DOPC/Lan; normalized $1/P_{DPH}$ values for (**c**) DOPC/Chol, (**d**) DOPC/Lan. Each data was normalized according to **Eq. (2-5)**. Dotted lines represent the $GP_{340,Laurdan}$ and $1/P_{DPH}$ values for DOPC and DPPC liposomes as references.

observed in DOPC/Chol=(7/3) and DOPC/Chol=(5/5), while other DOPC/sterol liposomes showed only one emission peak at 490 nm. Moreover, the recorded fluorescent spectra of Laurdan in each liposome showed the phase transition of liposomes when Chol concentration was increased, indicating the role of Chol in altering the membrane properties. This indicates that the Chol successfully form the L_o phase in proportional to its concentration in DOPC liposome. In addition, DPH, a widely used fluorescent probe used for investigating inner membrane fluidity ($1/P_{DPH}$), localized almost exclusively in the hydrocarbon cores of the phospholipid membrane. Changes in fluorescence anisotropy of DPH in the intact membranes indicated the fluidity of the inner membranes; the $1/P_{DPH}$ value for each liposome bilayer membrane was calculated and compared as shown in **Fig. 2-6 (c and d)**. On the other hand, effects of Lan on the membrane properties in the hydrophobic regions were not as significant.

Based on our previous reports (Hirose et al., 2015; Suga and Umakoshi, 2013), the data for membrane fluidities ($1/P_{DPH}$, *x* axis) and membrane polarities ($GP_{340,Laurdan}$, *y* axis) were plotted for various liposomes as shown in **Table 2-1**, and the phase states also shown in the **Fig. 2-7.**

It was found that by using DPH fluorescent probe, the threshold value of $1/P_{DPH}$ for DPPC phase transition is estimated to be $1/P_{DPH}$ = 6, while the value for membrane

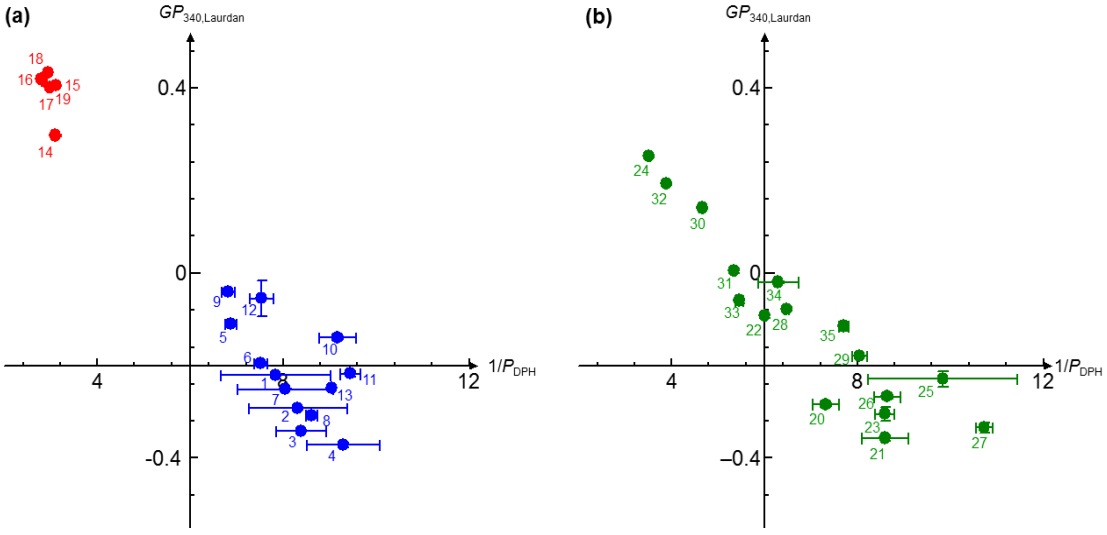

Fig. 2-7 Cartesian diagram for homogeneous liposome systems (**a**) and for heterogeneous liposome systems (**b**). See **Table 2-1** for assignment and details.

polarity determined by Laurdan is $GP_{340,Laurdan}$ = -0.2. Therefore, the threshold point in the Cartesian diagram is considered with $1/P_{DPH}$ = 6 and $GP_{340,Laurdan}$ = -0.2 (Cwiklik et

Table 2-1 Summary of the phase state and membrane properties for liposomes.

	Composition	T [°C]		Phase state	$1/P_{DPH}$	$GP_{340,Laurdan}$
(homogeneous system, l_d phase)						
1	DOPC	22	($>T_m$)	L_d	7.84	-0.22
2	DOPC	30	($>T_m$)	L_d	8.30	-0.29
3	DOPC	40	($>T_m$)	L_d	8.39	-0.34
4	DOPC	50	($>T_m$)	L_d	9.29	-0.37
5	POPC	19	($>T_m$)	L_d	6.88	-0.11
6	POPC	30	($>T_m$)	L_d	7.52	-0.19
7	POPC	40	($>T_m$)	L_d	8.05	-0.25
8	POPC	50	($>T_m$)	L_d	8.62	-0.30
9	DMPC	30	($>T_m$)	L_d	6.82	-0.04
10	DMPC	40	($>T_m$)	L_d	9.17	-0.13
11	DMPC	50	($>T_m$)	L_d	9.44	-0.21
12	DPPC	50	($>T_m$)	L_d	7.53	-0.05
13	bSM	50	($>T_m$)	L_d	9.04	-0.24
(homogeneous system. s_o phase)						
14	DMPC	19	($<T_m$)	S_o	3.10	0.29
15	DPPC	22	($<T_m$)	S_o	2.82	0.42
16	DPPC	30	($<T_m$)	S_o	2.79	0.41
17	DPPC	40	($<T_m$)	S_o	2.97	0.40
18	DSPC	25	($<T_m$)	S_o	2.95	0.43
19	bSM	25	($<T_m$)	S_o	3.11	0.40
(heterogeneous system)						
20	DOPC/DPPC=(75/25)	30			7.32	-0.28
21	DOPC/DPPC=(75/25)	50		L_d	8.59	-0.35
22	DOPC/DPPC=(50/50)	30			6.01	-0.09
23	DOPC/DPPC=(50/50)	50		L_d	8.59	-0.30
24	DOPC/DPPC=(25/75)	30			3.51	0.25
25	DOPC/DPPC=(25/75)	50		L_d	9.83	-0.22
26	DOPC/Ch=(90/10)	30			8.64	-0.26
27	DOPC/Ch=(90/10)	50			10.72	-0.33
28	DOPC/Ch=(70/30)	30			6.47	-0.07
29	DOPC/Ch=(70/30)	50			8.04	-0.17
30	DOPC/Ch=(50/50)	30			4.66	0.14
31	DOPC/Ch=(50/50)	50			5.34	0.004
32	DOPC/DPPC/Ch=(4/4/2)	30			3.88	0.19
33	DOPC/DPPC/Ch=(4/4/2)	50			5.45	-0.06
34	DOPC/SM/Ch=(6/2/2)	30			6.29	-0.02
35	DOPC/SM/Ch=(6/2/2)	50			7.70	-0.11

al., 2011). Obviously, the L_d phase liposomes appeared in the 1st and 4th quadrant ($1/P_{DPH}$>6), while the S_o phase liposomes appeared in the 2nd quadrant ($1/P_{DPH}$<6). The $GP_{340,Laurdan}$ values were >0 under T_m, and <0 above T_m. When a liposome shows similar properties to that in L_d phase, it could be in L_d phase (*disordered*). In similar manner, a liposome possessing similar properties to that in S_o phase, it could be in S_o phase (*ordered*). For heterogeneous liposome systems (green symbols plotted in (**b**)), some liposomes appeared between L_d-phase and S_o-phase clusters, indicating that they were in heterogeneous phases (L_d+L_o, L_d+S_o, *etc*.). It is notable that $1/P_{DPH}$ and $GP_{340,Laurdan}$ values could be insensitive to lipid/probe molar ratio (at least the range between 20/1 to 1000/1), indicating that the membrane properties evaluated by DPH and Laurdan can reflect the phase behavior of lipid bilayer systems.

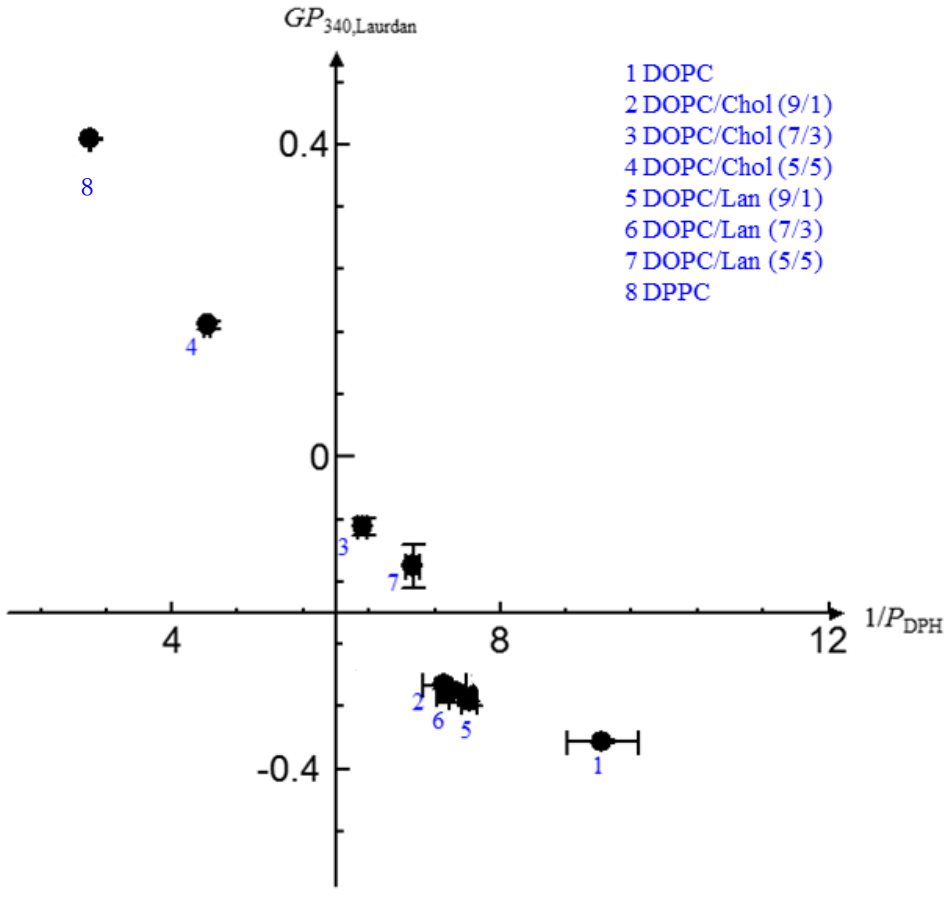

Fig. 2-8 Cartesian diagram for liposome modified with sterols based on $1/P_{DPH}$ and $GP_{340,Laurdan}$ values at 37 °C. When the liposome membrane becomes polar ($GP_{340,Laurdan}$ decrease), its fluidity becomes higher ($1/P_{DPH}$ increase).

A Cartesian diagram (Suga and Umakoshi, 2013) for the liposomes modified with 10, 30, and 50 mol% of sterols was prepared using data for membrane fluidity ($1/P_{DPH}$, *x*-axis) and polarity ($GP_{340,Laurdan}$, *y*-axis). Based on this Cartesian diagram for sterol-incorporated liposomes, the phase state of each liposome focusing on the hydrophobic region was determined as shown in **Fig. 2-8**.

The cross point of the *x*- and *y*-axes is the threshold point of the phase transition in S_o phase and L_d phase: using this method, the liposomes plotted in the 4th quadrant of the Cartesian diagram were considered be in the L_d phase. The data for phase state measurements of liposomes, obtained using DPH and Laurdan probes in our previous study, have been utilized in this study to estimate the boundary of phase state. In particular, a previous report showed that liposomes in the 1st quadrant such as DOPC/Chol=(7/3) could be in a heterogeneous phase, while liposomes in the 4th quadrant were in a homogeneous L_d phase (Suga and Umakoshi, 2013). DPPC and DOPC/Chol (5/5) in the 2nd quadrant were considered in ordered phases. The results also indicate that DOPC/Chol alters both the fluidity and polarity of membranes when increasing the amount of Chol from 0 to 50 mol%, indicating that Chol increases the order of the inner membrane. These results agree with those of previous reports regarding the effect of Chol on the membrane (Miñones et al., 2009). However, Lan slightly changed in both fluidity and polarity at 10 and 30 mol%, and GP_{340} values increase significantly at high concentration of Lan. Therefore, changes in both the polarity and fluidity of the interior of the membrane generally showed specific patterns for the presence of sterols, indicating the vital role of the sterol chemical structure in forming liposome membranes. The Cartesian diagram reflected variations in the membrane properties in the interior (or hydrophobic region) of the lipid bilayer, however, membrane characteristics in the hydrophilic region, the affinity of phospholipid molecules to sterols have not be inferred. Thus, the outer membrane was analyzed using other fluorescent probes with distinctive binding depths; this analysis is discussed in the next section.

3.3 Characterization of Hydrophilic Regions on the Membrane Surface

The surface membrane properties for DOPC/sterol liposomes were estimated by using TMA-DPH, ANS, and Prodan. Because no peak shifts of ANS or TMA-DPH were observed in DOPC/sterol liposomes, it was assumed that the binding location of probes did not change, and that the *in situ* environment around probes could be altered depending on the type and amount of sterols. The obtained data were normalized data are summarized in **Fig. 2-9**, **Fig. 2-11** and **Fig. 2-12**. Herein, the higher (z'~1) and lower (z'~0) z' values indicate the disordered and ordered membrane, respectively.

3.3.1 TMA-DPH Analyses of Membrane Fluidity of Liposome Surfaces

TMA-DPH binds to the phospholipid membrane surface, where it is assumed to embed into regions with a dielectric constant ε ~ 60.4 (**Fig. 2-3**). This indicates that TMA-DPH reflects membrane surface fluidity. The normalized $1/P_{\text{TMA-DPH}}$ values are shown in **Fig. 2-9** (**a**, DOPC/Chol; and **b**, DOPC/Lan). The results showed that the addition of Chol

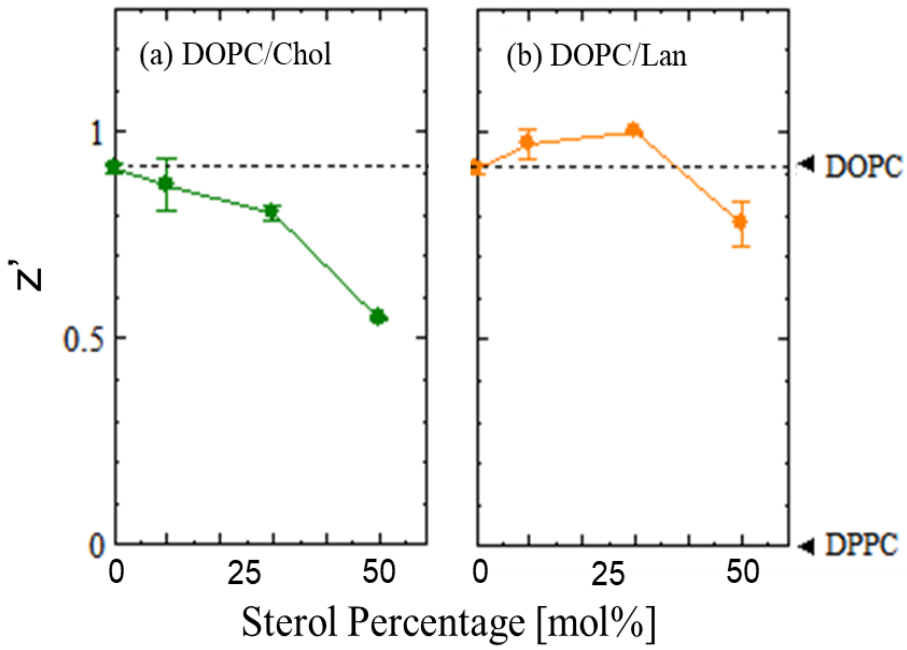

Fig. 2-9 Normalized membrane properties (z') in surface (hydrophilic region) investigated at 37 °C. The surface membrane fluidity, $1/P_{\text{TMA-DPH}}$ values for (**a**) DOPC/Chol and (**b**) DOPC/Lan.

reduced membrane fluidity, while Lan had little effect on membrane ordering. As illustrated in **Fig. 2-1**, Lan has two more methyl groups at 4C than the other sterols, which protect the β-surface of the planar steroid ring system and make the surface of the molecule rough. Thus, the molecular structure of Lan interferes with the interactions between phospholipid molecules in the hydrophilic region of the membrane surface, and then Lan reduces membrane order and increases fluidity by more than Chol.

3.3.2 ANS Analysis of Membrane Hydrophobicity

ANS shows low fluorescent intensity in polar environments and binds preferentially to hydrophobic cavities as shown in **Fig. 2-10** (Slavík, 1982**;** Stryer, 1965). Because the fluorescence emission peak of ANS depends on the surrounding hydrophobicity, the ANS emission peak wavelength can be used to monitor the microscopic environment around ANS in the lipid membrane. **Fig. 2-10** shows the fluorescent spectra of ANS 37 °C, for the liposomes in L_d phases (DOPC and POPC) and in S_o phases (DPPC and DSPC), where the emission intensity at 484 nm for DOPC liposome was defined as 100 [a.u.]. The results showed that all liposomes had the similar emission wavelengths (at 484 nm) but

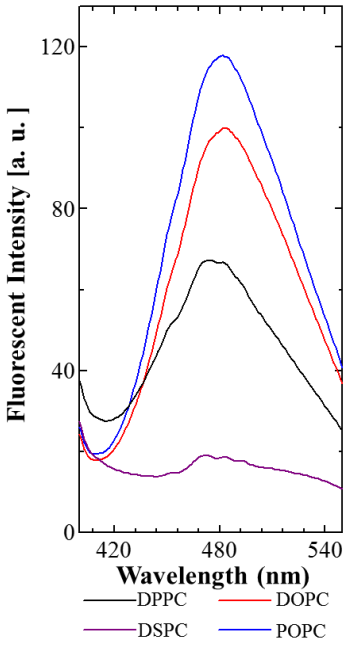

Fig. 2-10 Fluorescence spectra of ANS for different liposomes at 37 °C.

differences in intensities. It means that the same location of ANS but the different amount of bound ANS in the membrane.

Actually, the ANS probes bound to liposomes in L_d phases showed higher intensities than those in S_o phases. The ANS intensity in water was negligible. The liposomes in L_d phases have lower lipid packing densities (mean the headgroup area: 0.72 nm^2/molecule; more hydrophobic cavities), while the liposomes S_o phases have higher lipid packing densities (mean headgroup area: 0.48 nm^2/molecule) (Suga et al., 2013; Walde and Ichikawa, 2001). Thus, the lipid packing is critical factor for the degree in the exposure of hydrophobic core to water, where ANS can be distributed to such hydrophobic sites. Consequently, the amount of bound ANS will be higher and leads to the higher fluorescence intensity.

The location of ANS was estimated by emission peak (**Fig. 2-3**) (Ishigami et al., 2015): the binding location of ANS in DOPC liposome was regarded as the regions with dielectric constants ε ~ 26.5. It has also reported that ANS could be located near the phosphate group in the phospholipid membranes (Dhanikula and Panchagnula, 2008).

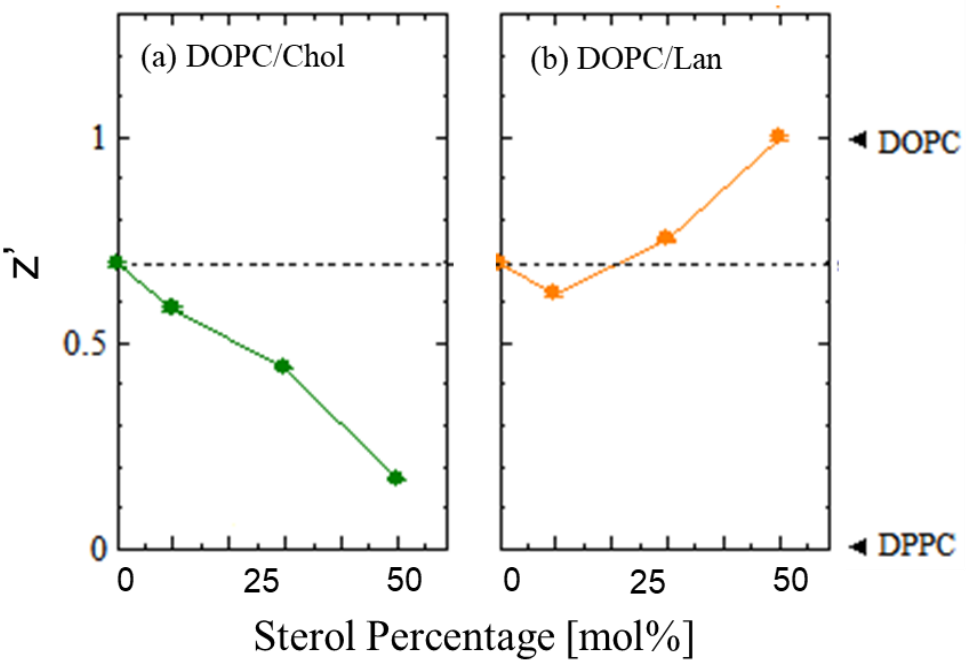

Fig. 2-11 Normalized membrane properties (z') in the surface hydrophobicity by ANS fluorescent probe at 37 °C, with (**a**) DOPC/Chol and (**b**) DOPC/Lan.

The membrane characteristics can be evaluated by comparing the fluorescence intensity of ANS at I_{484} as shown in **Fig. 2-3** and **Fig. 2-10**. **Fig. 2-11** shows the normalized I_{484} values for the disparity of ANS fluorescent intensity at 484 nm for DOPC/Chol and DOPC/Lan. In general, an increase in the percentage of Chol led to the increase of inner membrane packing. On the other hand, it is reported that the DOPC/Chol liposome (30 mol% Chol) rather decreased the packing with an increasing of the hydration dynamics near membrane surface (Mannock et al., 2006). Based on our result, the effects of 10 mol% of sterols raised the ANS fluorescent intensity, while 50 mol% of sterols decreased the intensity. This indicates that sterols and phospholipid molecules strongly interacted and the hydrogen bond network was formed at the membrane surface, when the higher amount of sterols are existing in the membrane. This can be explained by the differences in the chemical structures of each sterol at the surface region. Because the interaction between Lan and DOPC in the surface area is weaker than that of other sterols, the surface becomes flexible and contains many hydrogen bonds. Thus, it prevents the attack of ANS deeper into the membrane and leads to lower fluorescent intensity. This explains why Chol made the membrane more hydrophobic than Lan.

3.3.3 Prodan Analysis of Surface Membrane Polarity

The fluorescent intensity of Prodan in water was lower enough, as compared to that in liposome systems. Thus, the partitioning of probe in water hardly influences on the Prodan spectra in the presence of liposomes (Krasnowska et al., 1998; Cwiklik et al., 2011). By identifying the location of Prodan in the DOPC lipid membrane (**Fig. 2-3**) (Parasassi and Gratton, 1995; Cwiklik et al., 2011), the ε value around Prodan was estimated to be 43 in the DOPC membrane, indicating that Prodan binds to deeper (hydrophobic) regions in the membrane than TMA-DPH. Depending on the different fluorescent intensity of Prodan in liposomes and water systems (**Fig. 2-12**), the $GP_{340,\mathrm{Prodan}}$ values were calculated and normalized and are shown in **Fig. 2-13**. The normalized values for DOPC mixed with Chol ranged from 0 to 50 mol%, demonstrating that Chol increases membrane polarity, while DOPC/Lan membranes became hydrophilic around the Prodan-binding area. The structure of Lan contains one methyl group at 14C

that protects the α-face, whereas Chol contains none. Thus, Lan makes the membrane rougher and slightly bent compared to the effects of Chol (Mannock et al., 2006).

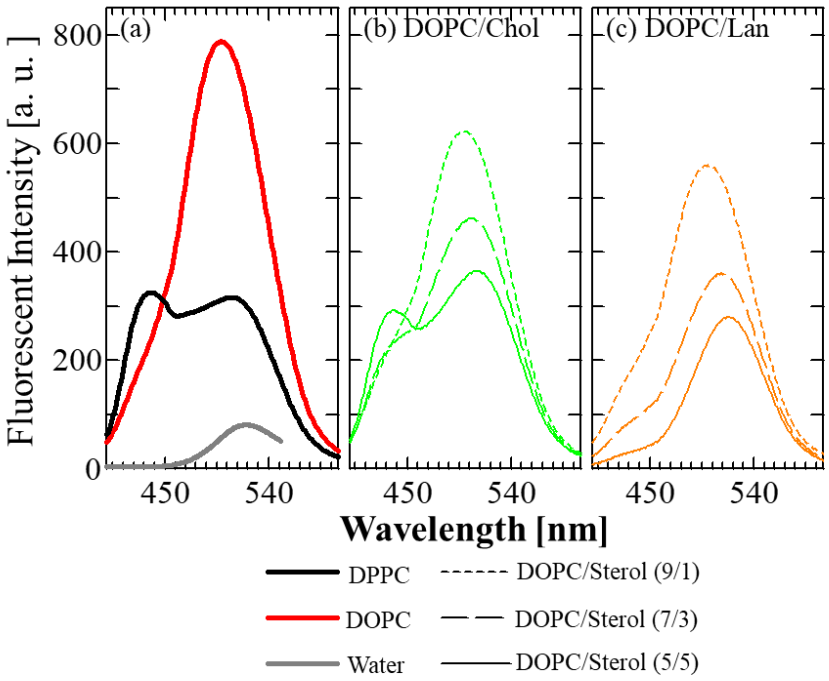

Fig. 2-12 Fluorescent spectra of Prodan in DOPC, DPPC liposomes and water (**a**), in DOPC/Chol liposomes (**b**) and DOPC/Lan liposomes (**c**).

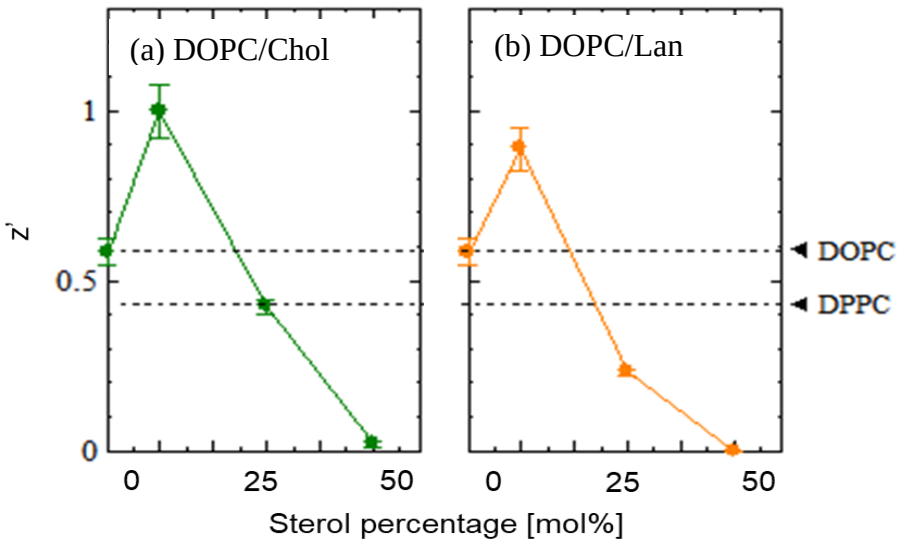

Fig. 2-13 Normalized membrane properties (z') of polarity in surface (hydrophilic region) investigated at 37 °C. The surface membrane polarity, $GP_{340Prodan}$ values for (**a**) DOPC/Chol and (**b**) DOPC/Lan.

4. Summary

In summary, cooperation between sterols in the phospholipid membranes changed the basic characteristics of the membranes from the surface to the interior. The effect of sterols on the membrane properties were analyzed using the fluorescent probes such as TMA-DPH, ANS, Prodan, Laurdan, and DPH. Although the sterols had similar molecule structures, our results revealed that each type of sterol had different and typical effects on each part of the membrane. **Fig. 2-14** summarizes the effect of 10 and 50 mol% sterols in DOPC membranes, wherein the normalized values of the surface membrane characteristics, such as membrane fluidity (by TMA-DPH), membrane hydrophobicity (ANS), and membrane polarity (Prodan), are compared. Given the different phase states of disordered liposomes (e.g., DOPC) and ordered liposomes (e.g., DPPC), the normalized data for DOPC and DPPC were considered as two landmarks, which is useful in comparing the properties of DOPC membranes modified with the sterol variants Chol and Lan. Compared to the DOPC membrane itself, liposomes modified with 10 mol% sterols such as Chol and Lan showed distinct properties. The results for these liposomes suggest that these membranes are more flexible on the surface and condensed in the

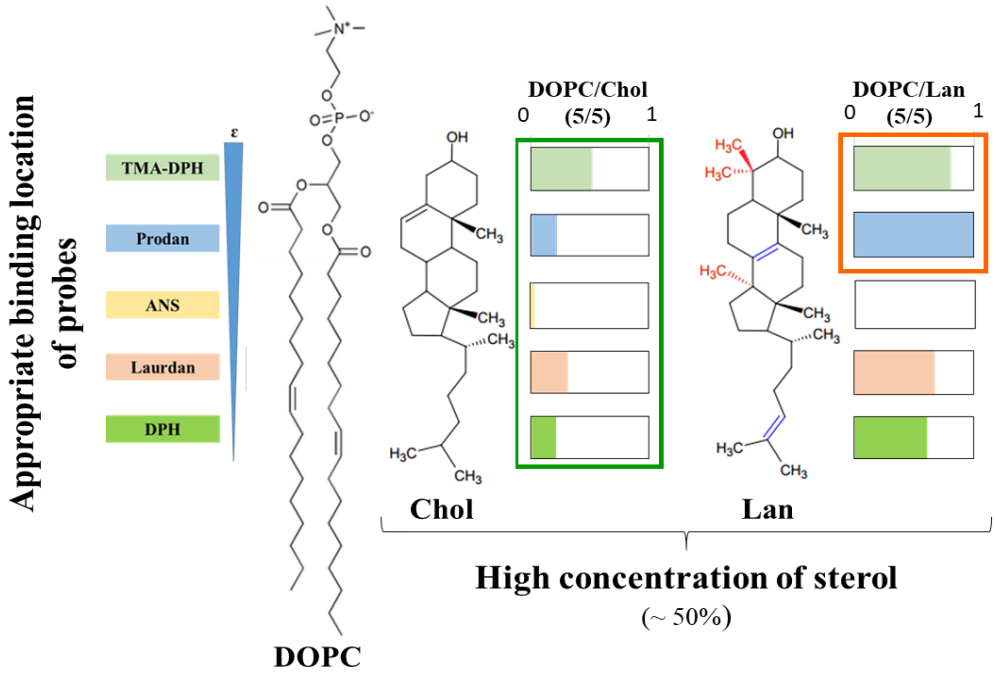

Fig. 2-14 Variation of membrane property chart for each kind of DOPC/sterol liposomes.

deeper region. After increasing the amount of each sterol to 50 mol%, the membrane property chart indicated that Chol condensed the membrane to the greatest extent in all areas, indicating that it interacted tightly with phospholipid molecules to decrease fluidity and increase hydrophobicity. Although Lan also condensed the membrane, the degree of its influence was lower than that of Chol, except at the binding location of Prodan which showed that the membrane in this region was more hydrophilic than with DOPC.

Chapter III

Thermodynamic Characteristics of Mixed Sterols/DOPC Monolayers on Water Subphase

1. Introduction

Cells are highly organized with multiple functional units or organelles defined by one or more lipid membranes. Individual membrane is specialized by containing specific proteins and typical lipid components that enable it to perform the unique role of that cell or organelle. Lipids are very diverse in both their respective structures and functions, and cells exquisitely control membrane composition. One intriguing issue is the specific role of lipids in modulating the physical properties of membranes (Nichols-Smith et al., 2004).

Lipids bilayers are well-known as highly complex structures of great importance for cells, because of their protective role and providing an environment for many important biochemical processes. Phospholipids and sterols have been found as major constituents of membranes surrounding eukaryote cells. The nature of phospholipids, their structural diversity, and content in bilayer determine the properties of the membrane. Whereas, Cholesterol (Chol) which is popular in animal is synthesized from Lanosterol (Lan). These sterol molecules that is of special significance as a regulator of membrane parameters, they can modulate membrane properties and influences the organization of the other lipid by for example changing their ordering, available area, and formation of domains of characteristic composition. However, despite numerous studies, it is still unclear how exactly sterols act and interact on membrane phospholipids. Several models have been proposed to describe the behavior of these compounds in mixed systems in considering only the issue of sterol/phospholipids interactions, such as the super lattice model (Somerharju, 2002), the condensed-complexes model (McConnell and Radhakrishnan, 2003), the umbrella model (Huang and Feigenson, 1999), and others.

McConnell and co-workers proposed a thermodynamic model of condensed complexes to explain a non-ideal behavior of Chol−phospholipid mixtures. Thus, the

existence of stable complexes was defined between Chol and respective phospho- and sphingolipids. The condensing effect of Chol on phospholipid membranes was predicted as comparing the occupied average area with expected area from the ideal mixing, based on the formation of these complexes (Ali et al., 2007; McConnell and Radhakrishnan, 2003; Somerharju, 2002). It is indicated that lipids and sterols can be regularly distributed into super lattices in bilayer (Chong et al., 2009). And the regular arrangement in phospholipid bilayers is stimulated by for example steric effects or geometric complementarity, charge−charge repulsion, or hydrophobic effects (Somerharju, 2002; Ali et al., 2007). According to super lattice models, the key role in Chol−phospholipid interactions play long-range forces between molecules of Chol, and it has been discussed in detail in a review by Somerharju *et al.* (Somerharju, 2002). Similar to the super lattice model, the umbrella model also predicted the regular distribution in Chol−phospholipid bilayers (Huang and Feigenson, 1999). In addition, the distribution of sterol in low and high concentrations and the effect of sterols on the membrane properties has been revealed, by using several fluorescent probes which bind from the outer into inner leaflets of membranes. Particularly, in unsaturated membrane, at 10 and 30 mol% Lan, the insignificant ordering effect of Lan in unsaturated lipid membrane was revealed, but multi focal fluorescent probes cannot indicate how Lan interact with membranes.

Liposomes or phospholipid bilayer have long been used as model membranes for studying the characteristic of the biological membranes and then utilizing for many applications as in pharmacy and cosmetic. However, it is required that liposome products must remain stable for a period of time under ambient storage conditions. Actually, liposomes are impressionable to aggregate and lead to the changes of vesicle sizes during the preservation. Additionally, the substance encapsulated by bilayer membranes could produce side effects. Under such these circumstances, liposome structures are obviously necessary to maintain the stable membrane until they move to the target destination. Therefore, the stability of liposomes which is always of huge interest, especially in pharmaceutical and pharmacological aspects and depend on their physicochemical properties as the interaction of constituents in the membranes (Sekiguchi et al., 1995). Monolayers of amphiphilic molecules which are established at aqueous environments as air/water interfaces, are of interest in a variety of disciplines (MacDonald and Simon,

1987). Specifically, the interest in physics and chemistry is in studying the magnitude and origin of the molecular interactions of a single layer of complex molecules positioned between two fluids (Gershfeld, 1976), while in biology, Gorter and Grendel were known as the first authors proposing that the bilayer as the foundation of bio-membranes (Gorter and Grendel, 1925). This conclusion was found on an entirely compression of lipid monolayer, hence it remains the relationship between molecular packing in monolayer and that in bilayers.

Apart from the mechanism of Chol−phospholipids interactions, the problem of the magnitude of the condensing effect of Chol on various membrane phospholipids also requires further analysis. Numerous studies on this subject (Gershfeld, 1976; Presti et al., 1982; Radhakrishnan and McConnell, 1999; Epand et al., 2002; Su et al., 2007; Bennett et al., 2009; Wydro et al., 2011) have indicated the relationship between the structure of chain(s) of phosphatidylcholines (PCs) and the magnitude of the area condensation, especially with reference to the sterol concentration and their derivatives still require discussion. Therefore, by using the monolayer technique, as Langmuir balance, thermodynamic properties of sterol-incorporated monolayer membrane can be investigated. The schematic of illustration for the analysis of membrane was shown in **Fig. 3-1**. Moreover, it is reported that at the high surface pressure, 30 mN/m, the properties of monolayer is similar to bilayer membrane (Sennato et al., 2005). Consequently, the monolayer analysis could be supported for analyzing the membrane properties.

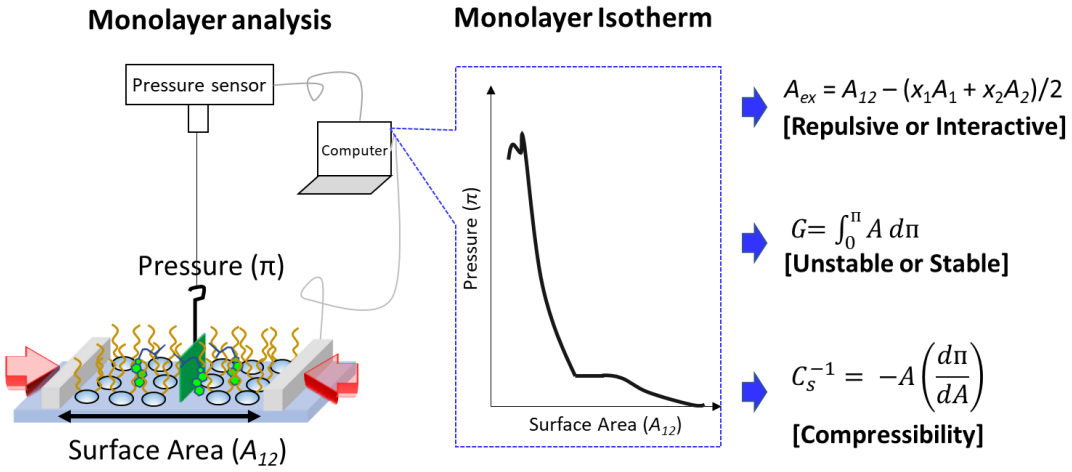

Fig. 3-1 The schematic of illustration for the analysis of monolayer membrane.

As reported in previous study that the membrane properties such as fluidity, polarity and hydrophobicity were carefully investigated by using several fluorescent probes which bind vertically from the surface into the inner membranes. However, fluorescent probes are well-known as indirect communicator depending on the surrounding elements as temperature, pH, etc…, and the insignificant ordering effect of Lan under 50 mol% were unable to distinct. To investigate a potential interaction between sterol and phospholipid molecules, pressure-area (π-A) isotherm were studied.

2. Materials and methods

2.1 Materials

1,2-Dioleoyl-*sn*-glycero-3-phosphocholine (DOPC) were purchased from Avanti Polar Lipids (Alabaster, AL). Chol and Lan and were synthetic products of high purity and purchased from Sigma-Aldrich (St. Louis, MO, USA). These products were stored in a refrigerator without the access of light. Other chemicals were purchased from Wako Pure Chemical Industry Ltd. (Osaka, Japan) and were utilized without further purification.

2.2 Monolayer preparation

Spreading solutions were prepared by weighting a proper amount of investigated compounds on the analytical balance and then dissolving each of the compound in chloroform solution at room temperature. Mixed solutions were prepared from the respective stock solutions of both compounds with the initial concentration of 4 mM. The final concentration of working solutions is 0.4 mM. Molecules in working solutions were spread on water subphase in the Langmuir trough. Surface pressure-area (π-A) isotherms were recorded with a KSV (Finland) Langmuir trough with the total area of 76.5 cm^2, equipped with two movable barriers, and placed on an anti-vibration table. Surface pressure (π) was measured with the accuracy of ±0.1 mN/m using a Wilhelmy plate made from platinum foil as a pressure sensor. After spreading, monolayers were left for 10 min to ensure the solvent evaporation, and afterwards the compression was initiated with a barrier speed of 3-4 $Å^2$ $molecule^{-1}$ min^{-1}.

2.3 Analyses of isotherms data

The compressibility modulus, C_s^{-1}, which reflects the physical phase state of membrane was calculated as the following equation (**Eq. 3-1**):

$$C_s^{-1} = -A\left(\frac{d\pi}{dA}\right) \quad \textbf{(3-1)}$$

where *A* is the mean area per molecule at specific surface pressure π.

The behaviors of sterols in mixed films were determined based on the excess area per molecule (A_{ex}) in the mixed monolayer calculated as the following **Eq. 3-2**:

$$A_{ex} = A_{12} - (A_1 x_1 + A_2 x_2) \quad \textbf{(3-2)}$$

where A_1, A_2 are mean area per molecule and x_1, x_2 are molar fractions of DOPC and sterols, respectively, at the given surface pressure. A_{12} is mean area per lipid molecule in the mixed system. Additionally, partial molecular areas of PCs in the mixed monolayers were calculated at π = 30 mN/m by a procedure in which tangents to the area-composition curve are extrapolated (Sennato et al., 2005). To analyze the interaction of sterol and phospholipid molecules in each binary monolayer, the Gibbs free energy of mixing (ΔG_{mix}) was calculated by **Eq. 3-3**:

$$\Delta G_{mix} = \Delta G_{ex} + \Delta G_{ideal} \quad \textbf{(3-3)}$$

with $\Delta G_{ex} = \int_0^{\pi} A\, d\pi = \int_0^{\pi} A_{12} - (A_1 x_1 + A_2 x_2) d\pi$
and $\Delta G_{ideal} = kT(x_1 ln x_1 + x_2 ln x_2)$

where *k* is the Boltzmann constant and *T* is temperature

3. Results and discussion

3.1 Surface pressure – area isotherms of sterol-DOPC mixtures

Compression isotherms for pure components of sterols and phospholipid were recorded and shown in **Fig. 3-2**. For unsaturated phospholipid like DOPC, the isotherm gradually increased, where no phase transition was observed. Compare to other sterols, the area per molecule of DOPC was largest at the range of 0 – 30 mN/m, it could reflect

the bulky head group of DOPC and kink structures of fatty acid chains including double bond. It is the indicated that the isotherm curve of DOPC was appropriate to the liquid phase at 28 ^{o}C. Because of the smaller molecule structures, Chol and its derivatives also shown the isotherms with relatively smaller headgroup, as compared to DOPC. Firstly, the isotherm of Chol started to raise sharply at 37 Å^2 /mol, while Lan showed higher lift-off area, which can be evident for bulky structure of Lan as compared to Chol. This observations indicate that the addition of methyl groups and double bonds created the cumbersome structures, increased the tilt of molecules with respect to the monolayer plane and reduced the packing effectiveness (Wydro et al., 2011).

According to **Fig. 3-2,** Lan isotherm shown the less tight packing molecules as compared to Chol. It could indicate that the best bulky head group of Lan with the addition of two methyl groups resulted in the extended surface and then leads to the arrangement of free Lan molecules occupying the larger area than Chol.

To understand the effect of each sterol in the surface of unsaturated phospholipid membrane, the mixtures of sterol with DOPC in the range of sterol percentage from 0 to 10, 30 and 50 mol% were prepared and the isotherms for mixed systems were shown in **Fig. 3-3**

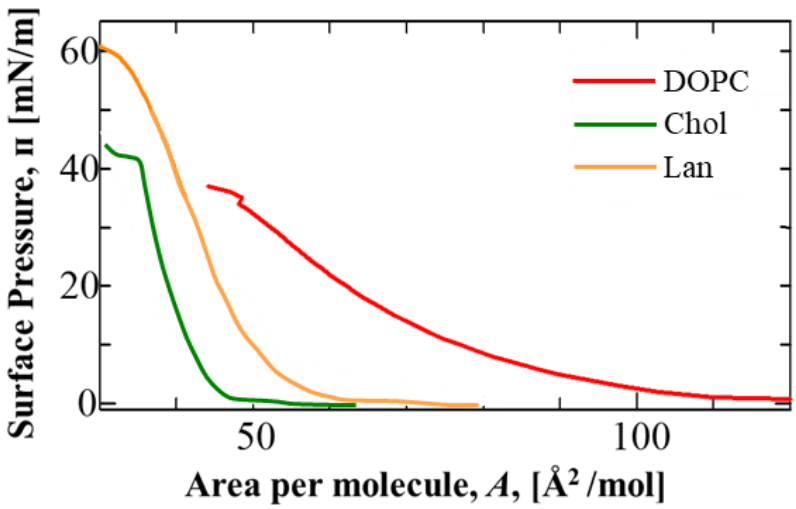

Fig. 3-2 Surface pressure-area (π-A) isotherms for pure component lipid films.

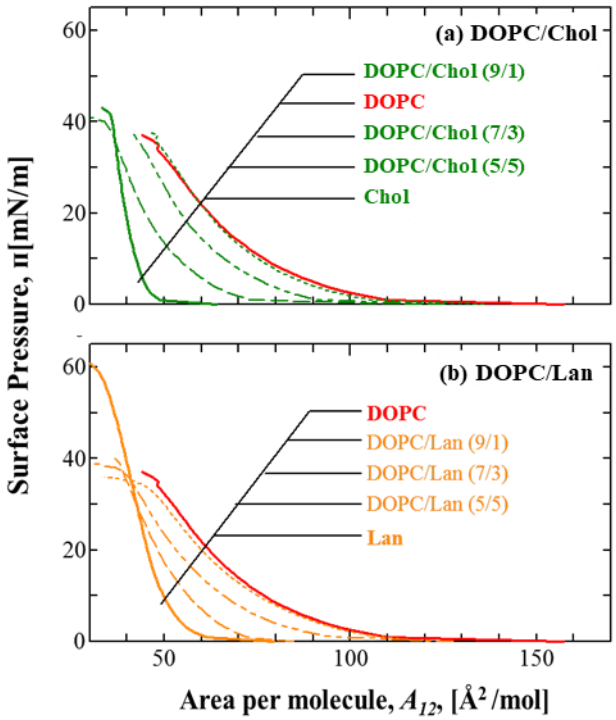

Fig. 3-3 Surface pressure-mean molecular area (π-A) isotherms for mixed monolayer of DOPC with Chol (**a**) and Lan (**b**).

By increasing the surface pressure (π), the compression isotherms for DOPC/Sterol mixture systems were recorded and shown in **Fig. 3-3**. When DOPC liposome was modified with sterols and the amount of sterols was adjusted from 10 to 30 and 50 mol%, the isotherms for each sterol were obtained. All these isotherms changed smoothly from the initial area until the area of collapse phase states. This meant that the packing of membrane changed and phase states of these mixture monolayers existed in the same states or no phase transition could be observed during the increase of pressure.

Especially, clear compression isotherms were obtained for Chol and Lan at 10, 30 and 50 mol%. The curve of these isotherms became to widen with the decrease of sterol amounts. These above results indicated Chol and Lan had more strong effect in the packing of membranes. These results also agree with the effect of sterols in the surface of membrane, such as in the region of ANS fluorescent probe binding (as shown in **Fig. 2-11**). Along with these clear shifted curves of DOPC with Chol and Lan mixtures, it is

indicated that they had more effectiveness in the packing or ordering of the surface membrane.

To gain the further insight into the specific effect of these sterol at the interface region of membrane, the physical state of membrane could be revealed by calculated the elastic moduli.

3.2 Effect of sterol type and content on membrane compressibility

The compressibility of DOPC-sterol membranes was compared by analyzing elastic moduli, C_s^{-1}, which reflects the interaction of molecules in mixed films and calculated following the **Eq. (3-1)**. It is indicated that the characteristic of lipid monolayer membrane correlated with the properties of bilayer membrane at the high surface pressure (Marsh,

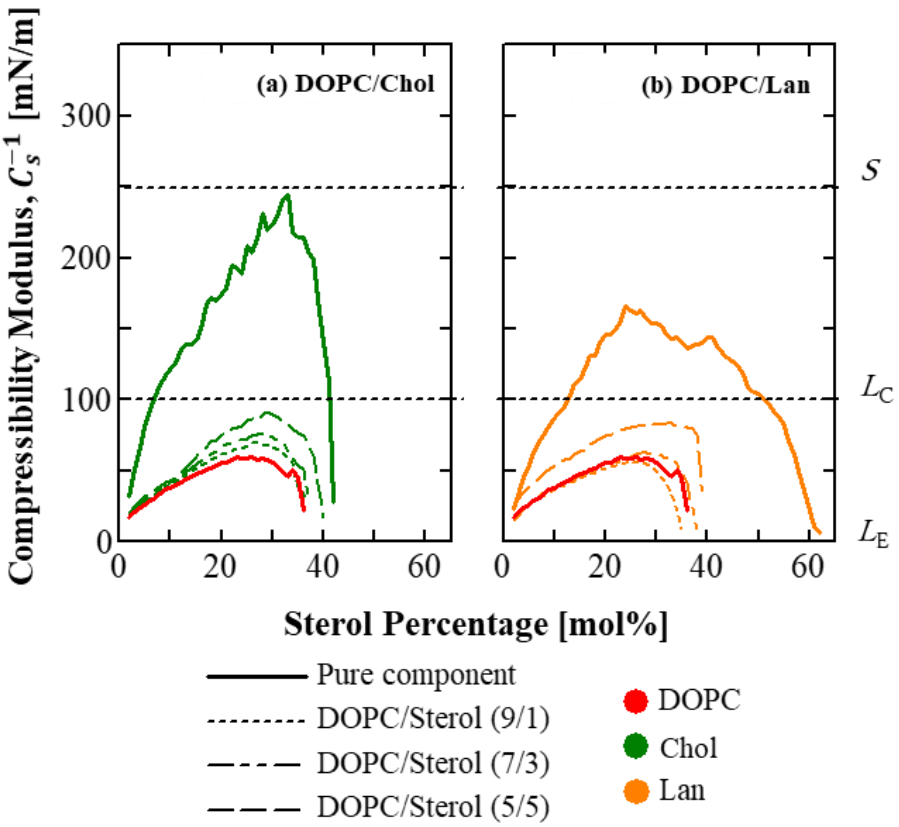

Fig. 3-4 Compression modulus vs. sterol percentage in DOPC monolayer with (**a**) DOPC/Chol and (**b**) DOPC/ Lan.

1996). Therefore, the further analysis of these obtained results has been performed at π = 30mN/m and the values of C_s^{-1} at 30 mN/m were also indicated in **Fig. 3-4**. Results revealed that pure sterols displayed the distinctive values, such as the highest compression moduli was observed by Chol, while followed by Lan. Both of them had similar peaks at surface pressure around 30 mN/m, the values of C_s^{-1} decreased with increasing pressure. At 30 mN/m, the compressibility modulus for Chol and Lan mixtures increased gradually, however, the values of compression for DOPC/Chol mixtures appropriating to each mol fraction (0.1, 0.3, 0.5 and 1.0) were always higher than that of Lan. According to Davies and Rideal (Davies and Rideal, Interfacial Phenomena 1963), the C_s^{-1} values are smaller than 100 mN/m, it means that the physical state of film in liquid-expand phase (L_E) and that values shift from 100 mN/m to 250 mN/m like liquid-condense phase (L_C), and over than 250 mN/m is solid phase (S). Therefore, all the mixtures of sterols from 10 to 50 mol% still keeps membranes in L_E, but in different scale of packing. It meant that Chol have more effect in condensing membrane than Lan. These distinctive effects of sterols in the physical phase state of membrane could be explained based on the differences in the configuration of each sterol. To acquire more detail about the interaction of sterols and phospholipids and the stability of films, the excess area and Gibbs free energy were calculated.

3.3 Excess area of mixed monolayer

The magnitude of the condensing effect of sterols on phospholipid monolayers could be verified with the excess area per molecules (A_{ex}). As shown in **Fig. 3-5**, the disparity between the ideal area (A_{id}, dotted line) and the mean area (A_{12}, solid circle) is defined as the excess area, A_{ex}, of the mixed film at 30 mN/m (**Eq. 3-2**). The negative values of excess area mean the ordering effect, while the positive values indicate the expanding of lipids in the membrane. It was clearly shown that Chol and Lan had the ordering effect in unsaturated membrane.

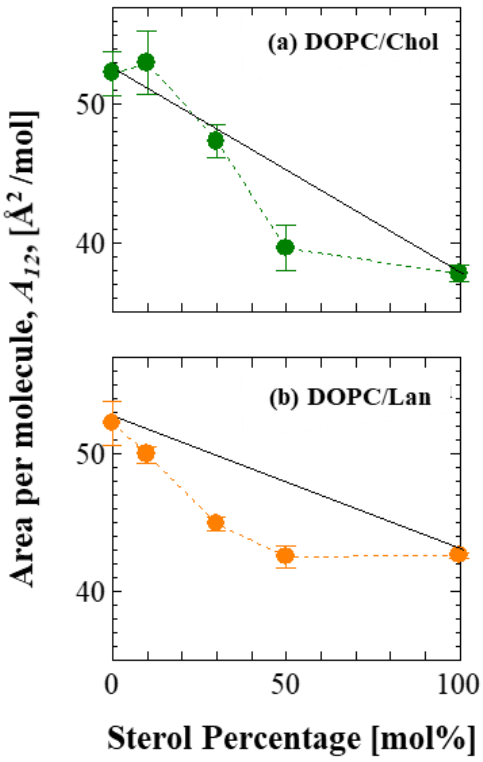

Fig. 3-5 Average molecular area of (**a**) DOPC/Chol and (**b**) DOPC/ Lan. Solid lines represent ideal area at each missing ratio.

3. 4 The Gibbs free energy

Following **Eq. 3-3**, the Gibbs free energy of mixing was calculated for each mixed monolayer at 30 mN/m surface pressure (**Fig. 3-6**). Obviously, the presence of sterols with appropriate amount like 10, 30 and 50 mol%, resulted in all negative values of ΔG_{mix}. It meant that all mixed systems became stability or miscibility, but their scales were distinctive. It is revealed that Chol and Lan had the similar tendency when increased their amounts up to 50 mol%. Specifically, with the 10 and 30 mol% of Chol, it shown the more stable membrane than the same amount of Lan. However, Lan shown the most stable membrane at 50 mol% with the lowest values for ΔG_{mix}. It could be the evidence for why Lan and Chol are rich in mammalian cell membranes, and the low amount of Lan does not affect membrane properties significantly.

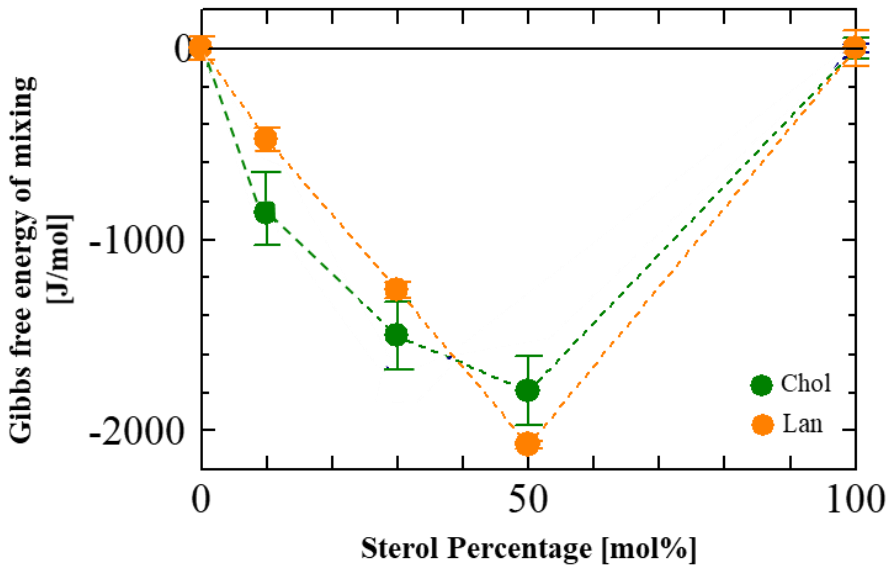

Fig. 3-6 Gibbs free excess energy of mixed monolayers at π = 30 mN/m.

The interaction forces between Chol and phospholipids, the hydrogen bonding and van der Waals, stabilized the membrane and enhanced its ordering in nonpolar region and subsequently increased the packing density of monolayers, as resulted in the decreased of excess area (Sabatini et al., 2008). It is also pointed out that the accommodation of Chol underneath the hydrated phosphocholine head group, known as the umbrella effect (Patzer et al., 1978; Holopainen et al., 2004). The elastic modulus of DOPC/Chol mixtures (**Fig. 3-4a**) were also evident the packing effect when increased the sterol amount from 0 to 50 mol% and the presence of Chol indicated the stable membrane (**Fig. 3-6**). The interaction of Chol with phospholipid molecules were speculated via the values of excess areas (**Fig. 3-5a**) and the expanding effect occurred at 10 mol% Chol, while 30 and 50 mol% Chol shown the condensing membranes. Thus, the figure of sterol attributed in unsaturated membrane was constructed like **Fig. 3-7** with low and high concentration of sterols.

Similar with the condensing effect of Chol, Lan also shown the clear ordering effect in DOPC monolayer, revealed via the values of C_s^{-1} in **Fig. 3-4b**. The elastic modulus shown that the mixed monolayers of Lan and DOPC shifted from the low elastic value of pure DOPC into high value of pure Lan. In another words, Lan also showed a potential to alter the phase state from the L_E to L_c, when increased Lan from 0 to 50 mol%. As

supported in **Fig. 3-5b**, the gradual increase of Lan amount led to the gradual decrease of the A_{ex} values, it was indicated that Lan had the strong interaction with DOPC molecules and led to the smaller membrane, as compared to the ideal mixtures with respective amount of Lan and DOPC. Moreover, these mixed systems also shown the high stability along with the high amount of sterols (**Fig. 3-6**).

In contrast to the stiffer structure of Chol, the addition of methyl at the benzene ring of Lan resulted in the cumbersome head and led to the distinctive effect in ordering unsaturated membrane. Obviously, pure Lan shown the largest area as compared to Chol (**Fig. 3-2**), but the mixture of Lan with DOPC proposed the almost smaller mean area than Chol at the same amount. However, the higher interaction of Lan with DOPC was revealed by the disparity of mean area and ideal area of mixed systems than Chol at the same amount. Therefore, it could be assumed that Lan had the high interaction between DOPC-sterols and sterol-sterols. Whereas, Chol has less interaction with DOPC (at 10 mol% of Chol) but the higher amount could lead to the aggregated sterols and could be form the domain at 30 mol%, and the increase to 50 mol% of Chol shown the more ordering membrane with smaller mean area. It also agrees with the results from the analysis of bilayer systems of DOPC and sterols by fluorescent probes, especially, DPH and Laudran fluorescent probes. For examples, the presence of Chol from 10 to 50 mol%, it changed the membrane from the liquid phase into the condensed phase. Finally, the model of sterol distribution was constructed and shown in **Fig. 3-7**.

In summary, both Chol and its derivatives like Lan impacted on the packing effect of membranes, but in different scales. The results from the elastic moduli proved that the increase of sterol amounts lead to the change phase state of mixed monolayers from the liquid expanding to near the liquid condense. Subsequently, the interaction of Chol and Lan with membranes were revealed via the excess area per molecules during the compression process. Finally, the all of them stabilized the mixed membrane when increased the amount up to 50 mol%. These results also agreed with our previous about the effect of these sterols in unsaturated phospholipid membranes, such as Chol had more effect in condensing membrane, while lesser effects were observed in Lan.

4. Summary

The condensing effect of sterol is accompanied by the ordering effect, manifests in the contraction of area per lipid molecules in the system of phospholipid incorporated with sterol. The magnitude of this effect was measured by calculation of the excess areas per lipid for mixed systems at high surface pressure, around 30 mN/m. At the minimum of A_{ex}, the condensing effect reaches the maximum.

It was found that in the case of saturated phospholipid molecules, the strongest condensation was observed as a minimum of A_{ex} at 30 % of Chol (Wydro et al., 2011). While, in this research, it is clearly shown that the strongest ordering effectiveness existed at 50 % of Chol in unsaturated phospholipid molecules, such as DOPC. It could be explained that the presence of double bond induces the bend of the chain, then leads to a limited ability to be tightly packed and thus inhibits the effect of sterol. Consequently, it required the higher concentration of Chol in condensing unsaturated membranes. The excess Gibbs free energy was also calculated to indicate the interaction between molecules in the mixed system or the stability of membranes. With the increase of Chol amount, the as reduced. It means that the increase of stable characteristic of membrane. Or in another words, the high affinity of Chol with DOPC molecules.

Compared to Lan, the condensing effects were indicated but quite difference with Chol. In particular, the A_{ex} values of DOPC/Lan mixture were almost negative at pressure below 30 mN/m, while an increase of compression modulus was obtained at Lan 50 mol%. Lan results provoked that the increase of Lan into 50 mol%, had more effect in condensing membrane as determined by the decrease of excess area, along with the reduced excess Gibbs free energy. While, the excess Gibbs free energy analysis revealed a favorable interaction between DOPC and Lan at high concentration which could be responsible to weak but sure ordering effect of Lan in unsaturated lipid bilayer.

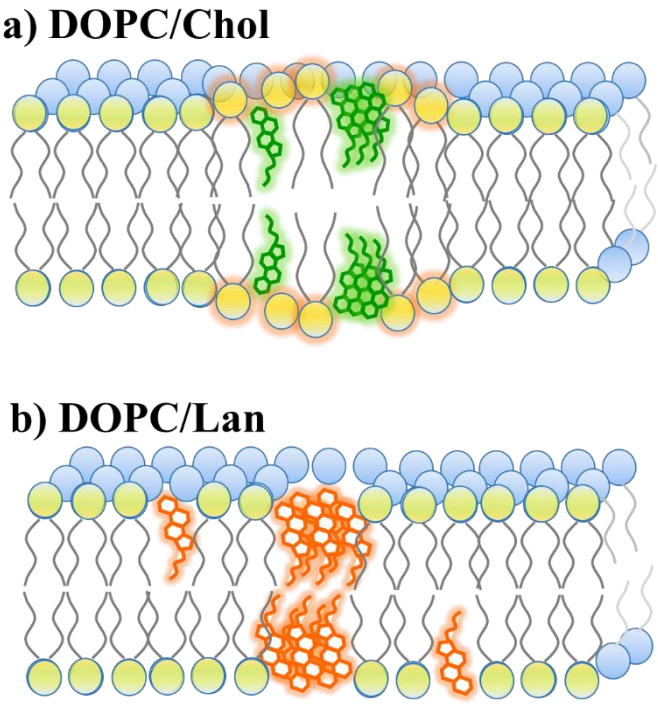

Fig. 3-7 Model of sterol distribution in unsaturated phospholipid membranes.

Chapter IV

Melting Temperature Dependent Interactions of Ergosterol with Unsaturated and Saturated lipids in Model Membranes

1. Introduction

Biological lipid membranes are widely studied, highly complex structures that regulate the cellular environment and are essential for many biochemical processes. Phospholipids and sterols are major constituents of cell membranes; their amphiphilic nature, structural diversity, and composition determine membrane properties (Karp 2004). Sterol molecules, in particular, are well known regulators of physicochemical membrane properties (e.g. fluidity, phase state, and permeability) (Bennett et al., 2009; Chang et al., 2008; Dynarowicz-Łątka and Hąc-Wydro, 2004; Epand et al., 2002), because they modulate the organization of other lipids by changing their ordering, available area, and formation of domains of characteristic composition. In higher eukaryotes, Cholesterol (Chol) is abundant, whereas Ergosterol (Erg) is found in lower eukaryotes such as protozoa, yeast, fungi and insects (Arora et al., 2004; Henriksen et al., 2004). Despite numerous studies focusing on Chol's impact on membrane properties, Erg and other sterols have not been studied nearly as extensively. Erg has an additional double bond in the steroid ring in comparison to Chol, as well as a double bond and an extra methyl group in the alkyl tail (**Fig. 4-1**). These structural differences enable Erg to exhibit distinctive

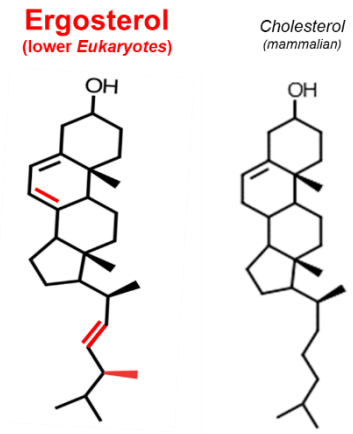

Fig. 4-1 Chemical structures of Erg and Chol.

effects in membranes (Bagiński et al., 1989; Hung et al., 2016). However, it is still unclear exactly how Erg behaves and alters membrane properties, as well as why Erg is the primary sterol in lower eukaryotes.

Past studies have concentrated on the distinctive roles of Erg and Chol in saturated diacylglycerophosphocholines such as 1,2-dipalmitoyl-*sn*-glycero-3-phosphatidylcholine (DPPC) and 1,2-dimyristoyl-*sn*-glycero-3-phosphatidylcholine (DMPC) (Bennett et al., 2009; Chang et al., 2008; Czub and Baginski, 2006; Miyoshi and Kato, 2015; Tierney et al., 2005). The smooth alpha-face together with the presence of the unsaturated acyl tail of Erg led to stronger interactions of Erg with saturated lipids, which resulted in Erg having a larger condensing effect than Chol, as reflected by the area per lipid (Czub and Baginski, 2006; Cournia et al., 2007; Urbina et al., 1995). Using x-ray diffraction, the effect of Erg and Chol on the thickness of bilayer membranes composed of binary mixtures of unsaturated, monounsaturated and saturated phospholipids such as 1,2-dioleoyl-*sn*-glycerol-3-phosphatidylcholine (DOPC), 1-palmitoyl-2-oleoyl-*sn*-glycero-3-phosphatidylcholine (POPC) and DMPC, respectively, was determined (Levine and Wilkins, 1971). The thickening effect of Erg on DMPC was less than one-third that of Chol (Hung et al., 2016). In addition, Erg slightly thinned POPC and DOPC, whereas Chol has been shown to thicken membranes with these above lipid types. The solubility of Erg was lower with increasing content of unsaturated lipids with DMPC > POPC > DOPC. Further, a spin-label electron paramagnetic resonance and NMR study indicated the ordering and disordering effect of Erg in unsaturated lipids (i.e., egg lecithin) and monounsaturated lipids such as POPC depended strongly on its concentration (Semer and Gelerinter, 1979).

To better understand the behavior of Erg, a comparative study with well-known Chol is meanwhile. For example, enhanced ordering was observed below 15 mol% Erg in egg lecithin, while above 25 mol% Erg there were no further ordering of POPC by Erg, presumably because the excess Erg is not intercalated among the POPC chains. Above these sterol amounts, the lipids were more disordered in the presence of Erg. In contrast to Erg, Chol showed a strong ordering effect in both egg lecithin and POPC membranes. These studies clearly reveal a difference between Erg and Chol effect on membranes,

however the studies did not clarify the interaction behavior of Erg in various lipid membranes in different phase states.

Bilayer vesicles (liposomes) have long been used as models for studying biological processes and are used in formulations of pharmaceuticals and cosmetics. Preventing liposome or vesicle aggregation and avoiding changes in size while maintaining substance encapsulation is required for applications. Obviously, stable bilayer membranes are necessary to maintain liposome structure during storage until they move to the target destination. The stability and physical properties of liposomes depend on the properties of their constituent molecules and their intermolecular interactions in the membrane (Sekiguchi et al., 1995). Lower eukaryotes such as fungi have membranes enriched with saturated phospholipids (Ridgway and McLeod 2015). Thus, measurements of Erg-modified lipid membrane properties enable a better understanding of the role of Erg and complement the more extensive studies of Chol.

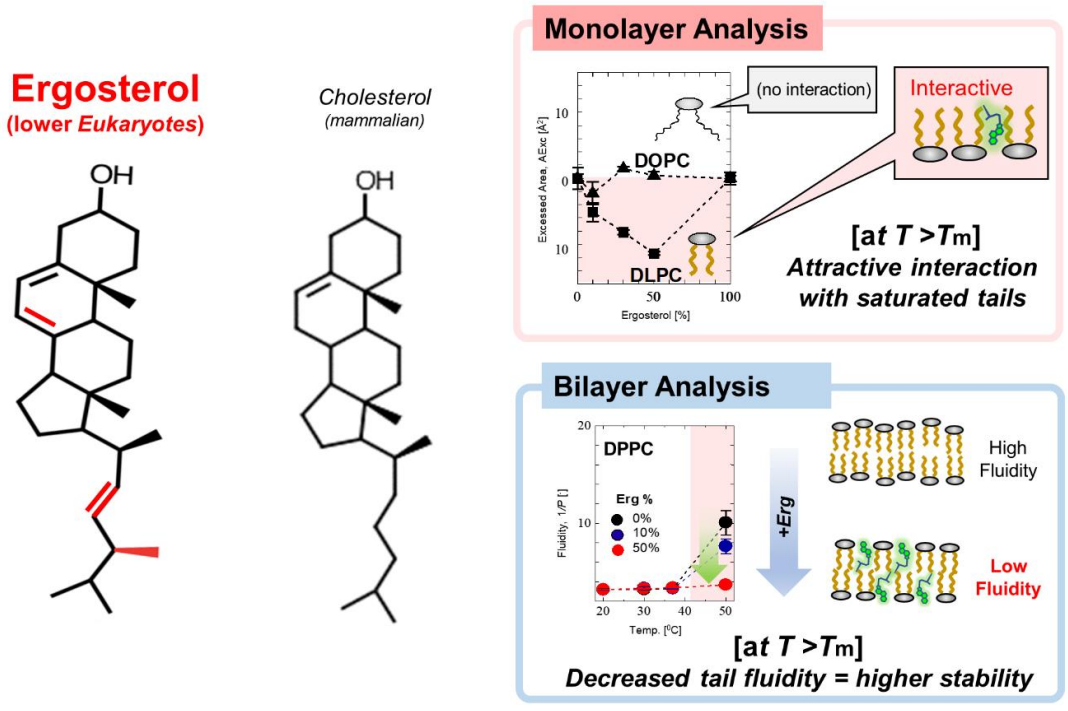

Fig. 4-2 Conceptual illustration of chapter IV

While numerous studies have investigated area condensation of various PCs and their mixtures with Chol (Bennett et al., 2009; Epand et al., 2002; Gershfeld, 1976; Wydro et al., 2011; Presti et al., 1982; Radhakrishnan and McConnell, 1999; Su et al., 2007), other sterols such as Erg are much less studied. The main objective of this research was to investigate the interaction behaviors of Erg in lipid membrane systems. Herein, saturated DPPC, 1,2-dilauroyl-*sn*-glycero-3-phosphocholine (DLPC), and unsaturated DOPC were employed. Monolayer isotherm measurements were employed to quantify the interaction of Erg with unsaturated and saturated phospholipids. The influence of Erg on the vesicular membrane polarity was investigated by a polarity-sensitive probe 6-lauroyl-2-dimethylamino naphthalene (Laurdan). The steady-state fluorescence polarization of 1,6-diphenyl-1,3,5-hexatriene (DPH) in Erg-modified vesicles was used to measure membrane fluidity with the various membrane compositions. Finally, the measurements and role of Erg in PC membranes are discussed by comparing to Chol (**Fig. 4-2**).

2. Materials and Methods

2.1 Materials

DOPC, DLPC, and DPPC were purchased from Avanti Polar Lipids (Alabaster, AL). Synthetic Erg (purity ≥95.0%) was purchased from Sigma-Aldrich (St. Louis, MO, USA). These products were stored in a refrigerator without exposure to light. Other chemicals were purchased from Wako Pure Chemical Industry Ltd. (Osaka, Japan) and were utilized without further purification.

2.2 Surface pressure-area (π-A) isotherm measurements

π-A isotherms were recorded on a pure water subphase at 28℃ with a KSV film balance (trough dimensions: width 60 mm, length 190 mm), equipped with two movable barriers, and placed on an anti-vibration table. Surface pressure was measured with an accuracy of ±0.1 mN/m using a Wilhelmy plate made from platinum foil. Spreading solutions were 0.4 mM of lipid in $CHCl_3$. A 30–40 μL of stock solution was spread onto a pure water subphase in a KSV film balance (trough dimensions: width 60 mm, length 190 mm, total area of 76.5 cm^2). After 10 min was allowed for the solvent to evaporate off, the surface pressure-area (π−A) isotherms were measured at a constant compression rate of 5 mm/min (ca. 300 mm^2/min), which corresponds to a compression rate of 3–4 $Å^2$ mean area per min. Using the obtained mean area per molecule data, the excess area per molecule (A_{ex}) of PC/Erg mixture systems was calculated as follows:

$$A_{ex} = A_{12} - (x_1A_1 + x_2A_2), \quad \textbf{(4 - 1)}$$

where A_{12} was the measured mean area per lipid molecule in the mixed monolayer, A_1 and A_2 are the mean area per molecule of the pure components at the given surface pressure, and x_1 and x_2 indicate the molar fractions. The total Gibbs excess free energy of mixing (ΔG_{mix}) was defined as follows:

$$\Delta G_{mix} = \Delta G_{ex} - \Delta G_{ideal}, \quad \textbf{(4 - 2)}$$

where the excess Gibbs free energy (ΔG_{ex}) was obtained by integrating A_{ex} with respect to the surface pressure, $\Delta G_{ex} = \int A_{ex} d\pi$, and the ideal Gibbs free energy of mixing (ΔG_{ideal}) was calculated by follows:

$$\Delta G_{ideal} = kT\,(x_1\ln(x_1) + x_2\ln(x_2)), \quad \textbf{(4 - 3)}$$

where k is the Boltzmann constant and T is absolute temperature (=301 K in this work).

The elastic modulus was defined as the product of the average area per molecule (A) and the slope of the π–A isotherm at a specific surface pressure.

$$C_s^{-1} = -A\mathrm{d}\pi/\mathrm{d}A \quad (\mathbf{4 - 4})$$

2.3 Vesicle preparation

Vesicle suspensions were prepared according to previous method. A chloroform solution including PC and Erg with a molar fraction of 0, 10, 30 and 50 mol% was dried in a round-bottomed flask by rotary evaporation under vacuum. To ensure mixing, the lipid films were dissolved in chloroform and evaporated two times. The lipid thin films were kept under a high vacuum for at least 3 hours and then hydrated at room temperature with 3 ml of water. The vesicle suspension was frozen at -80°C and thawed at 50°C. This freeze and thaw cycle were repeated five times. The vesicle suspensions were then extruded 11 times through two layers of polycarbonate membranes with mean pore diameters of 100 nm using an extruding device (Liposofast; Avestin Inc,. Ottawa, ON, Canada). The total lipid concentration was 20 mM in all cases. Prepared vesicle suspensions were kept in a refrigerator until use.

2.4 Fluorescence emission spectra of Laurdan

10 μL of 100 μM Laurdan in ethanol was mixed with 12.5 μL of vesicle suspension, and the sample solution was diluted with water to a total volume of 1 mL. The molar ratio of total lipid/probe was 100/1. The sample solutions were incubated for 2 hours at room temperature, and then the fluorescence spectrum of Laurdan was recorded with an excitation wavelength of 340 nm, at emission wavelengths from 400 to 600 nm. The membrane polarity ($GP_{340,\mathrm{Laurdan}}$) at different temperatures was determined from (Parasassi and Gratton, 1995; Suga and Umakoshi, 2013):

$$GP_{340,\mathrm{Laurdan}} = (I_{440} - I_{490}) / (I_{440} + I_{490}), \quad (\mathbf{4- 5})$$

where I_{440} and I_{490} are the emission intensities of Laurdan in a range of 440 and 490 nm wavelengths, respectively.

2.5 Fluorescence polarization measurements

To measure membrane fluidity, 0.4 μL of 100 μM DPH ethanol solution was mixed with 12.5 μL of vesicle suspension, and the sample solution was diluted with water to a total volume of 1 mL. The molar ratio of total lipid/probe was 250/1. Before fluorescence polarization measurements the samples were incubated at 20, 30, 40 and 50°C in the dark for at least 30 min. After incubation, the fluorescence polarization of DPH was measured using a fluorescence spectrophotometer (FP-8500, Jasco, Tokyo, Japan) (Ex. = 360 nm, Em. = 430 nm). Fluorescence polarizers were set on the excitation and emission light pathways. With the emission polarizer angle of 0°, the fluorescence intensities obtained with the emission polarizer angle 0° and 90° were defined as $I_{\perp}$ and $I_{/\!/}$, respectively. With the emission polarizer angle of 90°, the fluorescence intensities obtained with the emission polarizer angle 0° and 90° were defined as $i_{\perp}$ and $i_{/\!/}$, respectively. The polarization (P_{DPH}) was then calculated using:

$$P = (I_{/\!/} - GI_{\perp}) / (I_{/\!/} + GI_{\perp}), \qquad \textbf{(4 - 6)}$$

where G (= $i_{\perp}/i_{/\!/}$) is the correction factor. Since polarization is inversely proportional to fluidity,[2] the membrane fluidity was evaluated by the reciprocal of polarization (1/P) (Suga and Umakoshi, 2013; Taguchi et al., 2018).

3. Results and Discussion

3.1 Surface pressure - area isotherm studies

π-A isotherms were measured at 28℃ for pure lipids (DLPC, DOPC, DPPC, Erg) and lipid mixtures (**Fig. 4-3**). The melting temperatures (T_m) of DLPC, DOPC, and DPPC are −2, −17, and 41°C, respectively. In DLPC systems, the isotherms of DLPC/Erg (Erg: 10, 30 and 50 mol%) appeared between pure DLPC and Erg isotherms. The excess area (A_{ex}) values of DLPC/Erg at 30 mN/m were negative (**Fig. 4-3a**), indicating an attractive interaction between DLPC and Erg and tighter membrane packing. Typically, decreased A_{ex} values are also observed in the mixtures of fluid phase PC (saturated and unsaturated) and Chol (Wydro et al., 2011; Jurak, 2013). The Gibbs free energies of mixing (ΔG_{mix}) of DLPC/Erg monolayers were all negative (**Fig. 4-3b**), demonstrating that Erg is miscible in DLPC monolayers at least up to 50 mol%. The phase states of DLPC (T_m = −2℃) and DOPC (T_m = −17℃) membranes at 28 ℃ are liquid-disordered phase (L_d). In contrast to

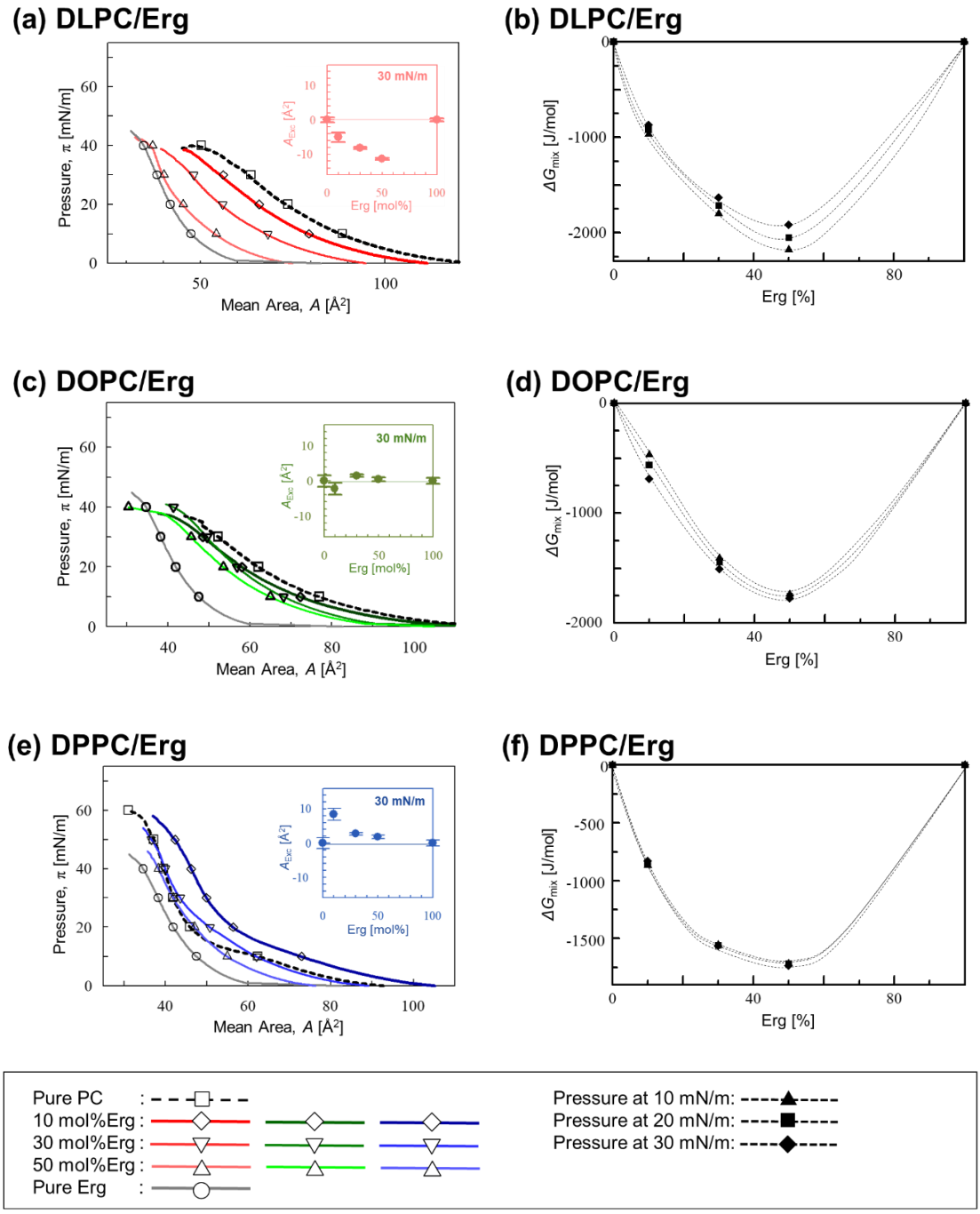

Fig. 4-3 π-A isotherms and variation in the Gibbs free energy of mixing (ΔG_{mix}) for DLPC/Erg **(a, b)**, for DOPC/Erg **(c, d)**, and for DPPC/Erg (**e, f**). Isotherms were measured on pure water subphase at 28 ℃. Insets of (a), (c), (e) represent A_{exc} values at 30 mN/m. Symbols indicate pure PC systems (□), PC with 10 mol% Erg (◇, ◆), PC with 30 mol% Erg (▽, ▼), PC with 50 mol% Erg (△, ▲), and pure Erg (○).

DLPC membranes, only a slight condensation effect was observed in DOPC monolayer at 10 mol% Erg and almost no change was observed with 30 and 50 mol% of Erg at and below a surface pressure of 30 mN/m (**Fig. 4-3c**). Because unsaturated acyl chains of DOPC are kinked, steric hindrance between DOPC and Erg could be significant. In addition, less ordering effects of Erg were reported in vesicle systems. The ΔG_{mix} values of DOPC/Erg mixtures were all negative, but less so than with DLPC (**Fig. 4-3d**). These findings suggest that Erg prefers to interact with saturated PC in monolayer systems.

The isotherm of pure DPPC system showed inflection points at ~7 mN/m and ~10 mN/m (Chang et al., 2008; Sabatini et al., 2008), revealing the solid ordered state (S_o) of DPPC membrane at this temperature. The addition of Erg (10, 30, and 50 mol%) increased mean areas in comparison to the expected values (ideal mixture of DPPC and Erg) (**Fig. 4-3e**). A positive A_{ex} value indicates a repulsive interaction between the molecules. In DPPC/Erg binary systems, the incorporation of Erg resulted in positive excess areas at 30 mN/m, suggesting that Erg disturbed the tight-packing of DPPC molecules. Although A_{ex} values of DPPC/Erg systems were all positive through the pressure range of 10–30 mN/m, the Gibbs free energy of mixing were negative (**Fig. 4-3f**). Given that Erg potentially disturbed the tight-packing of DPPC molecules, the monolayer structure could be stable and in liquid-ordered phase with high concentration of Erg similar to the liquid-ordered phase of cholesterol-DPPC (Sabatini et al., 2008). Consistent with these findings, an increased DPPC membrane elasticity with increased Erg was measured using micropipette aspiration. In addition, at high Erg content the membrane properties were consent with a liquid-ordered phase (Tierney et al., 2005).

At 30 mN/m the mean area of Erg was 39.19 ± 0.44 Å/molecule, and the maximum compressibility modulus (C_s^{-1}) was 108 ± 4 mN/m. Chol has been reported to have a mean area of 37.43 ± 0.59 Å/molecule and a much higher C_s^{-1} value 615 mN/m at 30 mN/m (Jurak, 2013). Thus, Chol should be more compressible than Erg under typical membrane such as DPPC, which is consistent with the lower area compressibility modulus of DPPC membranes containing Erg vs. Chol (Tierney et al., 2005). Chol induces condensation in both saturated and unsaturated PC monolayer systems (Dynarowicz-Łątka and Hąc-Wydro, 2004; Miyoshi and Kato, 2015; Tierney et al., 2005). It is also reported that the condensation effect of Erg is not so significant both for DPPC

Table 4-1 Maximum compressibility moduli (C_s^{-1}) and the corresponding surface pressures (π_{max}) measured in DLPC/Erg monolayers.

Erg [%]	DLPC		DOPC		DPPC	
	C_s^{-1} [mN/m]	π_{max} [mN/m]	C_s^{-1} [mN/m]	π_{max} [mN/m]	C_s^{-1} [mN/m]	π_{max} [mN/m]
0	72.9 ± 1.1	29	59.4 ± 1.8	26	195.1 ± 5.0	37
10	64.1 ± 4.4	25	57.3 ± 1.9	27	139.3 ± 4.2	39
30	73.2 ± 2.2	30	76.7 ± 1.0	30	152.7 ± 0.6	42
50	149.5 ± 8.6	36	65.3 ± 2.3	29	119.3 ± 2.8	37
100	108.0 ± 3.9	34	108.0 ± 3.9	34	108.0 ± 3.9	34

and DOPC monolayer systems (Miñones et al., 2009), consistent with our results. When Erg was incorporated into DMPC (T_m = 24℃) monolayer at 25℃, the maximum compressibility moduli of DMPC/Erg binary systems increased when compared to that of pure DMPC or Erg (Sabatini et al., 2008). A portion of DMPC molecules could be in a melted state (L_d phase) at this temperature, Overall, the average area per molecule in the mixture decreased indicating that Erg resulted in tighter membrane packing. This suggests that Erg can attractively interact with melted PCs ($T > T_m$). As described in **Table 4-1**, 50 mol% of Erg in DLPC monolayer increased the maximum compressibility moduli, however, no significant influence was observed in DOPC. Therefore, Erg condensed DLPC in monolayers at 28℃, where DLPC molecules are in melted state but could be more ordered – e.g. liquid condensed phase.

3.2 Effect of Erg in bilayer membrane polarities

Previous work has indicated that lipid monolayer characteristics at the high surface pressure correlate with bilayer membrane properties (Marsh, 1996). It is assumed that the

condensation effect of Erg in monolayer at π = 30 mN/m should be comparable with vesicular systems. To clarify the role of Erg in bilayer membrane systems, Erg-containing vesicle membranes were prepared and characterized by fluorescent probes (Bui et al., 2016; Lentz, 1993).

The fluorescent probe, Laurdan, is widely used to characterize the polar environment in vesicle membranes (Parasassi and Gratton, 1995; Klemm et al., 2009). The emission peak position of Laurdan corresponds to the membrane phase state: a sharp peak at around 440 nm for S_o phase, a broader peak at 440 nm for L_o phase (Watanabe et al., 2019; Suga and Umakoshi, 2013), and a broader peak at 490 nm for L_d phase. The addition of Erg in DLPC vesicles resulted in blue-shifted emission peaks (**Fig. 4-4a**), demonstrating that incorporation of Erg resulted in an ordered phase. In contrast, no peak shifts were found in DOPC/Erg vesicles (**Fig. 4-4b**), which reinforces our previous findings that Erg did not alter DOPC membrane properties. In DPPC vesicles, the presence of Erg led to a slight blue-shift (~4 nm) in the Laurdan emission peak (**Fig. 4-4c**), indicating that the membranes remained in the ordered phase. These results agreed well with the isotherm results that Erg enhanced DLPC membrane order, but had little to no effect in DOPC (Parasassi and Gratton, 1995). At 20°C, Erg significantly increased the ordering of DLPC membranes, but only had a small effect in DOPC membranes (**Fig. 4-5a**). With DPPC, below T_m there was no effect of Erg, but a dramatic ordering effect was observed above DPPC T_m (**Fig. 4-5b**). The addition of Erg increased the $GP_{340,Laurdan}$ values in DLPC/Erg vesicles at 50°C, but again no significant effects were observed in fluid phase DOPC/Erg vesicles. These results demonstrate that Erg molecules prefer to interact with saturated PC molecules at temperatures above T_m. systems. General polarization, *GP*, reflects the

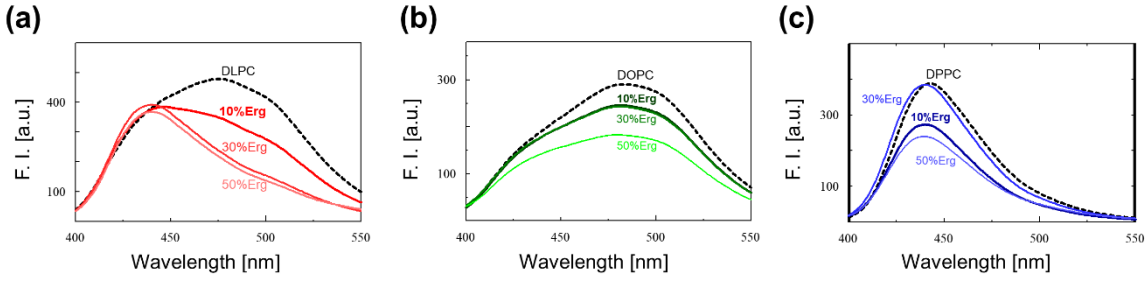

Fig. 4-4 Laurdan spectra obtained in DLPC/Erg (**a**), DOPC/Erg (**b**), and DPPC/Erg (**c**). Total concentrations of lipids and Laurdan were 100 and 1 μM, respectively. Measurements were carried out at 20°C.

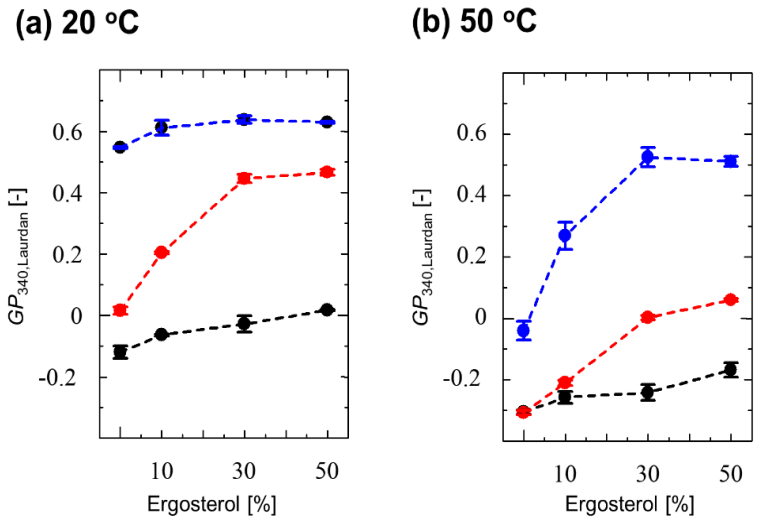

Fig. 4-5 Relationship between Erg content and membrane polarity ($GP_{340,Laurdan}$) at 20°C **(a)** and at 50 °C **(b)**. Colors indicate DLPC/Erg (red), DOPC/Erg (black), and DPPC/Erg (blue). Higher $GP_{340,Laurdan}$ values (> 0) mean ordered state, lower $GP_{340,Laurdan}$ values (< 0) mean disordered state. Data obtained with three repeatable experiments.

polarity of the vesicle: positive *GP* values (>0) represent ordered states while negative *GP* values (<0) represent disordered states

3.3 Temperature-dependency of membrane fluidities in PC/Erg vesicle systems

As DPH can bind to lipid tails (acyl chains) in the membrane interior, ($1/P_{DPH}$) is an important indicator used to characterize the fluidity of lipid bilayers. **Fig. 4-6** displays the measured ($1/P_{DPH}$) as a function of Erg mol% and temperature. The phase state of the membrane can be roughly estimated based on the $1/P_{DPH}$ values. Specifically, a higher $1/P_{DPH}$ value ($1/P_{DPH}$ >6) indicates a fluid phase membrane (L_d), while a lower $1/P_{DPH}$ value ($1/P_{DPH}$ <6) indicates an ordered membrane (S_o or L_o). Between 20 to 50°C, membrane fluidity of DLPC/Erg systems decreased with increasing addition of Erg. This indicates that Erg monotonically increases the ordering of saturated lipids above their melting point. On the other hand, unsaturated DOPC membrane fluidity was not altered by Erg. In DPPC/Erg systems, below T_m of DPPC (41°C), there was no significant change in the membrane fluidity. However, at temperature > T_m of DPPC, the fluidity of the pure DPPC membrane increased rapidly. Consistent with the findings with DLPC, the

inclusion of Erg in the saturated DPPC membrane above T_m significantly decreased membrane fluidity values in the order of 10, 30 and 50 mol% of Erg. For instance, while the $1/P_{DPH}$ value of the DPPC membrane decreased with a mere 10 mol% Erg, the value was still higher than 6, indicating that the membrane was still in the L_d phase. At 30 and 50 mol% Erg, the $1/P_{DPH}$ values were similar to pure DPPC under T_m, implying the mixed membranes remained in the L_o phase. The significant reduction of membrane fluidity in the presence of Erg at temperatures above T_m of saturated phospholipids demonstrate a preferential interaction of Erg with saturated, fluid phase PC and that Erg enhances the ordered phase as well as L_o phase in the membranes. As a result, the fluidity of DLPC/Erg and DPPC/Erg membranes decreased at temperatures above T_m. As saturated PC and Erg membranes can maintain a more ordered state at elevated temperatures. In particular, Erg had a much smaller effect in unsaturated membranes (Hung et al., 2016).

The ordering effect of Erg and Chol on DPPC was also compared via the fluidity values of mixed membranes containing 10, 30 and 50 mol%. As shown in **Fig. 4-7**, the $1/P_{DPH}$ values clearly show that below T_m neither sterol altered membrane fluidity. However, above the T_m of DPPC, Chol had a stronger ordering effect than Erg. For example, both Chol and Erg significantly reduced the $1/P_{DPH}$ values at 10 mol% sterol,

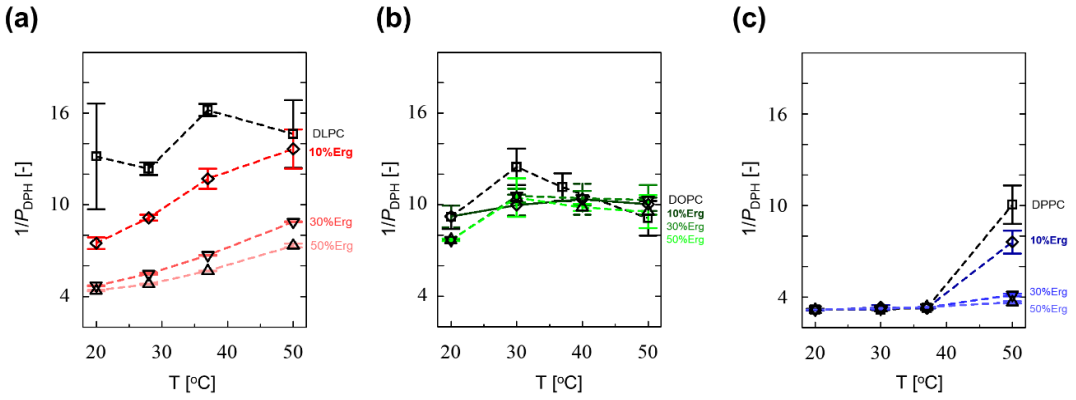

Fig. 4-6 Temperature dependency of membrane fluidity ($1/P_{DPH}$) for DLPC/Erg **(a)**, DOPC/Erg **(b)**, and DPPC/Erg (**c**). Total concentrations of lipids and DPH were 100 and 0.4 μM, respectively. Symbols indicate pure PC systems (□), PC with 10 mol% Erg (◇, ◆), PC with 30 mol% Erg (▽, ▼), and PC with 50 mol% Erg (△, ▲). Data obtained with three repeatable experiments.

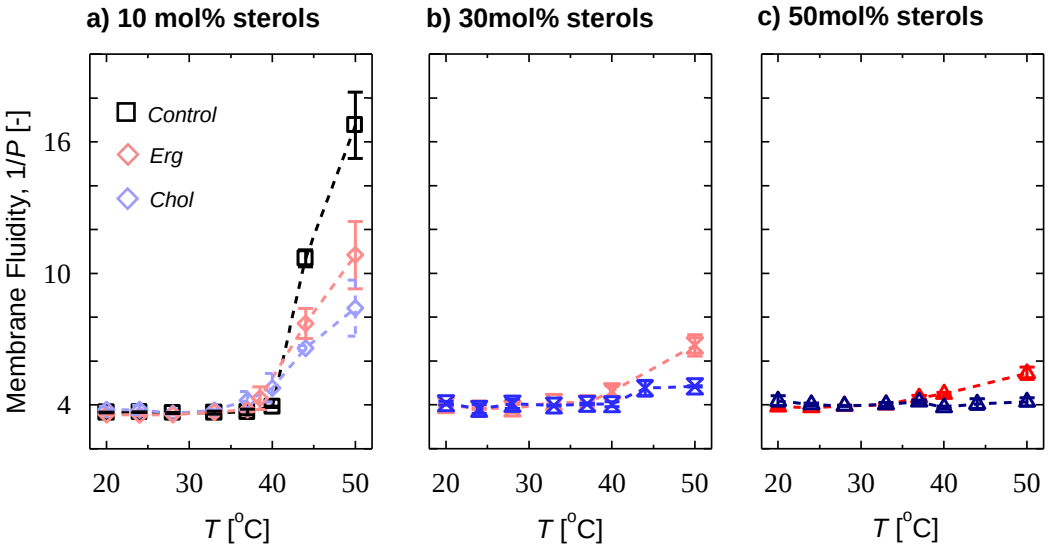

Fig. 4-7 The membrane fluidity of DPPC membranes containing Erg and Chol at 10 mol% (a), 30 mol% (b) and 50 mol% (c) at temperature ranges of 20 to 50 °C.

but Chol more than Erg. At higher concentration of sterols (30 and 50 mol%) membrane fluidity remained almost constant indicative of the liquid order phase in DPPC membranes with elevated sterol.

3.4 Discussion of possible roles for Erg in lipid membrane

Chol has been established to regulate and maintain a low membrane fluidity (Mitra et al., 2004; Mouritsen and Zuckermann, 2004). For instance, Hung *et al.* used high resolution X-ray diffraction to measure the thickness of saturated, monounsaturated and unsaturated phospholipid lipid bilayers containing Chol (Hung et al., 2007; Hung et al., 2016). Their work demonstrated that Chol induced the largest thickening effect in saturated (DMPC) lipid membranes. The thickness increase of monosaturated (1-stearoyl-2-oleoyl-*sn*-glycero-3-phosphocholine) and unsaturated (DOPC) phospholipid membranes were about 20% smaller than that of DMPC. High resolution X-ray diffraction by Hung *et al.* also revealed the condensing effect of Chol, however the effect of Erg was found to depend on membrane composition (Hung et al., 2016). The differences between Erg and Chol were explained by subtle differences in their structure and the type of acyl chains esterified to phospholipids. A simple and robust natural abundant two-dimensional 13C-NMR spectroscopy method has been used to investigate

order and dynamics in systems containing loosely coupled proton spin pairs, such as lipid bilayers. As evidenced from inter-proton pair order parameters (Urbina et al., 1998; Urbina et al., 1995; Sabatini et al., 2008), the results indicated that the ordering effects of sterols in membranes depended both on sterol structure and phospholipid acyl chains, being Erg < Chol for unsaturated phospholipid but the reverse for saturated lipid (Hsueh et al., 2005).

Furthermore, the results of previous ^{2}H-NMR studies with perdeuterated molecules also agreed with the ordering effect of Erg and Chol in membranes. Hsueh *et al*. argued that the addition of a methyl group at the tail and one double bond at C7-8 of the B-ring in the steroid ring system made Erg bulkier than Chol which limited Erg's ability to order unsaturated acyl chains (Hsueh et al., 2007). It is also reported that Erg ordered unsaturated membranes less strongly than Chol (Tierney et al., 2005), consistent with our studies. Similar to Chol, Erg has the potential to induce a L_o–like ordered phase. In the present study, Erg also slightly decreased the fluidity of DOPC vesicles. More significantly, Erg preferentially interacted with saturated phospholipids above T_m, reduced the membrane fluidity and stabilized the membrane structure of the composite membrane. Indeed, it acted very similarly although slightly less strongly than Chol (**Fig. 4-7**). The ring system in Erg is, in fact, known to be more planar than in Chol, and an additional double bond and a methyl group in the side chain of Erg make this moiety more rigid and oriented along the axis of the ring system (Arora et al., 2004). This feature may make Erg slightly less efficient in ordering saturated hydrocarbon chains. Such behaviors of Erg are important to explain the properties of lower eukaryote membranes as well as the roles of Erg in thermal resistance. Erg could be essential to provide ordered membrane structures of *Saccharomyces cerevisiae* (Abe and Hiraki, 2009).

Further, the fluidity results showed that Erg maintained membrane order over a large temperature range, even beyond T_m of the saturated lipid component. The affinity between Erg and saturated lipids could explain why Erg is the main sterol in lower eukaryotes, which contain saturated lipids as one of the dominant lipid species, while Chol is the sterol component of mammalian cell membranes, which are enriched in unsaturated lipids. As lower eukaryotes cannot control cellular temperature, the effect of Erg on membrane properties is extremely important to help maintain membrane fluidity homeostasis for

proper cellular functions. This also helps to clarify how fungi can function at high temperature as the concentration of saturated PC lipids increases under these conditions (Ramage et al., 2012; Grillitsch et al., 2014). Conversely, in mammalian membranes which are rich in unsaturated lipids, Chol is thought to be more effective in maintaining tight membrane packing and order. Comparing the chemical structure of Chol and Erg, it makes sense that Chol should have a larger condensing effect: Chol has a planar ring structure which enables PC molecules approaching from both sides, and no hindrance around hydroxyl group (Hénin and Chipot, 2006). While, the double bonds at the B ring and tail of Erg result in a bulky structure (Stevens et al., 2010), which will decrease intermolecular interaction with a kinked DOPC molecule and be slightly less efficient in ordering saturated DPPC. In summary, the interaction behavior and function of Erg depends on the membrane phase state and acyl chain structure. In particular, Erg only interacted and altered the membrane fluidity of saturated lipids above T_m.

4. Summary

Compared to Chol which ordered both saturated and unsaturated phospholipid membranes, Erg, Chol's derivative only altered the lipid packing of saturated phospholipid membranes at the melting state and had no effect on unsaturated lipid membranes. The results from monolayer isotherms indicated that increasing amounts of Erg led to changes in mixed monolayer phase state suggesting the formation of a liquid ordered phase with saturated acyl tail lipids above T_m. Additionally, the interaction of Erg in different membrane phase states were revealed via excess area per molecule analysis of isotherms. Erg was also found to modulate membrane fluidity in vesicles. The stabilization of low membrane fluidity in unsaturated lipids likewise clarified the function of Erg in lower eukaryotes. It is assumed that Erg preferentially interacts with saturated PC in the melted state, which maintains membrane stability and order at high temperature. By comparing the physicochemical functions of sterol molecules in lipid membranes, a plausible role for biological selection of Erg or Chol for different eukaryotes was suggested. As this work demonstrates, the selection of sterol component provides another means to optimize membrane properties for applications.

Chapter V

Ergosterol-Induced Ordered Phase in Ternary Lipid Mixture Systems of Unsaturated and Saturated Phospholipid Membranes

1. Introduction

Biological membranes are composed of phospholipid bilayers embedded with proteins, glycolipid, glycoproteins, and steroids. Membrane components and their composition vary according to organism, cell type, and membrane type (Singer and Nicolson, 1972; Spector and Yorek, 1985). Model membranes are constructed from self-assembled vesicles composed of saturated or unsaturated phospholipids and other amphiphilic molecules, such as Chol in animal cells, phytosterol, sitosterol, and stigmasterol in plant cells, Erg in fungal cells, and bacteriohopanetetrol or bacteriohopanaminotroil in bacterial cells (Dufourc et al., 1984). Chol induces the formation of liquid-ordered (L_o) membrane states known as lipid rafts (Marsh, 1996). Raft domains play an important role in modulating the structure, dynamics, and properties of membranes (Bloch, 1983; Rubenstein et al., 1979; Bacia et al., 2005) and are also thought to have an essential role in fundamental biological processes such as cell sorting, infectious diseases, asymmetric growth, and signal transduction (Dufourc et al., 1984). For instance, Erg, the predominant sterol in yeast, induces an L_o–like ordered phase and increases yeast tolerance to high ethanol concentrations (Hsueh et al., 2005).

The role of Chol in membrane properties and functions and the interactions between Chol and phospholipids have been well-studied; McConnell *et al*. reported the miscibility of Chol in phospholipid monolayers and bilayers (Rubenstein et al., 1979; Keller et al., 2000; Radhakrishnan and McConnell, 1999; Okonogi and McConnell, 2004; Radhakrishnan et al., 2000; Radhakrishnan and McConnell, 2005; McConnell and Radhakrishnan, 2008). Unlike Chol, Erg has a methyl group at

C24 of its side chain and two additional double bonds at 7C and 22C, which generate the distinctive effects of Erg (Bagiński et al., 1989; Hung et al., 2016). Many molecular dynamics studies have been conducted on Erg-phospholipid systems (Hung et al., 2016; Czub and Baginski, 2006; Cournia et al., 2007; Smondyrev and Berkowitz, 2001); however, their results do not concur, particularly regarding the condensing effect of Erg

(Mannock et al., 2006). It has been reported that the effects of Erg are dependent on membrane phospholipid composition. The interactions of Erg and Chol with saturated phospholipid membranes containing 1,2-dimilystoyl-*sn*-glycero-3-phosphocholine (DMPC) have been compared. It is known that the electron density profile and thickness of a pure lipid bilayer vary depending on the degree of hydration (Hung et al., 2016; Olah et al., 1991); however, in the presence of Erg or Chol, the electron density profile of the bilayer was independent of the degree of hydration (Hung et al., 2016; Franks, 1976). In addition, the roles of Erg and Chol differ in monolayer systems; Erg has a condensing effect with fully saturated lipids, whereas Chol has a condensing effect with both unsaturated and saturated lipids (Hung et al., 2016). Furthermore, the electron density profile of DMPC bilayers containing Chol is similar to that observed for pure DMPC in a gel phase, while membranes mixed with Erg are smoother and disordered (Hung et al., 2016).

The differences between Erg and Chol have also been clarified by evaluating their interactions with membranes containing unsaturated PCs (1,2-dioleoyl-*sn*-glycero-3-phosphocholine (DOPC) or 1-palmitoyl-2-oleoyl-*sn*-glycero-3-phosphocholine (POPC)). For concentrations of up to 20 mol%, Chol exhibited a strong condensing effect that thickened both membranes, whereas Erg had almost no condensing effect in these membranes (Hung et al., 2016). These results suggest that Erg has no ordering effect on the lipid acyl chains of DOPC and POPC; however, at concentrations of up to 25 mol%, Erg exhibited a small ordering effect (Urbina et al., 1998; Urbina et al., 1995; Hsueh et al., 2005). The effects of Erg on DMPC, POPC, and DOPC differ from those of Chol, particularly with unsaturated lipid acyl chains. Consequently, the phase diagrams of Chol in lipid membranes cannot be utilized to understand membrane state in the presence of its analog, Erg. Thus, phase diagrams for Erg with saturated and unsaturated lipids in binary and ternary lipid mixtures should be constructed and compared to those for Chol in similar lipid systems.

Considering previous findings, it is important to understand how Erg affects interaction behavior, condensing effects, and membrane phase states. In a DOPC bilayer, Chol dose-dependently altered the state of the bilayer (DOPC/Chol = 9/1, L_d; DOPC/Chol = 7/3, L_d+L_o; DOPC/Chol = 5/5, L_o) (Suga and Umakoshi, 2013), whereas Erg exhibited less ordering effects than Chol or Lan (Bui et al., 2016). Herein, we studied the effect of Erg in a model membrane composed of DOPC, 1,2-dipalmitoyl-*sn*-glycero-3-phosphocholine (DPPC), and sterol (**Table 5-1**). The experimental systems used here were bilayers (assessed using fluorescent probe analyses) and monolayers (assessed using surface pressure-area (π-A) isotherms). In the bilayer systems, the used of fluorescent probes with 1,6-diphenyl-1,3,5-hexatriene (DPH) and 6-lauroyl-2-dimethylamino naphthalene (Laurdan) enabled the ordering effects of Erg and Chol to be compared, with the plausible phase states of DOPC/DPPC/Erg ternary systems categorized as solid order (S_o, gel phase of pure phospholipid bilayers under phase transition temperature (T_m)), liquid-disordered (L_d), or liquid-ordered (L_o, sterol-induced ordered phase) phases.

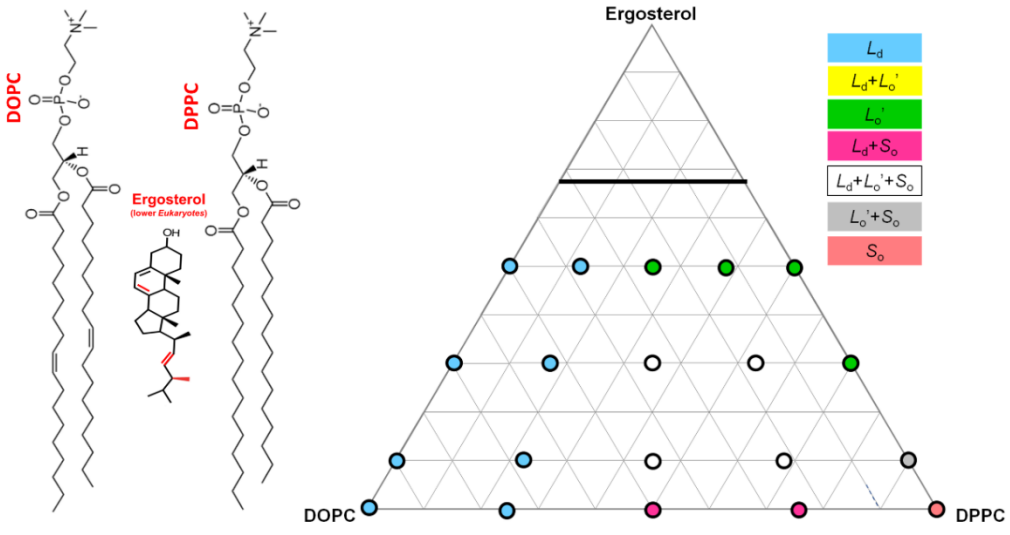

Fig. 5-1 Conceptual illustration of Chapter V.

Table 5-1 Lipid compositions studied in this work

Entry[*1]	Lipid composition (DOPC/DPPC/Erg)	Entry[*2]	Lipid composition (DOPC/DPPC/Chol)
a	75/25/0		
a-i	67.5/22.5/10	a-i’	67.5/22.5/10
a-ii	52.5/17.5/30	a-ii’	52.5/17.5/30
a-iii	37.5/12.5/50	a-iii’	37.5/12.5/50
b	50/50/0		
b-i	45/45/10	b-i’	45/45/10
b-ii	35/35/30	b-ii’	35/35/30
b-iii	25/25/50	b-iii’	25/25/50
c	25/75/0		
c-i	22.5/67.5/10	c-i’	22.5/67.5/10
c-ii	17.5/52.5/30	c-ii’	17.5/52.5/30
c-iii	12.5/37.5/50	c-iii’	12.5/37.5/50

[*1] Erg-modified memrbaneas are described without prime. The DOPC/DPPC ratio of systems a, b, and c are 3/1, 1/1, and 1/3, respectively. The stertol amout for systems -i, -ii, and -iii are 10%, 30%, and 50%, respectively.

[*2] Chol-modified membranes are decribed with prime (’)

2. Materials and Methods

2.1 Materials

1,2-Dioleoyl-*sn*-glycero-3-phosphocholine (DOPC) and 1,2-dipalmitoyl-*sn*-glycero-3-phosphocholine (DPPC) were purchased from Avanti Polar Lipids (Alabaster, AL). Synthetic high purity (≥ 95.0 %) Erg and Chol were purchased from Sigma-Aldrich (St. Louis, MO) and stored in a refrigerator without exposure to light. Other chemicals were purchased from Wako Pure Chemical Industry (Osaka, Japan) and were utilized without further purification.

2.2 Liposome preparation

Liposome suspensions were prepared according to a previously described method. Briefly, chloroform solutions of DOPC/DPPC/sterol were dried in a round-bottomed flask by rotary evaporation in a vacuum. To ensure mixing, the lipid films were dissolved in chloroform and evaporated three or four times. The thin lipid films were kept in a high vacuum for at least 3 h and then hydrated at room temperature with 3 mL of water. The vesicle suspension was frozen at -80 °C and thawed at 50 °C. This freeze-thaw cycle was repeated five times and the liposome suspensions were extruded through two polycarbonate membranes with mean pore diameters of 100 nm using an extruding device (Liposofast; Avestin, Ottawa, ON, Canada) 11 times. The total lipid concentration ([DOPC] + [DPPC] + [sterol]) was 20 mM in all cases. Prepared liposome suspensions (**Table 5-1**) were kept in a refrigerator until further use.

2.3 Evaluation of membrane fluidity

To measure membrane fluidity, 0.4 μL of ethanol solution including DPH (probe concentration: 100 μM) was mixed with 12.5 μL of liposome suspension and diluted with water to a total volume of 1 mL. The molar ratio of total lipid ([DOPC] + [DPPC] + [Erg])/DPH was 250/1. The samples were incubated at 20-50 °C in the dark for at least 30 min before DPH fluorescence polarization was measured using a fluorescence spectrophotometer (FP-8500; Jasco, Tokyo, Japan; Ex. = 360 nm, Em. = 430 nm). Fluorescence polarizers were set on the excitation and emission light pathways. At an emission polarizer angle of 0°, the fluorescence intensities obtained at 0° and 90° were defined as $I_{\perp}$ and $I_{/\!/}$, respectively. At an emission polarizer angle of 90°, the fluorescence intensities obtained at 0° and 90° were defined as $i_{\perp}$ and $i_{/\!/}$, respectively. Polarization (P) was calculated using the following equation:

$$P = (I_{/\!/} - GI_{\perp}) / (I_{/\!/} + GI_{\perp}), \quad \textbf{(5-1)}$$

where G ($i_{\perp}/i_{/\!/}$) is the correction factor. Since polarization is inversely proportional to fluidity (Lentz, 1993), membrane fluidity was calculated as the reciprocal of polarization ($1/P$). The membrane fluidity of the bilayer interior region was given by $1/P_{\mathrm{DPH}}$.

2.4 Evaluation of membrane polarity using Laurdan fluorescent probes

To measure membrane polarity, 10 μL of Laurdan fluorescent probe (probe concentration: 100 μM) was added to 12.5 μL of liposome solution (total lipid concentration: 20 mM) in 977.5 μL of water (molar ratio: total lipid ([DOPC] + [DPPC] + [Erg])/Laurdan = 100/1) and incubated for 2 h at 20-50 °C. The Laurdan fluorescence spectrum of each liposome was recorded at appropriate emission wavelengths (400-600 nm) at different temperatures with an excitation wavelength of 340 nm. Membrane polarity ($GP_{340,Laurdan}$) was calculated as follows (Parasassi and Gratton, 1995):

$$GP_{340,Laurdan} = (I_{440} - I_{490}) / (I_{440} + I_{490}), \quad \textbf{(5-2)}$$

where I_{440} and I_{490} are the Laurdan emission intensities at 440 and 490 nm, respectively.

2.5 π−A isotherm measurements

DOPC, DPPC, and Erg were dissolved in chloroform at a total concentration of 0.4 mM and 30 – 40 μL of the stock solution was spread onto a pure water subphase in a KSV film balance (trough dimensions: width, 60 mm; length, 190 mm; total area, 76.5 cm^2). After incubating for 10 min for the solvent to evaporate off, the surface pressure-area (π−*A*) isotherms were measured at a constant compression rate of 5 mm/min (ca. 300 mm^2/min), corresponding to a compression rate of 3–4 $Å^2$ mean molecule per min. The temperature of the subphase was maintained at 28 ± 1 °C and the total amount of lipid spread on the subphase was 30 nM. All experiments were repeated at least three times with satisfactory reproducibility.

2.6 Excess area analysis

The excess area (A_{exc}) of the lipid ternary mixture system was calculated from the π−A isotherms according to the following equation:

$$A_{exc} = A_{123} - A_{id} = A_{123} - (x_1A_1 + x_2A_2 + x_3A_3), \quad \textbf{(5-3)}$$

where A_{123} is the mean area obtained at an arbitrary pressure, A_{id} is the ideal value for the membrane composition, A_i is the mean area, and x_i is the molar fraction pure component (i = 1, DOPC; i = 2, DPPC; i = 3, Erg).

3. Results and Discussion

3.1 Erg induces an ordering effect in ternary systems

Membrane fluidity, $1/P_{DPH}$, is one of many indicators of the state of lipid bilayers (Suga and Umakoshi, 2013; Bui et al., 2016; Lentz, 1993). Using a DPH fluorescent probe, we measured and compared the membrane fluidity ($1/P_{DPH}$) of ternary mixtures of DOPC/DPPC/Erg and DOPC/DPPC/Chol (**Fig. 5-2**). The membrane fluidity of the DOPC and DPPC mixture decreased as the amount of DPPC increased, reflecting the increased packing of the membranes (Entries a, b, and c). For the ternary mixtures of sterols in membranes enriched with unsaturated DOPC (Entries (a-i)-(a-iii), and (a-i')-(a-iii')), the membrane fluidity values dramatically decreased with the addition of high concentrations of Chol (50 mol%; Entries a-iii', b-iii', and c-iii'), whereas Erg only slightly decreased membrane fluidity even at high concentrations. This indicates that Erg has an insignificant ordering effect in DOPC-enriched membranes. In the mixtures containing equal amounts of DOPC and DPPC (Entries (b-i)-(b-iii) and (b-i')-(b-iii')), both Chol and Erg exhibited a similar ordering effect at 10 mol% and slightly reduced membrane fluidity, particularly at temperatures above 28 °C (**Fig. 5-2b-i**). At 30 and 50 mol%, Erg and Chol both decreased the fluidity of the membrane to very low and similar values for temperatures below 28 °C. The membrane fluidity gradually increased at high temperatures with Erg and even higher temperatures with Chol (**Figs. 5-2b-ii, b-iii**), suggesting that Chol has a greater ordering efficiency than Erg.

In the systems enriched with saturated DPPC (Entries (c-i)-(c-iii) and (c-i')-(c-iii')), the effect of Erg on membrane order was weaker than that of Chol at 10 and 30 mol%; however, the effects of Erg and Chol were similar at 50 mol% which demonstrated the lowest $1/P_{DPH}$ values (**Figs. 5-2c-i, c-ii, and c-iii**). These results suggest that in ternary mixtures of dominant saturated membranes, Erg could reduce membrane fluidity alongside environmental temperature, whereas Chol enhanced the packing of both unsaturated and saturated lipid membranes. The effects of Erg and Chol in ternary mixtures were similar to those in binary mixtures of unsaturated and saturated phospholipids (Hung et al., 2016).

The effects of Erg and Chol on the phase state of the membrane can be approximated via membrane properties (Suga and Umakoshi, 2013; Abe and Hiraki, 2009); in particular,

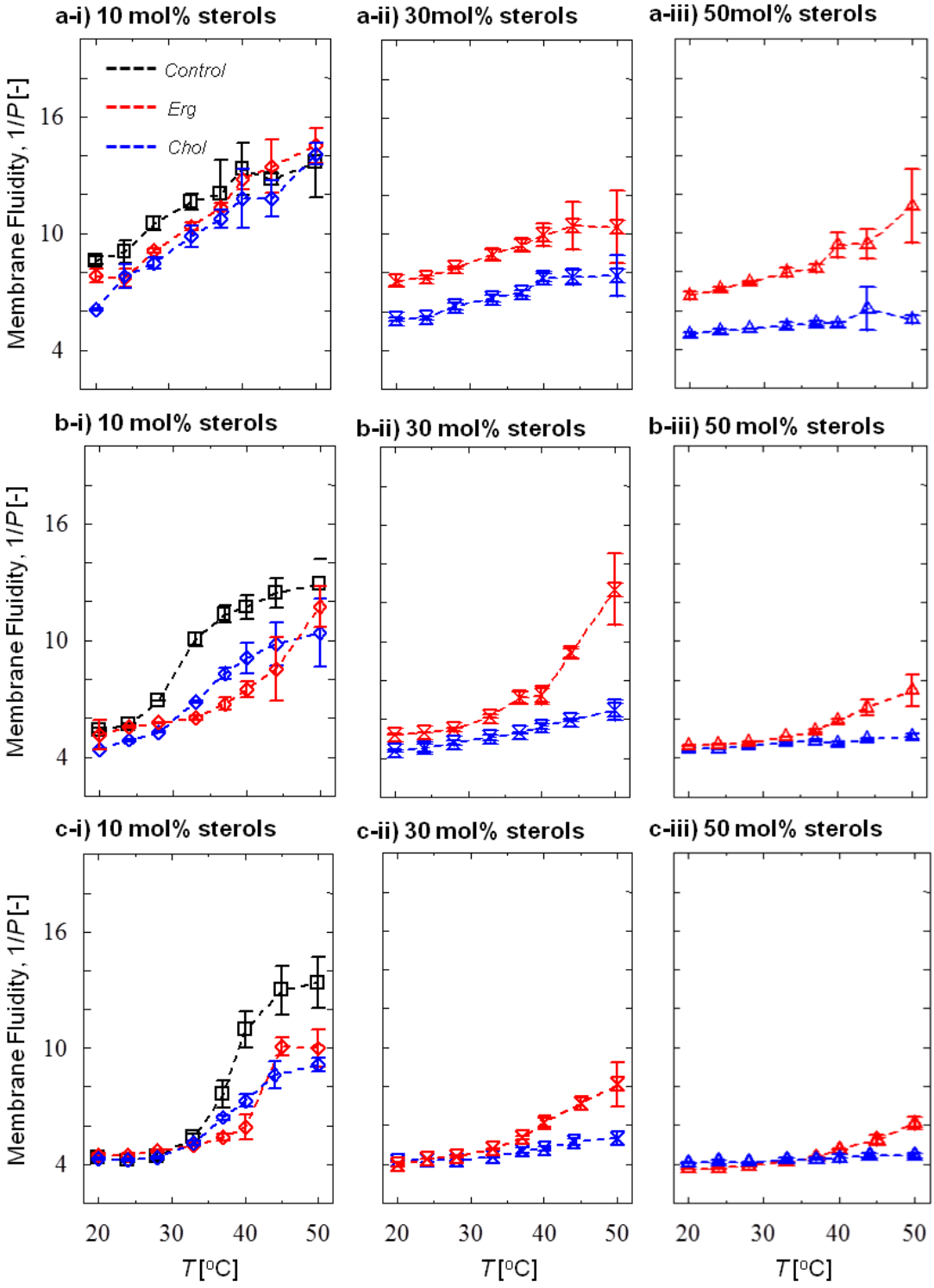

Fig. 5-2 Membrane fluidity (1/*P*) of DOPC/DPPC/sterol ternary bilayer systems. Measurements were carried out at the temperature range of 20 to 50 °C. Open square indicate the systems without sterols. The ratios of DOPC/DPPC are same in each panel. Detailed compositions are shown in **Table 5-1.**

a higher $1/P_{DPH}$ value (> 6) indicates a fluid phase membrane (L_d), whilst a lower $1/P_{DPH}$ value (< 6) indicates an ordered membrane (S_o or L_o). The membrane fluidity of DOPC/DPPC = 3/1 was greater than 6 at 20-50 °C, indicating an L_d phase. The addition of Erg at 10, 30, and 50 mol% decreased the $1/P_{DPH}$ values; however, the $1/P_{DPH}$ values were still higher than 6, indicating a L_d phase. For the systems without Erg (Entries a, b, and c), the membrane phase of L_d + S_o showed low fluidity at low temperatures and high fluidity at high temperatures. The presence of 10 and 30 mol% Erg in DPPC-enriched systems (Entries b-i, b-ii, c-i, c-ii) decreased $1/P$ values at 20-33 °C, resulting in a three phase mixture (L_d + S_o + L_o), whilst the addition of 50 mol% Erg drastically decreased membrane fluidity, even at high temperatures, and the $1/P_{DPH}$ value was typical of L_o-like phase membranes.

3.2 Effect of Erg on membrane polarity analyzed by Laurdan

Laurdan fluorescent probes have been widely utilized to characterize the polar environment of liposomal membranes (Suga and Umakoshi, 2013; Parasassi and Gratton,

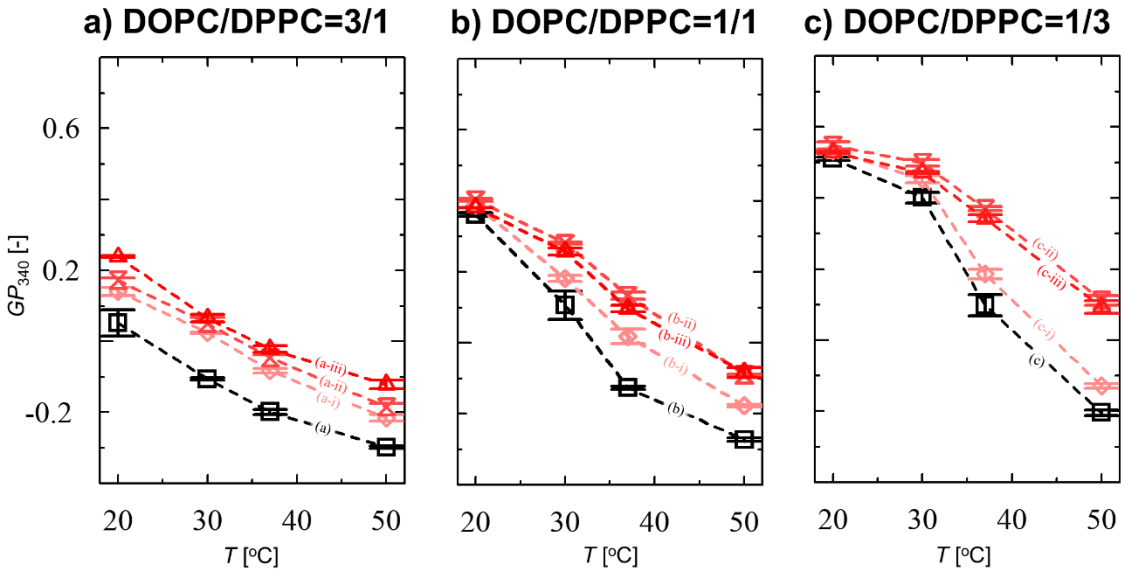

Fig. 5-3 GP_{340} values of DOPC/DPPC/Erg ternary mixtures. Left panel for systems a, a-i, a-ii, a-iii. Center panel for systems b, b-i, b-ii, b-iii. Right panel for systems c, c-i, c-ii, c-iii. Experiments were conducted at temperature range of 20 to 50 °C. Total concentrations of lipid ([DOPC]+[DPPC]+[Erg]) and Laurdan were 100 and 1 μM, respectively.

1995; Watanabe et al., 2019). The fluorescent intensity of Laurdan around 440 and 490 nm was recorded to calculate membrane polarity (GP_{340}). **Fig. 5-3** shows the alteration in membrane polarity values at 20 - 50 °C. A lower GP_{340} value indicates hydrophilic membranes with loose packing. At 20 °C (< T_m of DPPC), Erg altered membrane polarity in a dose-dependent manner, especially in systems enriched with saturated DPPC (Entries (c-i)-(c-iii)) at 50 °C, indicating that Erg can interact with PC molecules and make the membrane slightly ordered. At 50 °C (> T_m of DPPC), the GP_{340} values of the DOPC/DPPC binary mixtures were similar (ca. -0.3), revealing a L_d phase (Suga and Umakoshi, 2013). Higher levels of Erg can increase membrane order, with an increase in GP_{340} indicating an interaction between Erg and DPPC melting. Thus, Erg demonstrated higher membrane ordering efficiency in membranes enriched with saturated PCs at high temperatures.

3.3 Monolayer studies of Erg in ternary mixtures

Fig. 5-4 shows the π-A isotherms of ternary mixtures of DOPC/DPPC/Erg recorded at 28 °C. The isotherm of pure DOPC is smooth, indicating a L_d phase, whilst that of DPPC at temperatures below the T_m shows inflexion points, indicating a S_o phase (Chang et al., 2008; Sabatini et al., 2008). In the systems enriched with unsaturated DOPC (Entries (a-i)-(a-iii)), Erg did not decrease the mean area but caused an expansion in the isotherms, possibly due to its bulky structure (Cournia et al., 2007; Sabatini et al., 2008). The obtained isotherm curves were smooth and wide (**Fig. 5-4a**), which may be evidence of a L_d phase. In our previous study, the phase state of a DOPC/DPPC = 3/1 bilayer at 30 °C was shown to be fully disordered (L_d) (Suga and Umakoshi, 2013); thus, Erg did not alter the phase state of systems enriched with unsaturated lipids at the monolayer level. Unlike Erg, Chol decreased the surface area of membranes with more unsaturated phospholipid molecules and the obtained area was smaller than ideal mixing area, implying that Chol induced membrane condensation (Keller et al., 2000; Veatch and Keller, 2002; Stottrup et al., 2005).

The surface pressure of biological membranes is assumed to be higher than that of model membranes (Marsh, 1996; Sennato et al., 2005). As for ternary mixtures of Chol, membranes containing more saturated acyl chains and Erg had a lower molecular area

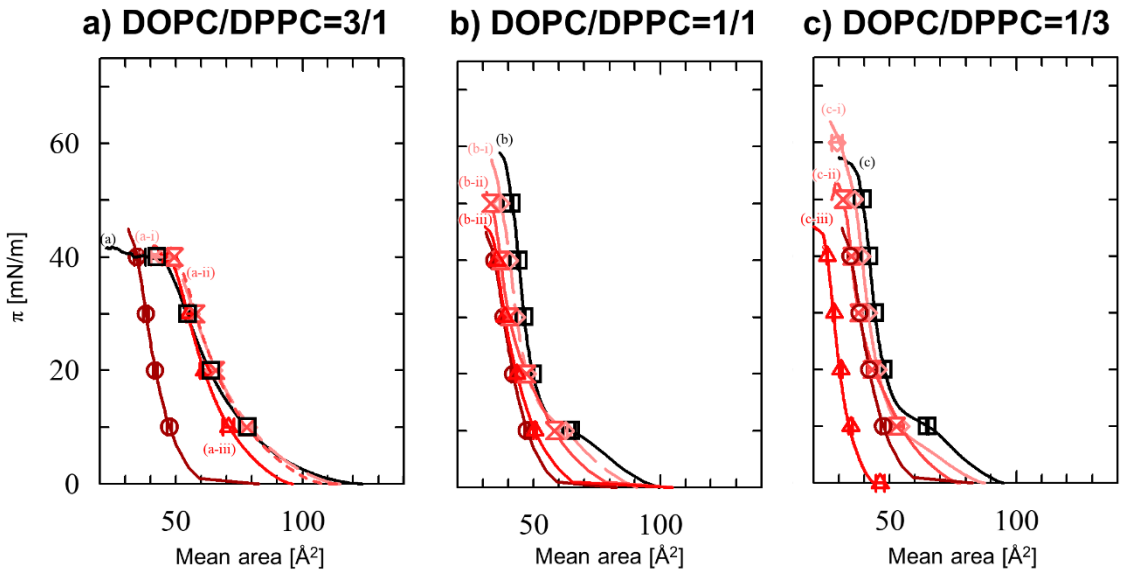

Fig. 5-4 Surface pressure-area (π-A) isotherms for ternary mixtures at 28 °C. Left panel for systems a, a-i, a-ii, a-iii. Center panel for systems b, b-i, b-ii, b-iii. Right panel for systems c, c-i, c-ii, c-iii. The symbol, circle, indicates the isotherm of pure Erg.

and compressibility than enriched unsaturated phospholipid membranes (Stottrup et al., 2005). In the systems enriched with unsaturated DOPC (Entries c, c-i) and those with equal amounts of DOPC and DPPC, Erg decreased the mean area at each surface pressure. In addition, the inflexion points disappeared with increasing amounts of Erg. The decrease in the mean area suggests that Erg has a similar condensing effect to Chol (Veatch and Keller, 2002; Miñones et al., 2009; Keller et al., 2000), whilst the smooth isotherms suggest the dissapearance of the solid phase (**Figs. 5-4b and c**). A transition from S_o to liquid phase has been observed for saturated PC at temperatures below the T_m with the addition of Erg at low surface pressure (Sabatini et al., 2008). Bending points were observed in the isotherms of systems b, b-i, c, and c-i, indicating the coexistence of S_o and liquid phases. Additionally, increasing levels of Erg gradually decreased the mean area. For systems with Erg ≥ 30 mol% (except a-ii and a-iii), the monolayers were in liquid phase (with no inflection points) and condensing effects were observed, suggesting the formation of an L_o-like ordered phase.

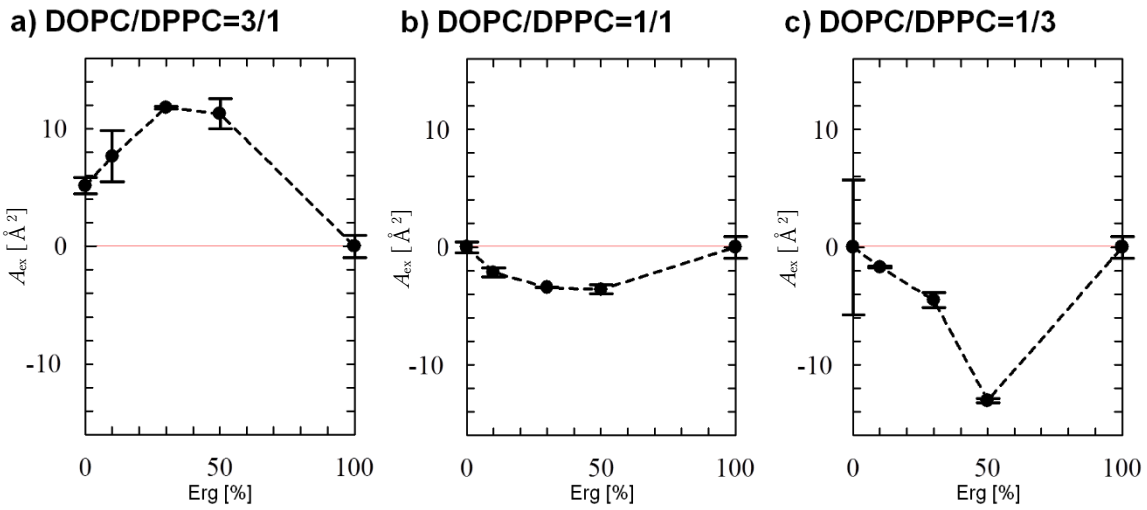

Fig. 5-5 A_{ex} values at π = 30 mM/m. Left panel for systems a, a-i, a-ii, a-iii. Center panel for systems b, b-i, b-ii, b-iii. Right panel for systems c, c-i, c-ii, c-iii.

To better quantify the interactions between Erg and PC molecules, the excess area (A_{ex}) was calculated from the experimental and ideal mixing areas (**Fig. 5-5**). Herein, A_{ex} values of 30 mN/m were used to estimate sterol-lipid interactions in the bilayer membranes. At 30 mN/m, the mean areas of pure DOPC, DPPC, and Erg were 52.24 ± 1.61, 41.94 ± 0.36, and 38.23 ± 0.93 Å^2/molecule, respectively. Disparity between the mean area of the ternary lipid mixture (A_{123}) and the ideal value (A_{id}, red line) was defined as the excess area. Condensing effects can be caused by attractive interactions between lipids, which are indicated by negative A_{ex} values, whereas positive A_{ex} values indicate expanding effects between molecules due to repulsive interactions (Radhakrishnan and McConnell, 2005; Kurniawan et al., 2017). In ternary mixtures of DOPC/DPPC = 3/1, the A_{ex} was large and positive (**Fig. 5-5a**), suggesting that the incorporation of Erg into unsaturated PC-enriched disordered membranes made the membranes loosely-packed. In the binary mixture systems of DOPC/Erg, no attracting interactions were observed (data not shown). These results reveal that the L_d phase state of DOPC/DPPC = 3/1 membranes is not affected by Erg.

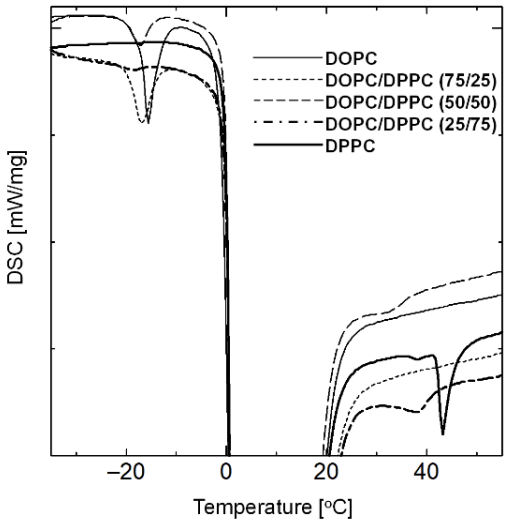

	ΔH_{DOPC}	ΔH_{DPPC}	$\Delta H_{boundary}$
DOPC	-1.95 J/g	-	0
DOPC/DPPC (75/25)	-1.31 J/g (74.1%)	-	-0.45 J/g (25.9%)
DOPC/DPPC (50/50)	-0.64 J/g (40.4%)	-0.16 J/g (10.1%)	-0.79 J/g (49.5%)
DOPC/DPPC (25/75)	-0.11 J/g (7.8%)	-0.51 J/g (36.4%)	-0.78 J/g (55.8%)
DPPC	-	-1.22 J/g	0

ΔH_{DOPC} : phase transition enthalpy of DOPC
ΔH_{DPPC} : phase transition enthalpy of DPPC
$\Delta H_{boundary} = \sum(\Delta H_{DOPC} + \Delta H_{DPPC}) - (\Delta H_{DOPC} + \Delta H_{DPPC})$

Fig. 5-6 DSC analysis of DOPC/DPPC liposomes. Based on the obtained ΔH values, the fraction of total boundary lipid in DOPC/DPPC 3/1 (75/25), 1/1 (50/50) and 1/3 (25/75) were 25.9%, 49.5%, 55.8%, respectively. The mean boundary DPPC (i.e. not in S_o state) in DOPC/DPPC 3/1, 1/1 and 1/3 was 25 mol%, 37.8 mol% and 36.0 mol%, respectively.

Conversely, in the systems with equal amounts of DOPC and DPPC (Entries (b-i)-(b-iii)) and those enriched with saturated DPPC (Entries (c-i)-(c-iii)), the incorporation of Erg resulted in negative excess areas, suggesting that the condensed state of the membrane is due to attractive interactions between Erg and PC molecules (**Figs. 5-5b and c**). Similarly, a condensing effect has been observed in ternary mixture systems including Chol (Keller et al., 2000; Veatch and Keller, 2002; Stottrup et al., 2005). This could suggest that interactions between Erg and saturated PC form an ordered phase. In binary mixtures of DPPC/Erg, positive A_{ex} values were observed at the same temperature (data not shown), indicating that Erg and DPPC may be immiscible at temperatures below the T_m. According to calorimetry analysis, boundary DPPC lipids (i.e., DPPC molecules not in S_o phase) exist in DOPC/DPPC mixtures (**Fig. 5-6** and **Table 5-2**). The phase transitions of DOPC/DPPC liposomes were revealed by differential scanning calorimetry (DSC) analysis (**Fig. 5-6**). It was found that the DPPC liposome indicated a phase

Table 5-2 Phase transition enthalpy of DPPC [kcal/mol]

DOPC/ DPPC	$\Delta H_{DOPC+DPPC}$ (1)	$\Delta H_{DOPC/DPPC}$ (2)	(2) - (1)
10/0	0.00	0.00	0.00
7/3	2.54	0.00	-2.54
5/5	4.92	0.49	-4.43
3/7	5.42	3.55	-1.87
0/10	7.38	7.38	0.00

transition temperature (T_m) at 41 °C. The enthalpy (ΔH) for DOPC and DPPC were calculated (**Table 5-2**). In the case of liposome mixture ((1) DOPC liposome + DPPC liposome), the ΔH values showed a liner relationship with DPPC concentration. In contrast, the DOPC/DPPC binary mixtures (2) showed the decreased ΔH values lower than those of liposome mixtures. It is therefore suggested that DPPC molecules are not fully in solid ordered (S_o) phases. Thus, Erg may interact with saturated PCs in a melted state. The total effects of Erg on DOPC/DPPC mixtures may therefore make the membrane more ordered.

3.4 Phase diagram of DOPC/DPPC/Erg bilayers

The phase diagram of DPPC/DOPC/Erg in 20 vol% ethanol at 22 °C has been shown to mimic yeast cell biomembranes (Vanegas et al., 2012; Ma and Liu, 2010; You et al., 2003; Arroyo-López et al., 2010) that can tolerate high alcohol concentrations during anaerobic fermentation. Generally, short-chain alcohols partition the lipid-water interface, with hydrocarbons positioned next to the lipid acyl chains and the hydroxyl group facing the solvent (Adachi et al., 1995; Barry and Gawrisch, 1994; Kranenburg et al., 2004; Feller et al., 2002). The behavior of ternary supported bilayer systems was investigated using atomic force microscopy and fluorescence microscopy (Vanegas et al., 2012) and phase behavior was determined by Texas Red DHPE fluorescent probe partitions. The phase diagram of lipid systems in 20 vol% ethanol clearly showed that an increase in unsaturated lipids and/or Erg could prevent the formation of the interdigitate

phase and maintain membrane thickness during fermentation (Vanegas et al., 2012). Compared to the phase diagram (20 °C) of DOPC/DPPC/Erg in the absence of ethanol, the membrane phase state was quite similar to that of enriched unsaturated lipid membranes in the disordered phase. In membranes with high amounts of saturated lipids, the membrane was mainly S_o phase in the absence of ethanol but a mixture of S_o, L_d, and L_o phases in the presence of ethanol at low temperatures. Depending on the surrounding environment, alterations in lipid and Erg content could produce fungi or yeast cells that can tolerate and survive in high ethanol conditions.

The temperature-dependence of the $1/P$ value can approximate the phase state of lipid bilayers: in S_o phase (e.g., pure DPPC) $1/P$ values are low ($1/P < 4$) and almost constant below the T_m; in L_o phase (e.g., DOPC/Chol 50/50) $1/P$ values are lower but gradually increase as the temperature increases (Suga and Umakoshi, 2013). Although it can be difficult to judge the phase state based on the $1/P$ value itself, case studies can help determine the membrane state (**Figs. 5-7** and **5-8**).

Considering the temperature dependency of the $1/P$ values, the phase states of DOPC/DPPC/Erg ternary systems were estimated as follows. Systems enriched with unsaturated DOPC (Entries (a)-(a-iii)) could be L_d phase (at 28 °C), otherwise membranes are in a more ordered state due to the presence of DPPC and Erg. In monolayer systems, smooth isotherms were obtained with similar membrane compositions, whereas systems b, b-i, c, and c-i could be S_o phase (at 28 °C) due to inflection points in the monolayer isotherms. These findings are summarized in a plausible phase diagram (**Fig. 5-9a**) which was compared with that of Chol (**Fig. 5-9b**). Erg exhibited less ordering effects in unsaturated lipids such as DOPC (Bui et al., 2016), whilst the addition of Erg led to the formation of L_o–like ordered phases (systems b-ii, b-iii, c-i, c-ii, c-iii)). The formation of an ordered phase can be confirmed via membrane properties (**Fig. 5-10**), which fulfill the criteria $1/P < 6$ and $GP_{340} > 0$. At temperatures above the T_m of DPPC, 30 and 50 mol% Erg eliminated disordered phases. When the temperature increased and was higher than the T_m of saturated lipids, Erg exhibited strong interactions and changed the membrane phase. In ternary lipid mixture systems, Erg could interact with: 1) boundary DPPC molecules (not in S_o phase) at temperatures below the T_m; and 2) melted DPPC molecules

at temperatures above the T_m. Therefore, DOPC and DPPC are immiscible boundary lipids that do not associate with the S_o domain. Erg (≥ 30 mol%) may interact with these lipids and enable an organism to maintain "ordered" membrane states and resist membrane disordering.

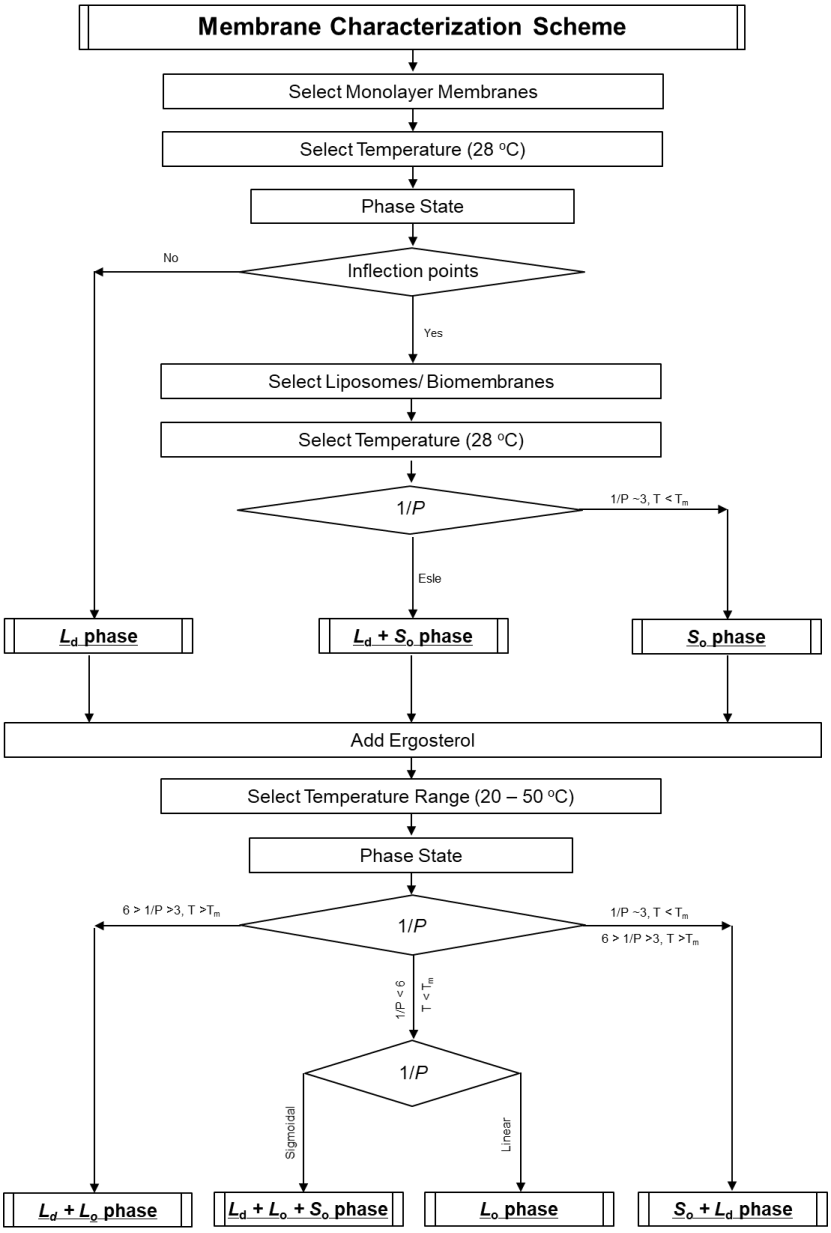

Fig. 5-8 Scheme for constructing the phase diagram for DOPC/DPPC/Erg ternary mixtures based on the inflection point of monolayer isotherms and membrane fluidity (1/*P*) herwise, $L_d + L_o$ phase.

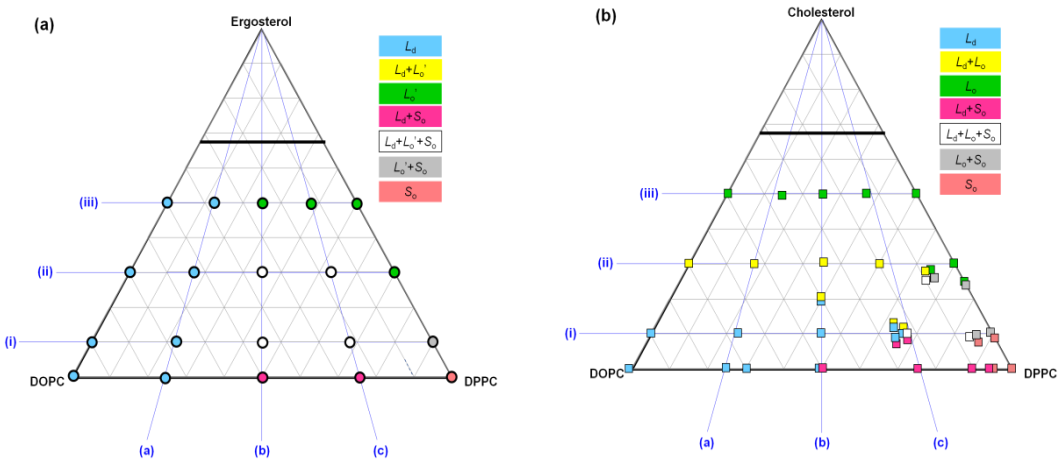

Fig. 5-9 (**a**) Plausible phase diagrams of DOPC/DPPC/Erg bilayers at 28 °C. Phase state are decided based on data obtained in this work. L_o' indicates Erg-induced ordered phase. (**b**) Modified phase diagram of DOPC/DPPC/Chol bilayers at 28 °C. Phase states and phase boundaries are drawn based on reported works, including our previous ones (Suga and Umakoshi, 2013); (Vanegas et al., 2012); (Cicuta et al., 2007); (Ishigami et al., 2015); (Uppamoochikkal et al., 2010); (Wolff et al., 2011).

For comparison, a modified phase diagram (at 28 °C) of DOPC/DPPC/Chol bilayers was produced according to the literature (Suga and Umakoshi, 2013; Vanegas et al., 2012; Cicuta et al., 2007; Ishigami et al., 2015; Uppamoochikkal et al., 2010; Wolff et al., 2011). By using the fluorescent probes Laurdan and DPH, Chol was clearly shown to be the effective molecule and was able to order both saturated and unsaturated phospholipids (Suga and Umakoshi, 2013). Based on physicochemical membrane property analyses of DOPC/DPPC/Chol ternary systems, Chol generally produces ordered membranes. Compared to membrane phase states at 28 °C, Chol is more effective than Erg at ordering membranes. Due to the affinity between Erg and saturated lipids, Erg decreased the solid phase and formed the ordered phase. According to these findings, a plausible mechanism for the regulation of biological membrane ordering in lower eukaryotes (e.g., fungi, which are enriched in saturated lipids) by Erg can be assumed. In contrast, Chol regulates membranes enriched with unsaturated lipids in mammalian cell membranes. Previous studies have reported that Chol has a greater condensing efficiency, plays an important role in regulating membrane thickness, and maintains a more constant membrane fluidity

(Mouritsen and Zuckermann, 2004; Mitra et al., 2004). Via Erg, ectothermic species such as lower eukaryotes can stabilize membrane fluidity and polarity independently of the environmental temperature, thus clarifying how fungi can survive at high temperatures (Ramage et al., 2012).

3.5 Possible roles of Erg and Chol in lipid membranes

Both of the investigated sterols (Erg and Chol) were found to interact differently with the studied PCs (DOPC and DPPC). Mixtures of Chol with DOPC, DPPC, or DOPC/DPPC always had smaller surface areas at the monolayer level (Minones, et al. 2009). At the bilayer level, Chol increased membrane thickness (Hung et al., 2016) and decreased membrane fluidity (**Fig. 5-2**). The presence of Erg in unsaturated lipid membranes or enriched unsaturated lipid membranes exhibited a much more obvious difference in the interaction with phospholipids compared to Chol. Chol induced strong condensing effects in DOPC, while Erg had a lesser ordering effect on the lipid chains of DOPC. These results agree with previous NMR studies, which reported that Erg had reduced ordering effects (Urbina et al., 1998; Urbina et al., 1995; Hsueh et al., 2005). The interactions of Erg and Chol with saturated phospholipids (DMPC) were also clarified. In a pure lipid bilayer, the electron density profile and thickness changed with the degree of hydration over a relative humidity range of 95–100 %; however, with Chol in the bilayer membranes, the electron density profile became independent of the degree of hydration. Conversely, membranes containing Erg noticeably varied with humidity and the electron density profile of DMPC containing Erg was smoother, indicating less order among the lipid-sterol molecules (Hung et al., 2016). In membranes enriched with DPPC, a saturated phospholipid, both Erg and Chol exhibited an ordering effect that decreased $1/P$ values (**Fig. 5-2**). These results contradict almost all previous studies, which found that the chain-ordering and condensing effects of Erg were stronger than those of Chol (Czub and Baginski, 2006; Cournia et al., 2007; Smondyrev and Berkowitz, 2001; Cournia et al., 2007; Smondyrev and Berkowitz, 2001; Pencer et al., 2005). Therefore, the effects of Erg and Chol also depend on lipid acyl-chains.

This study also suggested that small differences in the chemical structures of sterols could determine the effects of Erg and Chol in lipid membranes. In particular, Erg is

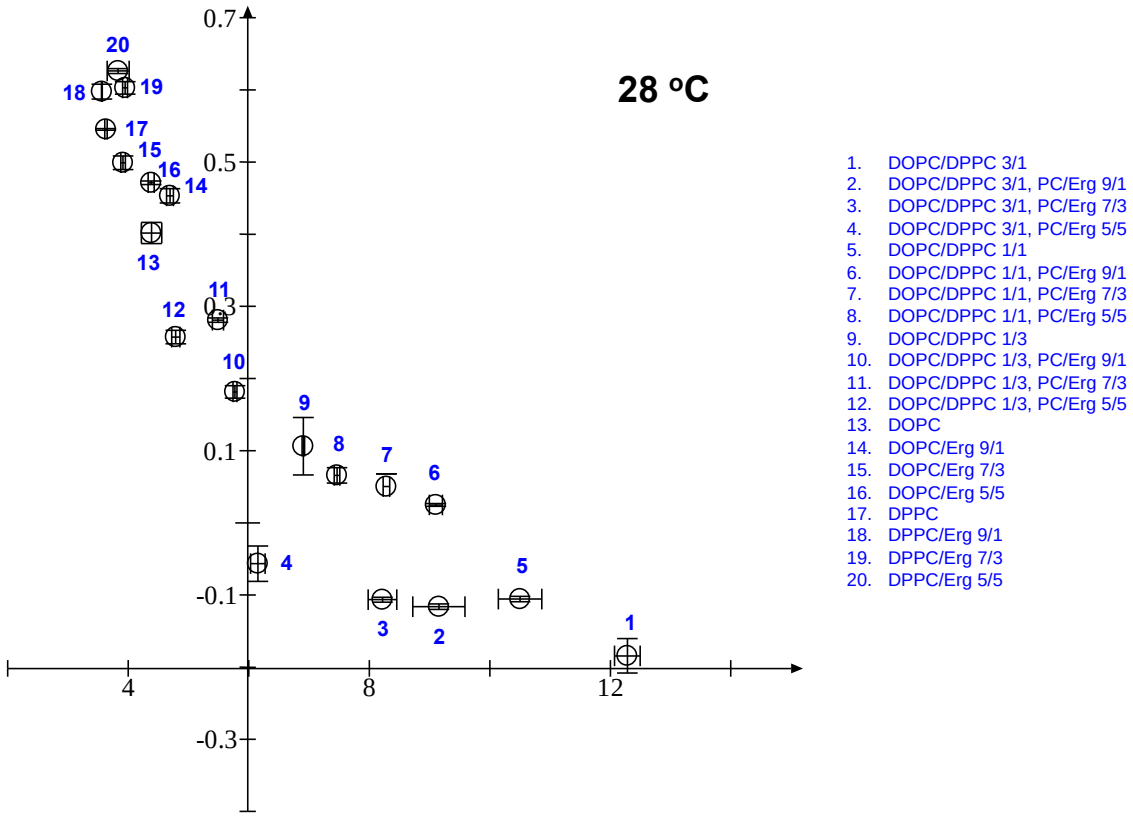

Fig, 5-10 Cartesian diagram for DOPC/DPPC/Erg ternary mixtures at 28 °C, based on membrane fluidity (1/*P*) and membrane polarity (GP_{340}). When the liposome membrane becomes polar (GP_{340} decrease), its fluidity increases (1/*P* increase). The membranes showing high fluidity (1/*P* >6) and in hydrophilic (GP_{340} <0) are estimated as liquid-disordered phase (L_d). For details of Cartesian diagram analysis, see following reports (Suga and Umakoshi, 2013).

stiffer and more rigid than Chol since it possesses two additional double bonds, one in its steroid ring and one in its alkyl chain. This inherent stiffness causes the Erg molecule to align with the membrane; however, angle distributions indicated that Chol is more closely aligned with the membrane (Cournia et al., 2007; Pandit et al., 2004). Conformational restrictions on sterol tail dihedral angles arising from the membrane environment were clarified via the vacuum simulation of sterols at different temperatures. The results indicated that the double bond in the sterol tail causes conformational differences and affects structural properties. Additional experiments on the radial distribution functions of the sterol hydroxyl hydrogen against water oxygen indicated that the associated

hydration numbers for Chol were higher than those for Erg, since Chol is closer to the lipid/water interface than Erg. The additional double bond in the Erg steroid ring causes its solvation to differ to that of Chol; for example, the Erg ring has a higher probability of solvation by both the *sn*1 and *sn*2 DPPC chains than Chol (Czub and Baginski, 2006; Cournia et al., 2007; Pandit et al., 2004).

Liposome systems have long been used as models to study biological processes and applied to pharmaceuticals (drug delivery systems) and cosmetics. Designing a rigid membrane is important for stabilizing the liposome during blood circulation and preventing the permeation of the encapsulated content. The stability and physical properties of liposomes depend on the interactions and properties of their constituent molecules (Sekiguchi et al., 1995). Our findings suggest that Erg can be used to modulate and maintain the stability of liposomal delivery systems.

4. Summary

Erg altered the packing state of DOPC/DPPC mixtures. Based on the dependence of membrane fluidity (1/*P*) and polarity (GP_{340}) on environmental temperatures, the ordering effect of Erg in ternary systems was revealed. Supported by monolayer π-A isotherms, the condensing effect of Erg in mixed membranes was also investigated. The interaction of Erg with phospholipids was estimated, with Erg preferentially interacting with saturated lipids such as DPPC. Using a combination of bilayer and monolayer studies, the role of Erg in membranes was clarified and the membrane phase states were determined for mixtures of DOPC/DPPC/Erg and compared with DOPC/DPPC/Chol systems. Our results showed that Erg had higher efficiency for ordering membranes enriched in saturated DPPC. The ordering effect of Erg was significant at high temperatures (> T_m of DPPC), resulting in stable membrane properties during heating. These functions of Erg can be utilized to design liposome systems for model biological membranes or for drug delivery. This study demonstrates that the selection of sterol components provides another means of optimizing membrane properties for different applications.

Chapter VI

General Conclusion

Liposomes are considered an ideal biomimetic environment and are potential functional carriers for important molecules such as sterols. With respect to regulation of self-assembly, the behaviors of sterol molecules (except Chol) in the self-assembled membranes have not been thoroughly investigated. In this study, to analyze the fundamental behaviors of steroid molecules in fluid membranes, Chol and its derivatives, such as Erg and Lan, incorporated in phospholipid membranes were carefully carried out by monolayer and bilayer studies.

In Chapter II, the behaviors of Chol and Lan in the unsaturated membrane have been thoroughly investigated via the exposed signal from multiple fluorescent probes in bilayer systems. By indicating the dielectric constant for each probe, the location of probes were pointed out as probes prefer binding from the outer to inner membrane leaflets. Therefore, the basic characteristics of membrane such as fluidity, polarity and hydrophobicity were revealed. Consequently, the stronger effectiveness of Chol in altering the behavior of unsaturated phospholipids was clarified and compared with Lan to point out the little difference in chemical structures having significant effects. It is thus required to investigate the detail interaction of sterol with membranes in the surface region to understand how each sterol change the property of membrane.

In Chapter III, the detail interaction behaviors of sterols, especially Lan, with phospholipid molecules which shown insignificant effect in regulating membrane properties at low concentration (Chapter II) were extendedly investigated in the surface areas by monolayer systems. Actually, the binary mixtures of Chol and Lan with phosphatidylcholines were analyzed using a Langmuir balance for recording force-area (π-A). Thus, the expanding or condensing effect in force-area (π-A) isotherms due to varying sterol concentrations and the differences in the monolayer physical state were accessed. Examination of the excess free energy of mixing revealed the stability of binary monolayers containing sterols; the differences are emphasized in the range of surface

pressure values found in natural membranes. The results surely confirmed that Lan had interaction with membrane even at 10 and 30 mol% which expressed the weak effect in modulating membrane characteristics in Chapter II.

In Chapter IV, applying both bio-membrane characterization methods presented in Chapter II and III, the interaction behavior and the regulation of Chol derivatives, Erg, dominant sterol in lower eukaryote membranes, in various membrane conditions were clarified. The negative excess areas of mixed membrane in Langmuir monolayer indicated the attractive interaction between molecules at different membrane states. In addition, the elastic modulus and Gibbs free energy demonstrated the stability or well-mixed membranes. Furthermore, signals from fluorescent probes of DPH and Laurdan referring membrane fluidity and polarity in bilayer systems indicated the distinctive interaction behaviors of Erg in different membrane states which depend on a range of temperatures. The changes in membrane properties reflected that Erg had potential condensation effects in melting states of saturated phospholipid membranes.

In Chapter V, the phase diagram of Erg in ternary mixtures of unsaturated and saturated phospholipids were next constructed and comparable with that of Chol, by using multiple fluorescent probes in Chapter II, Langmuir isotherm analysis in Chapter III and the interaction behaviors and function of Erg in Chapter IV. Supporting by these studies, the role of Erg in modulating membrane phase states in mixed phospholipid films were estimated and finally exhibited in phase diagrams. Compared to Chol in the same lipid systems, Chol had both ordering efficiencies in unsaturated and saturated membranes, while Erg only had strong effect in condensing the fluid states of melted saturated phospholipid films. Via this phase diagram, the model membrane composition could be easy to determine and design as model membranes for further studies

Based on the findings in this study, the phospholipid membrane properties could be fully investigated from the surface to inner regions by the characterization methods based on monolayer and bilayer systems. Via membranes characteristics, the roles of membrane components were clarified such as sterols and phospholipid types. Especially, the evolution pathways of sterols in membranes could be explained by the regulation of

membrane properties. These effective methods are useful full to characterize or further design drug carriers such as allergy disease and mycosis, or biomimetic membranes for investigate other bio-interaction between molecules (sterols with drug agents) or biosynthesis pathways of sterols which occur in the membranes.

Suggestion for Future Works

1. The role of Ergosterol in antifungal agent activities

Erg plays important role in the regulation of membrane properties, especially fluidity and structure, as well its present has been known as a target for the activity of antifungal agents for decades. An antifungal agent is a drug that selectively eliminates fungal pathogens from a host with minimal toxicity to the host. Recently, there are many drug agents applied for treatments. For examples, polyene antifungal drugs which interact with sterol in the cell membranes to form channels through which small molecules leak from the inside of the fungal cell to the outside. The mechanism interaction between drug and fungal molecules have not been elucidated, and the questionnaire is how to regulate these interactions. In the future work, the effect of membrane properties regulated by Erg will be characterized and analyzed to elucidate the interaction mechanism in membrane lipids, and the effectiveness of antifungal activities.

As indicated in Chapter IV and V, based on the interaction behavior Erg in melted phospholipid membranes, Erg can maintain membrane properties. Therefore, in this study, liposome membranes embedded with antifungal drug will be design with binary lipid systems containing both saturated and saturated lipids, but they will be enriched unsaturated phospholipids. The poor amount of saturated lipid as DLPC (L_d) (T_m = -2 ^oC) will form the domain which will be responsible for the recognition of and the fusion of fungal membrane and liposome drug carriers. After the membrane fusion, dominant unsaturated lipids from liposomes will insert into the fungi membrane to alter fungal membrane, and continuously, Erg will intercalate with antifungal agent to induce the formation of pore. Which stimulate the fungal components leak through membrane and lead to the cell death (**Fig. S1**).

In this study, characterization methods in Chapter II (multi-focal membrane properties by fluorescent probes) and Chapter III (the surface membrane properties indicated by monolayer study) will be employed to design the liposome drug carriers with optimal lipid compositions to protect the antifungal drug agents and support for the next

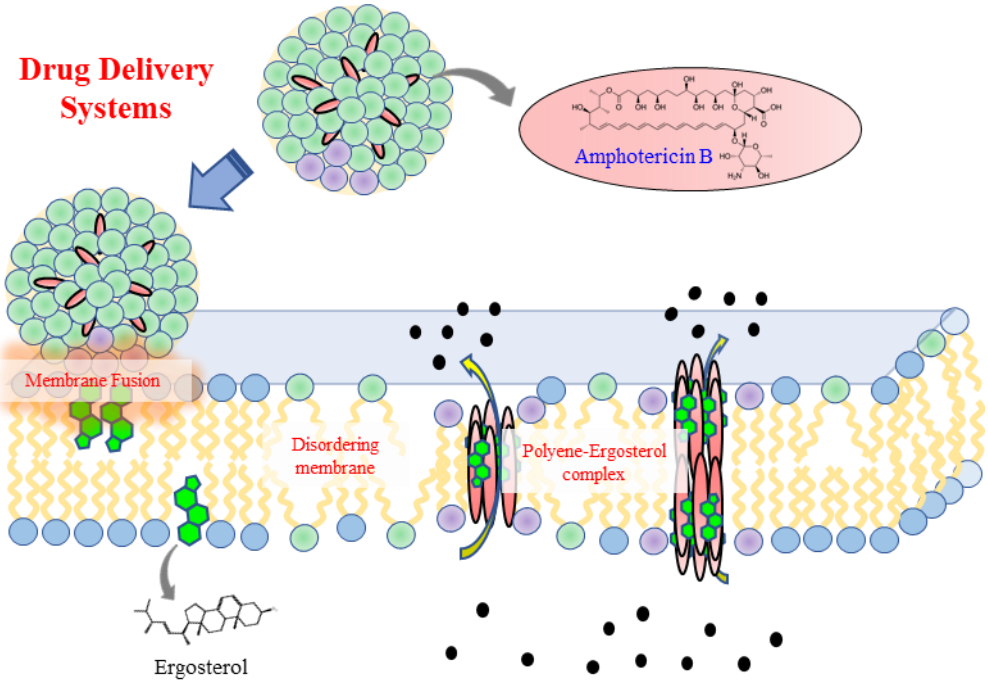

Fig. S1 Schematic for the mechanism of interaction between antifungal drug and ergosterol in membrane.

fusion stages. Via the properties of membrane during the fusion, the interaction mechanism of drug with fungal membrane will be elucidated. Finally, the drug carriers will be modified to enhance the activity of fungal agents

2. Characterize reconstructed membrane properties applied for membrane chiral selection

Relating to the utilization of amino acids, biological systems tend to favor and utilize L-amino acids over D-amino acids. However, a recently discovered deep sea bacteria strain, *Nautella sp.* strain A04V, exhibits an unusual characteristic of utilizing D-amino acids as nutrient source. In particular, these bacteria tend to favor D-amino acids more than L-amino acids, when they are harvested in minimal media (Kubota et al., 2016). While a nearby identical strain of this bacteria that was found in shallow sea waters favors L-amino acids. Previous research has only observed the A04V bacteria strain's preferential uptake towards D-amino acids, but no research has been done for investigating the reason behind the utilization of D-amino acids.

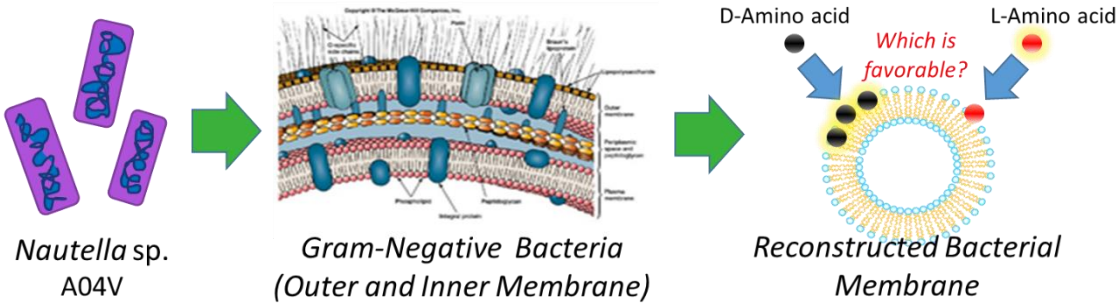

Fig. S2 Roles of bacteria membrane in chiral selection.

In our previous report, it has been reported that liposomes, constructed by phospholipids, showed the chiral recognition of L-amino acids (Ishigami et al., 2015). This suggests that the self-assembled membrane structure assists the chiral selective adsorption of amino acids onto the membrane. Therefore, in this research, the possible roles of A04V bacterial cell membrane were focused. To confirm the direct contribution of cell membrane components in D-amino acid uptake, the membrane lipids were extracted from bacteria, and then the reconstructed liposomes were prepared. Physicochemical membrane properties of reconstructed liposomes were investigated based on characterization methods as shown in Chapter II and Chapter III. Finally, the absorption behavior of amino acids onto the membrane was evaluated and optimized.

The experiments were conducted by several steps. Firstly, bacteria A04V were cultured in Marine Broth (MB) and harvested at the stationary phase (OD600 about 1.8) for extraction of lipids from outer, inner and whole bacterial membranes. Then, lipids from each membrane were reconstructed into liposomes and liposome membrane properties will be evaluated by fluorescent probes. Subsequently, the chiral selection in reconstructed membrane relating to membrane properties will be elucidated to finally design membranes inspired from bacteria membrane properties.

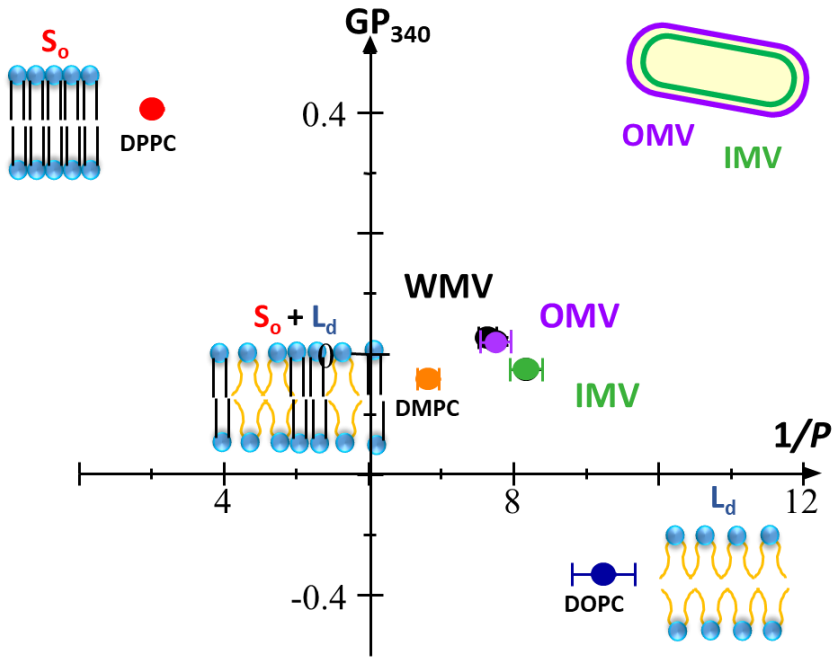

Fig. S3 Properties of reconstructed bacteria membranes indicated by DPH and Laurdan fluorescent probes at 30 ^{o}C.

Properties of reconstructed bacterial membranes analyzed by DPH and fluorescent probes

Lipids from outer (OMV), inner (IMV) and whole (WMV) bacterial membranes were extracted by Bligh and Dyer method. Consequently, the membrane properties were investigated by DPH and Laurdan fluorescent probes which refer the membrane fluidity (1/*P*) and polari\ty (GP_{340}), respectively **(Fig. S3)**. The results indicate that the membrane fluidity of reconstructed liposomes was higher as well as liposomes in disordered phase, while the membrane was rather hydrophobic (dehydrated). Previously, it is suggested that the hydrophobic environment (GP_{340}>0) plays an important role to enhance chiral selectivity (Ishigami et al., 2015). It is expected that the unique membrane properties of reconstructed liposomes contribute to adsorb amino acids selectively.

The absorption behavior ò Valine in reconstructed membranes

To investigate the absorption behavior of amino acids onto liposome membranes, D- and L-Valine (D-/L-Val) were selected as target molecules. Within 235 hours of

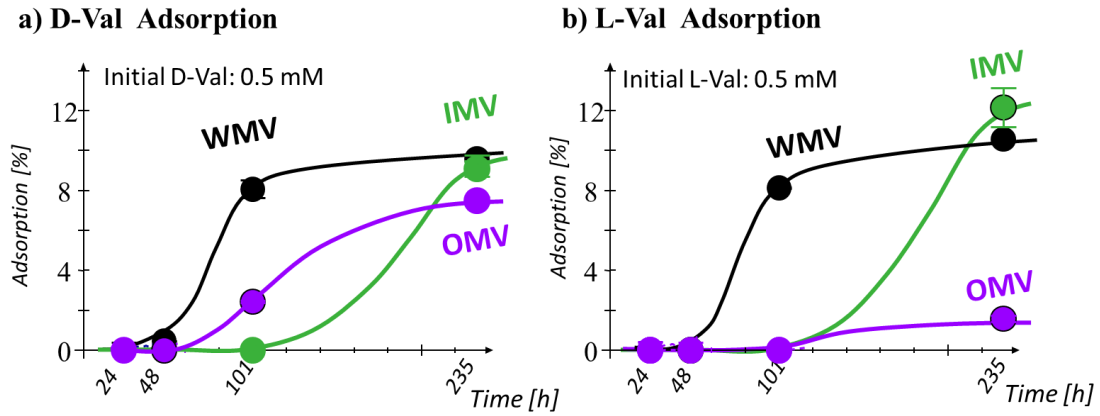

Fig. S4 The absorption behavior of reconstructed bacterial membranes with D- Val or L-Val.

incubation, the adsorption of D-Val was higher than that of L-Val in OMV, while in IMV and WMV the absorption of both D- and L-Val were equally (**Fig. S4**). This suggests that the outer bacterial membrane has a potential to interact with D-Val.

Conclusion and Future Plan

By using the reconstructed membrane from deep sea bacteria membrane, it was indicated that the absorption of D-amino acid related to the presence of membrane lipids. In next steps, lipids from outer bacteria membrane will be reconstructed and utilized for checking the absorption of D-Val. Then, lipid components from both outer and whole membranes will be identified to indicate the special lipid uptake D-amino acids. Finally, it will be reconstructed in liposome and regulated in properties to control the uptake of amino acids.

3. Control of membrane properties for regulating the interaction of membrane protein

The overexpression of proteins in cells are relating to tumors, especially the activation of epidermal growth factor receptor (EGFR) in membranes by interacting to epidermal growth factor (EGF). The purpose of this study is the control the activity of EGFR in membranes by regulating membrane properties (**Fig. S5**).

Liposomes with well-designed properties are as well-known as promising vehicles for drug carriers and model membranes for investigating the interaction of macromolecules occurring in the natural membranes. Thus, in this proposal study, liposomes modified with sterols like Chol, Lan and Erg will be employed to investigate and then control the mechanism interaction of membranes with EGFR. Finally, the liposome membranes will be designed and utilize as lipid therapies.

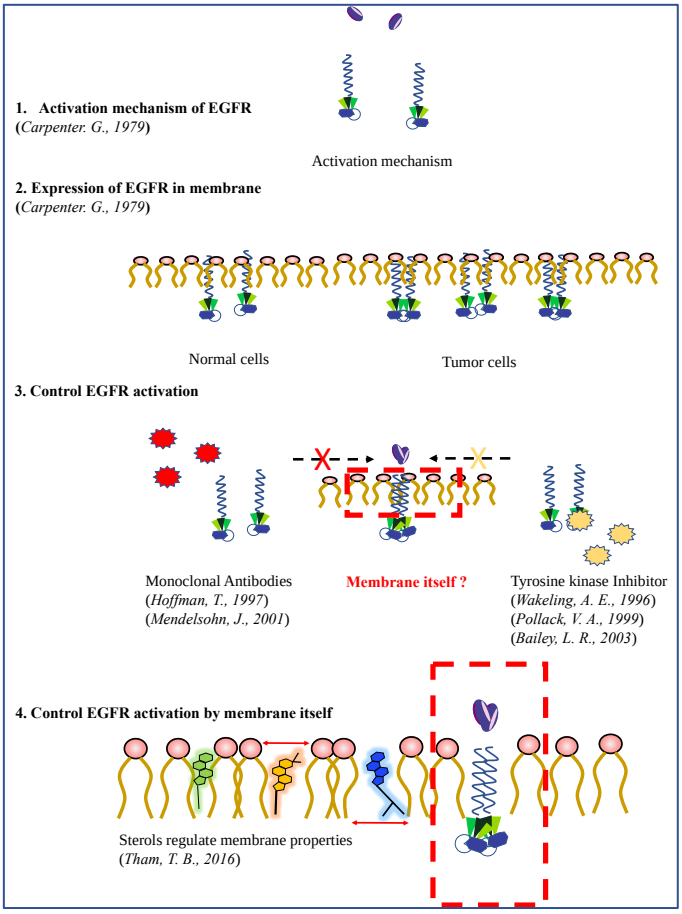

Fig. S5 The regulation of epidermal growth factor by membrane properties.

Nomenclatures

P	= Fluorescent polarization of probes imbedded in membranes	[-]
$1/P$	Membrane fluidity	[-]
G	Correction factor	[-]
GP_{340}	General polarization calculated at exciting light at 340 nm	[-]
z’	Normalize values	[-]
ε	Dielectric constant	[-]
I	Fluorescent intensity	[a. u.]
π	Surface pressure	mN/m
A	Surface area	$Å^2$/mol
ϕ	Quantum yield	[-]
C_s^{-1}	Compression modulus	mN/m
G	Gibbs free energy	[J]
I_{474}/I_{518}	Fluorescent intensity of ANS	[-]

List of Abbreviations

Chol	Cholesterol
Lan	Lanosterol
Erg	Ergosterol
DOPC	1,2-Dioleoyl-*sn*-glycerol-3-phosphocholine
DPPC	1,2-Dipamiltoyl-*sn*-glycerol-3-phosphocholine
DMPC	1,2-Dimyristoyl-*sn*-glycerol-3-phosphocholine
DLPC	1,2-Dilauroyl-*sn*-glycerol-3-phosphocholine
NMR	Nuclear magnetic resonance
Ld	Liquid disordered
Lo	Liquid ordered
So	Solid ordered
TMA-DPH	1-(4-Trimethylammoniumphenyl)-6-Phenyl-1,3,5-Hexatriene p-Toluenesulfonate
DPH	1-6-Phenyl-1,3,5-Hexatriene p-Toluenesulfonate
Prodan	N,N-Dimethyl-6-propionyl-2-naphthylamine
ANS	8-Anilino-1-naphthalenesulfonic acid
Laurdan	6-Dodecanoyl-N,N-dimethyl-2-naphthylamine
MLVs	Multi lamellar vesicles
LUVs	Large unilamellar vesicles
T_m	Melting temperature
E_x.	Excited wavelength
E_m.	Emission wavelength

References

Abe, F., and T. Hiraki. 2009. "Mechanistic role of Erg in membrane rigidity and cycloheximide resistance in Saccharomyces cerevisiae." *BBA–Biomembranes* 1788: 743-752.

Abrams, F. S., and E. London. 1993 . "Extension of the parallax analysis of membrane penetration depth to the polar region of model membranes: use of fluorescence quenching by a spin-label attached to the phospholipid polar headgroup." *Biochemistry* 32: 10826-10831.

Adachi, T., H. Takahashi, and I. Hatta. 1995. "Interdigitated structure of phospholipid-alcohol systems studied by x-ray diffraction ." *Biophys. J.* 68: 1850–1855.

Aden, H., R. Michael, A. Heinz, L. Peter, and P. Georg. 2008. "Differential modulation of membrane structure and fluctuations by plant sterols and cholesterol." *Biophys.* 94: 3935-3944.

Ali, M. D., K. H. Cheng, and Huang, J. 2007. "Assess the nature of cholesterol-lipid interactions through the chemical potential of Chol in phosphatidylcholine bilayers." *Proc. Natl. Acad. Sci. USA* 104: 5372–5377.

Ali, R., H. C. Kwan, and J. Huang. 2007. "Proc. Natl. Acad. Sci. U.S.A. ." *Assess the nature of cholesterol-lipid interactions through the chemical potential of Chol in phosphatidylcholine bilayers* 104: 5372-5377.

Ando, J., M. Kinoshita, J. Cui, H. Yamakoshi, K. Dodo, K. Fujita, M. Murata, and M. Sodeoka. 2015. "Sphingomyelin distribution in lipid rafts of artificial monolayer membranes visualized by Raman microscopy." *Proceedings of the National Academy of Sciences of the United States of America* 112: 4558-4563.

Andrew, J. B., W. W. Jong, A. T. Kathryn, and J. W. Michael. 2008. "Growth hormone receptor; mechanism of action." *Journal of Biochemistry & Cell Biology* 40: 1984-1989.

Arora, A., H. Raghuraman, and A. Chattopadhyay. 2004. "Influence of Chol and Erg on membrane dynamics: A fluorescence approach." *Biochemical and Biophysical Research Communications* 328: 920-926.

Arroyo-Lopez, F. N., Z. Salvado, and A. Querol. 2010 . "Susceptibility and resistance to ethanol in Saccharomyces strains isolated from wild and fermentative environments ." *Yeast* 27: 1005–1015.

Bacia, K., P. Schwille, and T. Kurzchalia. 2005. "Sterol structure determines the separation of phases and the curvature of the liquid-ordered phase in model membranes ." *Proc. Natl. Acad. Sci. USA* 102: 3272-3277.

Banginski, M., A. Tempczyk, and E. Borrowshki. 1989. "Comparative conformational analysis of Chol and Erg by molecular mechanics." *Eur. Bipphys. J.* 17: 159-166.

Barclay, J. L., L. M. Kerr, L. Arthur, J. E. Rowland, C. N. Nelson, M. Ishikawa, E. M. Aniello, M. White, P. G. Noakes, and M. J. Waters. 2010. ", In vivo targeting of the growth hormone receptor (GHR) Box1 sequence demonstrates that the GHR does not signal exclusivelythrough JAK2." *Mol. Endocrinol* 24: 204–217.

Barnard, R., and M. J. Waters. 1997. "The serum GH binding protein: pregnant with possibilities." *J. Endocrinol* 153: 1-14.

Barry, J. A., and K. Gawrisch. 1994 . "Direct NMR evidence for ethanol binding to the lipid-water interface of phospholipid bilayers ." *Biochem.* 33 : 8082–8088.

Beck, J. G., D. Mathieu, C. Loudet, S. Buchoux, and E. J. Dufourc. 2007. "Plant sterols in "rafts": a better way to regulate membrane thermal shocks." *FASEB J.* 21: 1714-1723.

Bennett, W. F. D., J. L. MacCallum, and D. P. J. Tieleman. 2009. "Thermodynamic Analysis of the Effect of Chol on Dipalmitoylphosphatidylcholine Lipid Membranes." *Am. Chem. Soc.* 131: 1972-1978 .

Bernsdorff, C, and R. Winter. 2003. "Differential properties of the sterols cholesterol, ergosterol, sistosterol, trans-7-hydroChol and Lan on DPPC bilayer order." *J. Phys. Chem.* 107: 10658.

Bisson, L. F. 1990 . "Stuck and sluggish fermentations ." *Am. J. Enol. Vitic.* 50: 107–119.

Bittman, R. 1997. "Has nature designed the Chol side chain for optimal interaction with cholesterol?" In *Cholesterol: Its Functions and Metabolism in Biology and Medicine*, edited by R. Bittman, 145-172. New York: Plenum Press.

Bloch, K. E. 1983. "Sterol structure and membrane function." *CRC Crit. Rev. Biochem.* 14: 47-92.

Bloom, M., and Mouritsen O. G. 1988. "The evolution of membranes." *Can. J. Chem.* 66: 706–712.

Brooks, A. J., and M. J. Waters. 2010. "The growth hormone receptor: mechanism of activation and clinical implications." *Nat. Rev. Endocrinol* 6: 515-525.

Brown, D. A., and E. London. 2000. "Structure and function of sphingolipid- and cholesterol-rich membrane rafts." *J. Biol. Chem.* 275: 17221–17224.

Brown, R. J., J. J. Adams, R. A. Pelekanos, Y. Wan, W. J. McKinstry, and K. Palethorpe. 2005. "Model for growth hormone receptor activation based on subunit rotation within a receptor dimer." *Nat. Struct. Mol. Biol.* 12: 814-821.

Bui, H. T., H. Umakoshi, K. X. Ngo, M. Nishida, T. Shimanouchi, and R. Kuboi. 2008. "Liposome membrane itself can affect gene expression in the Escherichia coli cell-free translation system." *Lamgmuir* 24: 10537-10542.

Cevc, G. 1990. "Membrane electrostatics." *Biochim. Biophys. Acta.* 1031: 311-382.

Chang, L. C., Y. Y. Chang, and C. S. Gau. 2008. "Interfacial properties of Pluronics and the interactions between Pluronics and cholesterol/DPPC mixed monolayers." *J. Colloid Interf. Sci.* 322,: 263-273.

Chattopadhyay, A., and E. London. 1987. "Parallax method for direct measurement of membrane penetration depth utilizing fluorescence quenching by spin-labeled phospholipids." *Biochemistry* 39-45: 26.

Chen, Z., Y. Sato, I. Nakazawa, and Y. Suzuki. 1995. "Interactions between bacteriohopane-32, 33, 34, 35-tetrol and liposomal membranes composed of dipalmitoylphosphatidylcholine." *Biol. Pharm. Bull* 18: 477-480.

Chong, P. L., W. Zhu, and B. Venegas. 2009. "On the lateral structure of model membranes containing cholesterol." *Biochim. Biophys. Acta* 1788: 2-11.

Cicuta, P., S. L. Keller, and S. L. Veatch. 2007 . "Diffusion of Liquid Domains in Lipid Bilayer Membranes." *J. Phys. Chem. B.* 111: 3328−3331.

Coskun, U., M. Grybeck, D. Drechdel, and K. Simons. 2011. "Regulation of human EGF receptor by lipids." *Proc. Natl. Acac. Sci. USA* 108: 9044-9048.

Cournia, Z., G. M. Ullmann, and J. C. Smith. 2007. "Differential effects of cholesterol, Erg and Lan on a dipalmitoyl phosphatidylcholine membrane: A molecular dynamics simulation study." *J. Phys. Chem. B.* 111: 1786–1801.

Cwiklik, L., A. J. A. Aquino, M. Vazdar, P. Jurkiewicz, J. Pittner, M. Hof, and H. Lischka. 2010. "Absorption and fluorescence of PRODAN in phospholipid bilayers: A combined quantum mechanics and classical molecular dynamics study." *J. Phys. Chem. A* 115: 11428-11437.

Czub, J., and M. Baginski. 2006. "Comparative molecular dynamics study of lipid membranes containing Chol and ergosterol." *Biophys. J.* 90: 2368-2382.

Dahl, C., Dahl, J., and K. Bloch. 1980. "Effect of alkyl-substituted precursor of Chol on artificial and natural membranes and on the viability of Mycoplasma capricolum." *Biochemistry* 19: 1462–1467.

David, A. M., N .A. H. L. Ruthven, and N. M. Ronald. 2006. "Comparative calorimetric and spectroscopic studies of the effects of Lan and Chol on the thermotrophic phase behavior and organization of dipalmitoylphosphatidinecholine bilayer membranes." *Biophys. J.* 91: 3327–3340.

Davies, J. T., and E. K. Rideal. 1963. "Interfacial Phenomena." 265. New York: Academic Press. 1963. *Interfacial Phenomena.* New York and London: Academic Press.

Davies, M. A., H. F. Schuster, J. W. Brauner, and R. Mendelsohn. 1990. "Effects of Chol on conformational disorder in dipalmitoylphosphatidylcholine bilayers. A quantitative IR study of the depth dependence." *Biochemistry* 29: 4368-4373.

Davis, J. H. 1993. "The molecular dynamics, orientation order, and thermodynamic phase equilibria of cholesterol/phosphatidylcholine mixtures." In *Chol in membrane models*, edited by L. Finegold, 67-136. Boca Raton: CRC Press.

Demchenko, A. P., Y. Mely, G. Duportail, and A. S. Klymchenko. 2009. "Monitoring biophysical properties of lipid membranes by environment-sensitive fluorescent probes." *Biophysical Journal* 96: 3461-3470.

DeMeyer, F., and B. Smit. 2009. "Effect of Chol on the structure of a phospholipid bilayer." *Proceedings of the National Academy of Sciences of the United States of America* 106: 3654-3658.

Desmond, E., and S. Gribaldo. 2009. "Phylogenomics of Sterol Synthesis: Insights into the Origin, Evolution, and Diversity of a Key Eukaryotic Feature." *Genome Biol. Evol.* 1: 364-381.

Dhanikula, A. B., and R. Panchagnula. 2008. "Fluorescence anisotropy, FT-IR spectroscopy and 31-P NMR studies on the interaction of paclitaxel with lipid bilayers." *Lipids* 43: 569-579.

Dingle, J. T., J. L. Gordon, B. L. Hazleman, C. G. Knight, D. P. Thomas, N. C. Phillips, I. H. Shaw, et al. 1978. "Novel treatment for joint inflammation." *Nature* 271: 372-373.

Dluhy, R. A., R. Mendelsohn, H. L. Casal, and H. H. Mantsch. 1983. "Interaction of dipalmitoylphosphatidylcholine and dimyristoylphosphatidylcholine-d54 mixtures with glycophorin. A Fourier transform infrared investigation." *Biochemistry* 22: 1170-1177.

Dufourc, E. J., E. J. Parish, S. Chitrakorn, and I. C. P. Smith. 1984. "Structural and dynamical details for the cholesterol-lipid interaction as revealed by deuterium NRM." *Biochemistry* 23: 6062–6071.

Duong, B. T. T., T. T. Bui, D. T. Quyen, T. T. Nguyen, and V. Q. Dong. 2013. "Molecular cloning, expression and purification of Bovine hormone (bST) in Eschrichia coli." Hanoi, : National Biotechnology Conference.

Dutta, P., J. B. Peng, B. Lin, J. B. Ketterson, M. Prakash, P. Georgopoulos, and S. Ehrlich. 1987. "X-ray diffraction studies of organic monolayers on the surface of water." *Physical Review Letters* 58: 2228-2231.

Dynarowicz-LAtka, P., and K. Haac-Wydro. 2004. "Interactions between phosphatidylcholines and Chol in monolayers at the air/water interface." *Colloids Surf. B* 37: 21-25.

Elie, D., and G. Simonetta. 2009. "Phylogenomics of Sterol Synthesis: Insights into the Origin, Evolution, and Diversity of a Key Eukaryotic Feature." *Genome Biol Evol* 1: 364–381.

Endress, E., K. Bayerl, S. Prechtel, C. Maier, R. Merkel, and T. M. Bayerl. 2002. "The effect of cholesterol, Lan and Erg on lecithin bilayer; mechanical properties at molecular and microscopic dimensions: a solid-state NMR and micropipette study." *Langmuir* 18: 3293–3299.

Epand, R. F., R. Kraayenhof, G. J. Sterk, H. W. Wong, and R. M. Epand. 1996. "Fluorescent probes of membrane surface properties." *Biochim Biophys Acta.* 1284: 191-195.

Epand, R. M., A. D. Bain, B. G. Sayer, D. Bach, and E. Wachte. 2002. "Properties of mixtures of Chol with phosphatidylcholine or with phosphatidylserine studied by 13C magic angle spinning nuclear magnetic resonance." *Biophys. J.* 83: 2053-2063.

Feller, S. E., C. A. Brown, and K. Gawrisch. 2002 . "Nuclear Overhauser enhancement spectroscopy cross-relaxation rates and ethanol distribution across membranes ." *Biophys. J.* 82: 1396–1404.

Franks, N. P. 1976. "Structural analysis of hydrated egg lecithin and Chol bilayers. I. X-ray diffraction." *J. Mol. Biol.* 100: 345–358.

Gaines, G. L. 1966. *Insoluble Monolayers at Liquid/Gas Interfaces.* New York.

Gershfeld, N L. 1976. "Physical chmistry of lipid films at fluid interfaces." *Annu. Rev. Phys. Chem.* 27: 3489-368.

Gorter, E, and F Grendel. 1925. "On biomolecular layers of lipoids on the cromocytes of the blood." *J. Exp. Med.* 41 (4): 439-443.

Gryczynski, I., J. Malicka, Y. Shen, Z. Gryczynski, and J. R. Lakowicz. 2002. "Multiphoton excitation of fluorescence near metallic particles: Enhanced and localized excitation." *J. Phys. Chem.* 106: 2191-2195.

Gumi-Audenis, B., L. Costa, F. Carl, F. Comin, F. Sanz, and M. I. Giannotti. 2016. " Structure and nanomechanics of model membranes by atomic force microscopy and spectroscopy: Insights into the role of Chol and sphingolipids." *Membranes* 6: 58.

Halling, K. K., and J. P. Slotte. 2004. "Membrane properties of plant sterols in phospholipid bilayers as determined by differential scanning calorimetry, resonance energy transfer and detergent-induced solubilization." *Biochimica et Biophysica Acta - Biomembranes* 1664: 161-171.

Hayashi, K., T. Shimanouchi, K. Kato, T. Miyazaki, A. Nakamura, and H. Umakoshi. 2011. "Span 80 vesicles have a more fluid, flexible and “wet” surface than phospholipid liposomes." *Colloids Surf. B: Biointerfaces* 87: 28–35.

Helen, W. 2015. "Biological membranes." *Esssays in biochemistry* 59: 43-69.

Henin, J., and C. Chipot. 2006. "Hydrogen-bonding patterns of Chol in lipid membranes." *Chem. Phys. Lett.* 425: 329-335.

Henon, S., and J. Meunier. 1991. "Microscope at the Brewster angle: direct observation of first-order phase transitions in monolayers." *Rev Sci Instrum* 62: 936-939.

Henriksen, J., A. C. Rowat, and J. H. Ipsen. 2004. "Vesicle fluctuation analysis of the effects of sterols on membrane bending rigidity." *Eur. Biophys. J.* 33: 732–741.

Henriksen, J., A. C. Rowat, E. Brief, Y. W. Hsueh, J. L. Thewalt, M. J. Zuckermann, and J. H. Ipsen. 2006. "Universal behavior of membranes with sterols." *Biophys. J.* 90 : 1639-1649.

Hirose, M., Ishigami, T., Suga, K., Umakoshi, H. 2015. "Liposome membrane as a platform for the l-Pro-Catalyzed michael addition of trans-β-Nitrostyrene and acetone." *Langmuir* 31: 12968–12974.

Hodzic, A., M. Rappolt, H. Amenitsch, P. Laggner, and G. Pabst. 2008. "Differential Modulation of Membrane Structure and Fluctuations by Plant Sterols and Cholesterol." *Biophysical Journal* 94: 3935-3922.

Holopainen, J. M., A. J. Metso, J. P Mattila, A. Jutila, and P. K. J. Kinnunen. 2004. "Evidence for the lack of a specific interaction between Chol and sphingomyelin." *Biophys. J.* 86: 1510-1520.

Honig, D., and D. Mobius. 1991. "Direct visualization of monolayers at the air–water interface by Brewster angle microscopy." *J Phys Chem* 95: 4590-4592.

Hsueh, Y.-W., K. Gilbert, C. Trandum, M. Zuckermann, and J. Thewalt. 2005. "The effect of Erg on dipalmitoylphosphatidylcholine bilayers: A deuterium NMR and calorimetric study ." *Biophys. J.* 88: 1799-1808.

Huang, J., and G. W. Feigenson. 1999. "A microscopic interacrion model of maximum solibility of." *Biophys. J.* 76: 2142-2157.

Hung, W.-C., M.-T. Lee, H. Chung, Y.-T. Sun, H. Chen, N. E. Charron, and H. W. Huang. 2016. "Comparative Study of the Condensing Effects of Erg and Cholesterol." *Biophys. J.* 110: 2026-2033.

Ihle, J. N., and D. G. Gilliland. 2007. "Jak2: Normal function and role in hematopoietic disorders." *Curr. Opin. Genet. Dev.* 17: 8-14.

Ipsen, J. H., O. G. Mouritsen, and M. Bloom. 1990. "Relationship between lipid membrane area, hydrophobic thickness, and acyl-chain orientational order." *Biophys. J.* 57: 405–412.

Ishigami, T., K. Suga, and H. Umakoshi. 2015. "Chiral Recognition of l-Amino Acids on Liposomes Prepared with l-Phospholipid." *ACS Appl. Mater. Interf.* 7: 21065-21072.

Israelachvili, J. N. 1992. *Intermolecular and Surface Forces: With Applications to Colloidal and Biological Systems (.* London: Academic Press.

James, A. S., and A. Sterling. 2012. "Wheaten, Paulo F. Almeida. Phase separation and fluctuations in mixtures of a saturated and an unsaturated phospholipid." *Biophys. J.* 102: 2526–2535.

Jurak, M. 2013. "Thermodynamic aspects of Chol effect on properties of phospholipid monolayers: Langmuir and Langmuir-Blodgett monolayer study." *J. Phys. Chem. B* 117: 3496-3502.

Kakoli, M., U. B. Iban, T. Tomohiko, W. Graham, and M. E. Donald. 2004. "Modulation of the bilayer thickness of exocytic pathway membranes by membrane proteins rather than Chol ." *Proc. Natl. Acad. Sci. USA* 1001: 4083-4088.

Kannenberg, E., A. Blume, R. N. McElhaney, and K. Poralla. 1983. "Monolayer and calorimetric studies of phosphatidylcholines containing branched-chain fatty

acids and of their interactions with Chol and with a bacterial hopanoid in model membranes." *BBA-Biomembranes* 733: 111-116.

Kannenberg, E., K. Poralla, and A. Blume. 1980. "A Hopanoid from the thermo-acidophilic Bacillus acidocaldarius condenses membranes." *Naturwissenschaften* 67: 458-459.

Karen, S., M. Juha-Pekka, and K. J. K. Paavo. 2008. "Interfacial behavior of Cholesterol, Ergosterol, and Lan in Mixtures with DPPC and DMPC." *Biophysical Journal* 95: 2340-2355.

Karp, G. 2004. *Cell and Molecular Biology: Concepts and Experiments, 4th edition.* Wiley and Sons. New York.

Keller, S. L., T. G. Anderson, and H. M. McConnell. 2000. "Miscibility critical pressures in monolayers of ternary lipid mixtures." *Biophys. J.* 79: 2033-2042.

Kjaer, K., J. Als-Nielsen, C. A. Helm, L. A. Laxhuber, and H. Mohwald. 1987. "Ordering in lipid monolayers studied by synchrotron x-ray diffraction and fluorescence microscopy." *Physical Review Letters* 58: 2224-2227.

Klemm, R. W., C. S. Ejsing, M. A. Surma, H. J. Kaiser, M. J. Gerl, J. L. Sampaio, Q. Robillard, et al. 2009. "Segregation of sphingolipids and sterols during formation of secretory vesicles at the trans-Golgi network." *J. Cell Biol.* 185: 601-612.

Koynova, R., B. Tenchov, L. Wang, and R. C. Macdonald. 2009. "Hydrophobic moiety of cationic lipids strongly modulates their transfection activity." *Mol. Pharm.* 6: 951-958.

Kranenburg, M., M. Vlaar, and B. Smit. 2004 . "Simulating induced interdigitation in membranes ." *Biophys. J.* 87: 1596–1605.

Krasnowska, E .K., E. Gratton, and T. Parasassi. 1998. "Prodan as a membrane surface fluorescence probe: Partitioning between water and phospholipid phases." *Biophys. J.* 74: 1984-1993.

Kurniawan, J., K. Suga, and T. L. Kuhl. 2017. "Interaction Forces and Membrane Charge Tunability: Oleic Acid Containing Membranes in Different pH Conditions ." *BBA-Biomembr* 1859 : 211-217 .

Lentz, B. R. 1989. "Membrane “fluidity” as detected by diphenylhexatriene probes." *Chem. Phys. Lipids* 50: 171–190.

Lentz, B. R. 1993. "Use of fluorescent probes to monitor molecular order and motions within liposome bilayers ." *Chem. Phys. Lipids* 64: 99-116.

Leonard, A., and A. Milon. 1993. "Modulation of membrane hydrophobic thickness by cholesterol, cycloartenol and hopanoid. A solid state 2H-NMR Study." *Bull. Magn. Reson* 15: 124-127.

Levine, Y. K., and M. H. F. Wilkins. 1971. "Structure of oriented lipid bilayers." *Nat. New Biol.* 230: 69–72.

Li, H., P. M. Bartold, C. Z. Zhang, R. W. Clarkson, W. G. Young, and M. J. Waters. 1998. "GH and IGF-1." *Endocrinology* 139: 3855-3862.

Lichanska, A. M., and M. J. Waters. 2008. ", How growth hormone controls growth, obesity and sexual dimorphism." *Trends Genet.* 24: 41-47.

Lingwood, D., and K. Simons. 2010. "Lipid rafts as a membrane-organizing principle." *Science* 327: 46-50.

Losche, M,, E. Sackmann, and H. Mohwald. 1983. "A fluorescence microscopic study concerning the phase diagram of phospholipids." *Ber Bunsenges Phys Chem* 87: 848-852.

Lu, X., A. W. Gross, and H. F. Lodish. 2006. "Active conformation of the erythropoietin receptor: Random and cysteine-scanning mutagenesis of the extracellular juxtamembrane and transmembrane domains." *J. Biol. Chem.* 281: 7002-7011.

Ma, M., and Z. L. Liu. 2010 . "Mechanisms of ethanol tolerance in Saccharomyces cerevisiae." *Appl. Microbiol. Biotechnol* 87: 829–845.

MacDermaid, C. M., H. K. Kashyap, R. H. Devane, W. Shinoda, J. B. Klauda, M .L. Klein, and G. Fiorin. 2015. "Molecular dynamics simulations of cholesterol-rich membranes using a coarse-grained force field for cyclic alkanes." *Journal of Chemical Physics* 143: 243144.

MacDonald, R. C., and S. A. Simon. 1987. "Lipid monolayer states and their relationships to bilayers." *Biophysics* 4089-4093.

MacGregor, R. B., and G. and Weber. 1981. "Fluorophores in polar media: spectral effects of the Langevin distribution of electrostatic interaction." *Ann. N. Y. Acad. Sci.* 24: 140-154.

Maier, O., V. Oberle, and D. Hoekstra. 2002. "Fluorescent lipid probes: some properties and applications (a review)." *Chem Phys Lipids* 116: 3-18.

Mannock, D. A., R. N. A. Lewis, and R. N. McElhaney. 2006. "Comparative colorimetric and spectroscopic studies of the effects of Lan and Chol on the thermotropic phase behavior and organization of dipalmitoylphosphatidylcholine bilayer membranes." *Biophys. J.* 91: 3327-3340.

Marsh, D. 1996. "Lateral pressure in membranes." *Biochim. Biophys. Acta* 1286: 183-223.

McConnell, H. M., and A. Radhakrishnan. 2003. "Condensed complexes of Chol and phospholipids ." *Biochim. Biophys. Acta* 1610: 159-173.

McConnell, H., and A. Radhakrishnan. 2008. "Molecular motion at the critical point in lipid membranes ." *Biophys. J.* 95: L22-L24.

McMullen, T. P. W., and R. N. McElhaney. 1996. "Physical studies of cholesterol–phospholipid interactions." *Curr. Opin. Coll. Interf. Sci.* 1: 83–90.

Miao, L., M. Nielsen, J. Thewalt, J. H. Ipsen, M. Bloom, M. J. Zuckermanm, and O. G. Mouritsen. 2002. "From Lan to cholesterol: structure evolution and differential effects on lipid bilayers." *Biophys. J.* 82: 1429-1444.

Minones, J. J., S. Pais, J. Minones, O. Conde, and L. P. Dynarowicz. 2009. "Interactions between membrane sterols and phospholipids in model mammalian and fungi cellular membranes — A Langmuir monolayer study." *Biophys. Chem.* 140: 69-77.

Mitra, K., I. Ubarretxena-Belandia, T. Taguchi, G. Warren, and D. M. Engelman. 2004. "Modulation of the bilayer thickness of exocytic pathway membranes by membrane proteins rather than Chol ." *Proc. Natl. Acad. Sci. USA* 1001: 4083-4088.

Miyoshi, T., and S. Kato. 2015. "Detailed Analysis of the Surface Area and Elasticity in the Saturated 1,2-Diacylphosphatidylcholine/Chol Binary Monolayer System." *Langmuir* 31: 9086-9096.

Montich, G. G., J. J. Cosa, and B. Maggio. 1988. "Interaction of 1-anilinonaphthalene 8-sulfonic acid with interfaces containing cerebrosides, sulfatides and gangliosides." *Chem. Phys.* 49: 111-117.

Morrow, M. R., D. Singh, D. Lu, and C. W. Grant. 1995. "Glycosphingolipid fatty acid arrangement in phospholipid bilayers: Chol effects." *Biophys. J.* 68: 179-186.

Mouritsen, O. G., Zuckermann, M. J. 2004. "What's so special about cholesterol?" *Lipids* 39: 1101–1113.

Nagimo, A., Y. Sato, and Y. Suzuki. 1991. "Electron spin resonance studies of phosphatidylcholine interacted with Chol and with a hopanoid in liposomal membrane." *Chem. Pharm. Bull* 39: 3071-3074.

Nyberg, F., and M. Hallberg. 2013. "Growth hormone and cognitive function." *Nat. Rev. Endocrinol* 9: 357-365.

Okonogi, T. M., and H. M. McConnell. 2004 . "Contrast Inversion in the Epifluorescence of Cholesterol-Phospholipid Monolayers." *Biophys. J.* 86: 880-890.

Olah, G. A., H. W. Huang, and Y. L. Wu. 1991 . "Location of ion-binding sites in the gramicidin channel by x-ray diffraction." *J. Mol. Biol.* 218: 847–858.

Oleary, T. J. 1993. "Vibrational spectroscopy of cholesterol-lipid interactions." In *Chol in Membrane Models*, edited by L. Finegold, 175-195. Boca Raton: CRC Press.

Pandit, S. A., S. Vasudevan, S. W. Chiu, R. J. Mashl, E. Jacobsson, and H. L. Scott. 2004 . "Complexation of phosphatidylcholine lipids with cholesterol." *Biophys. J.* 86: 1345-1356.

Parasassi, T., A. M. Giusti, E. Gratton, E. Monaco, M. Raimondi, G. Ravagnan, and O. Sapora. 1994b. ". Evidence for an increase in water concentration in bilayers after oxidative damage of phospholipids induced by ionizing radiation ." *Int. J. Radiat. Biol.* 65: 329–334.

Parasassi, T., and E. Gratton. 1995. "Membrane lipid domains and dynamics as detected by Laurdan fluorescence." *J. Fluoresc.* 5: 59−69.

Patzer, E. J., R. R. Wagner, and Y. Barenholz. 1978. "Chol oxidase as a probe for studying membrane organization." *Nature* 274: 394-395.

Pawez, W., K. Sabina, and L. Marta. 2011. "Variations in the condensing effect of Chol on saturated versus unsaturated phosphatidylcholines at low and high sterol concentration ." *Langmuir* 27: 5433-5444.

Pencer, J., M. P. Nieh, T. A. Harroun, S. Krueger, C. Adams, and J. Katsaras. 2005. "Bilayer thickness and thermal response of dimyristolylphosphatidylcholine unilamellar vesicle containing cholesterol, Erg and lanosterol: a small-angle neutron scattering study." *Biochim. Biophys. Acta* 1720: 84-91.

Penfold, J., and R. K. Thomas. 1990. "The application of the specular reflection of neutrons to the study of surfaces and interfaces." *Journal of Physics: Condensed Matter* 2: 1369-1412.

Pike, L. J. 2009. "The challenge of lipid rafts." *J. Lipid Res.* 50: S323-S329.

Poralla, K., E. Kannenberg, and A. Blume. 1980. "A glycolipid containing hopane isolated from the acidophilic, thermophilic Bacillus acidocaldarius, has a cholesterol-like function in membranes." *FEBS Letters* 113: 107-110.

Presti, F. T., J R. J. Pace, and S. I. Chan. 1982. "Cholesterol-phospholipid interaction in membranes. 2. Stoichiometry and molecular packing of cholesterol-rich domains." *Biochemistry* 21: 3831–3835.

Radhakrishnan, A., and H. M. J. McConnell. 1999. "Cholesterol−Phospholipid Complexes in Membranes." *Am. Chem. Soc.* 121: 486–487.

Radhakrishnan, A., and H. McConnell. 2005. "Condensed complexes in vesicles containing Chol and phospholipids ." *Proc. Nat. Acad. Sci. U.S.A.* 102: 12662-12666.

Radhakrishnan, A., T. G. Anderson, and H. M. McConnell. 2000. "Condensed complexes, rafts, and the chemical activity of Chol in membranes." *Proc. Nat. Acad. Sci. U.S.A.* 97: 12422-12427.

Ramage, G., R. Rajendran, L. Sherry, and C. Williams. 2012. "Fungal biofilm resistance ." *Int. J. Microbiol.* 2012: 528521.

Reiter, R., H. Motschmann, H. Orendi, A. Nemetz, and W. Knoll. 1992. "Ellipsometric Microscopy. Imaging Monomolecular Surfactant Layers at the Air–Water Interface." *Langmuir* 8: 1784-1788.

Ribeiro, N., S. Streiff, D. Heissler, M. Elhabiri, A.M. Albrecht-Gary, M. Atsumi, M. Gotoh, L. Desaubry, Y. Nakatani, and G. Ourisson. 2007. "Reinforcing effect of bi- and tri-cyclopolyprenols on 'primitive' membranes made of polyprenyl phosphates." *Tetrahedron* 63: 3395-3407.

Ridgway, N. D., and R.S. McLeod. 2015. *Biochemistry of Lipids, Lipoproteins and Membranes.* 6. Amsterdam: Elsevier B. V.

Roche, Y., P. Gerbeau-Pissot, B. Buhot, D. Thomas, L Bonneau, J. Gresti, S. Mongrand, J. M. Perrier-Cornet, and F. Simon-Plas. 2008. "Depletion of phytosterols from the plant plasma membrane provides evidence for disruption of lipid rafts." *FASEB Journal* 22: 3980-3991.

Rubenstein, J. L., B. A. Smith, and H. M. McConnell. 1979. "Lateral diffusion in binary mixtures of Chol and phosphatidylcholines." *Proc. Natl. Acad. Sci. USA* 15-18: 76.

Sabatini, K., J. P. Mattila, and P. K. J. Kinnunen. 2008. "Interfacial behavior of cholesterol, ergosterol, and Lan in mixtures with DPPC and DMPC." *Biophys. J.* 95: 2340-2355.

Saenz. 2010. "Hopanoid enrichment in a detergent resistant membrane fraction of Crocosphaera watsonii: implications for bacterial lipid raft formation." *Org. Geochem* 41: 853-856.

SAenz, J. P., D. Grosser, A. S. Bradley, T. J. Lagny, Oksana Lavrynenko, M. Broda, and K. Simons. 2015. "Hopanoids as functional analogues of Chol in bacterial membranes." *Proceedings of the National Academy of Sciences of the United States of America* 112: 11971-11976.

Saenz, J. P., E. Sezgin, P. Schwille, and K. Simons. 2012. "Functional convergence of hopanoids and sterols in membrane ordering." *Proc. Natl Acad. Sci. USA* 109: 14236-14240.

Saito, H., and N. Suzuki. 2007. "Distributions and sources of hopanes, hopanoic acids and hopanols in Miocene to recent sediments from ODP Leg 190, Nankai Trough. ." *Org Geochem* (38): 1715–1728.

Sankaram, M. B., and T. E. Thompson. 1991. "Cholesterol-induced fluid-phase immiscibility in membranes ." *Proc. Natl. Acad. Sci. USA* 88: 8686-8690.

Sato, Y., Z. Chen, and Y. Suzuki. 1995. "Thermodynamic effects of hopanoids on synthetic and bacterial phospholipid membranes." *Chem. Pharm. Bull* 43: 1241-1244.

Schaller, H. 2003 . "The role of sterols in plant growth and development." *Prog Lipid Res.* 3 (42): 163-75.

Schonbrunn, E., S. Eschenburg, K. Luger, W. Kabsch, and N. Amrhein. 2000. "Structural basis for the interaction of the fluorescence probe 8-anilino-1-naphthalene

sulfonate (ANS) with the antibiotic target MurA." *Proc Natl Acad Sci USA* 97: 6345-6349.

Sekiguchi, A., H. Ogino, H. Yamauchu, and M. Abe. 1995. "Molecular unteractions between phospholipids and glycolipids in a lipid bilayer." *Colloids and Surfaces B: Biointerfaces* 287-296.

Semer, R., and E. Gelerinter. 1979. "A spin label study of the effects of sterols on egg lecithin bilayers." *Chem. Phys. Lipids* 23: 201–211.

Sennato, S., F. Bordi, C. Cametti, C. Coluzza, A. Desideri, and S. Rufini. 2005. "Evidence of domain formation in cardiolipin−glycerophospholipid mixed Monolayers. A thermodynamic and AFM study." *J. Phys. Chem. B* 109: 15950-15957.

Sessions, A. L., L. Zhang, P. V. Welander, D. V. Doughty, R. E. Summons, and D. K. Newman. 2013. "Identification and quantification of polyfunctionalized hopanoids by high temperature gas chromatography-mass spectrometry." *Organic Geochemistry* 56: 120-130.

Shimizu, T., M. Masuda, and H. Minamikawa. 2005. "Supramolecular Nanotube Architectures Based in Amphiphilic Molecules." *Chem. Rev.* 105: 1401-1443.

Simons, K., and E. Ikonen. 1997. "Functional rafts in cell membranes." *Nature* 387: 569–572.

Simons, K., and E. Ikonen. 2000. "How cells handle cholesterol." *Science* 290: 1721–1726.

Singer, S. J., and G. L. Nicolson. 1972. "The fluid mosaic midel of the structure of cell membranes." *Science* 175: 720-731.

Slavik, J. 1982. "Anilinonaphthalene sulfonate as a probe of membrane composition and function." *Biochim. Biophys. Acta.* 694: 1-25.

Slotte, J. P. 1999. "Sphingomyelin-Chol interactions in biological and model membranes." *Chem. Phys. Lipids* 102: 13–27.

Smondyrev, A. M., and M. L. Berkowitz. 2001 . "Molecular dynamics simulation of the structure of dimyristoylphosphatidylcholine bilayers with cholesterol, ergosterol, and lanosterol." *Biophys. J.* 80: 1649–1658.

Somerharju, P. 2002. "Pyrene-labeled lipids as tools in membrane biophysics and cell biology." *Chem Phys Lipids* 116: 57-74.

Somerharju, P., J. A. Virtanen, and C. K. Hon. 1999. "Lateral organisation of membrane lipids. The superlattice view." *Biochim. Biophys.* 1440: 32-48.

Spector, A. A., and M. A. Yorek. 1985. "Membrane lipid composition and cellular function." *J. Lipid Res.* 1015-1035.

Stephanie Nichols-Smith, Shia-Yen Teh, Tonya L. Kuhl. 2004. "Thermodynamic and mechanical properties of model mitochondrial membranes." *Biochimica et Biophysica Acta* 1663: 82-88.

Stevens, M. M., A. R. Honerkamp-Smith, and S. L. Keller. 2010. "Solubility limits of cholesterol, lanosterol, ergosterol, stigmasterol, and β-sitosterol in electroformed lipid vesicles." *Soft Matter* 6: 5882-5890.

Stockton, G. W., and I. C. Smith. 1976. "A deuterium nuclear magnetic resonance study of the condensing effect of Chol on egg phosphatidylcholine bilayer membranes. I. Perdeuterated fatty acid probes." *Chem. Phys. Lipids* 17: 251-263.

Stottrup, B. L., D. S. Stevens, and S. L. Keller. 2005. "Miscibility of ternary mixtures of phospholipids and Chol in monolayers, and application to bilayer systems." *Biophys. J.* 88: 269-276.

Stryer, L. 1965. "The interaction of a naphthalene dye with apomyoglobin and apohemoglobin. A fluorescent probe of non-polar binding sites." *J. Mol. Biol.* 13: 482-495.

Stubbs, C. D., C. Ho, and S. J. Slater. 1995. "Fluorescence techniques for probing water penetration into lipid bilayers." *J. Fluorescence* 5: 19-28.

Su, Y., Q. Li, L. Chen, and Z. Yu. 2007. "Condensation effect of cholesterol, stigmasterol, and sitosterol on dipalmitoylphosphatidylcholine in molecular monolayers." *Colloids Surf., A* 293: 123-129 .

Suga, K., and H. Umakoshi. 2013. "Detection of Nano-sized Sized Ordered Domains in DOPC/DPPC and DOPC/Ch Binary Lipid Mixture Systems of Large Unilamellar Vesicles Using a TEMPO Quenching Method." *Langmuir* 29: 4830-4838.

Suga, K., T. Tanabe, and H. Umakoshi. 2013. "Heterogeneous cationic liposomes modified with 3β-N-[(N′, N′-dimethylamino)ethyl]carbamoylChol can induce partial conformational changes in messenger RNA and regulate translation in an escherichia coli cell-free translation system." *Langmuir* 29: 1899-1907.

Suga, K., T. Tanabe, H. Tomita, T. Shimanouchi, and H. Umakoshi. 2011. "Conformational change of single-stranded RNAs induced by liposome binding." *Nucleic Acids Res.* 39: 8891-8900.

Szabo, G. 1974. "Dual mechanism for the action of Chol on membrane permeability." *Nature* 252: 47-49.

Taguchi, S., K. Suga, H. Hayashi, Y. Okamoto, H.-S. Jung, H. Nakamura, and H. Umakoshi. 2018. "Systematic Characterization of DMPC/DHPC Self-Assemblies and Their Phase Behaviors in Aqueous Solution." *Colloids Interf.* 2: 73-88.

Talbot, H. M., D. F. Watson, J. C. Murrell, J. F. Carter, and P. Farrimond. 2001. "Analysis of intact bacteriohopanepolyols from methanotrophic bacteria by reversed-phase high-performance liquid chromatography-atmospheric pressure chemical ionisation mass spectrometry." *Journal of Chromatography A* 921: 175-185.

Tierney, K. J., D. E. Block, and M. L. Longo. 2005. "Elasticity and phase behavior of DPPC membrane modulated by cholesterol, ergosterol, and ethanol." *Biophys. J.* 89: 2481-2493.

Tran, R., S. Ho, and P. Dea. 2004. "Effects of ethanol on lipid bilayers with and without cholesterol: the distearoylphosphatidylcholine system ." *Biophys. Chem.* 110: 39–47.

Uchiyama, S., Y. Matsumura, A.P. De Silva, and K. Iwai. 2003. "Fluorescent Molecular Thermometers Based on Polymers Showing Temperature-Induced Phase Transitions and Labeled with Polarity-Responsive Benzofurazans ." *Anal. Chem.* 75: 5926-5935.

Umakoshi, H, and K. Suga. 2013. "Use liposome as a designable flatform for molecular recognition from "Statistical separation" to "Recognitive separation"." *Solvent Extr. Res. Dev. Jpn.* 20: 1-13.

Umakoshi, H., K. Suga, H. T. Bui, M. Nishida, T. Shimanouchi, and R. Kuboi. 2009. "Charged liposome affects the translation and folding steps of in vitro expression of green fluorescent protein." *J. Biosci. Bioeng.* 108: 450-454.

Umakoshi, H., M. Yoshimoto, T. Shimanouchi, R. Kuboi, and I. Komasawa. 1998. "Model system for heat-induced translocation of cytoplasmic beta-galactosidase across phospholipid bilayer membrane." *Biotechnol. Progr.* 1998: 218-226.

Uppamoochikkal, P., S. Tristram-Nagle, and J. Nagle. 2010. "Orientation of tie-lines in the phase diagram of DOPC/DPPC/Chol model biomembranes." *Langmuir* 26: 17363-17368.

Urbina, J. A., B. Moreno, W. Arnold, C. H. Taron, P. Orlean, and E. Oldfield. 1998. "A carbon-13-nuclear magnetic resonance spectroscopic study of inter-proton pair order parameters: A new approach to study order and dynamics in phospholipid membrane systems." *Biophys. J.* 75: 1372-1383.

Urbina, J. A., S. Pekerar, H. B. Le, J. Patterson, B. Montez, and E. Oldfield. 1995. "Molecular order and dynamics of phosphatidylcholine bilayer membranes in the presence of cholesterol, Erg and lanosterol: a comparative study using 2H-, 13C- and 31P-NMR spectroscopy." *Biochim. Biophys. Acta.* 1238: 163–176.

Vaknin, D., K. Kjaer, J. Als-Nielsen, and M. Losche. 1991. "Structural properties of phosphatidylcholine in a monolayer at the air/water interface: Neutron reflection study and reexamination of x-ray reflection measurements." *Biophysical Journal* 59: 1325-1332.

Vanegas, J. M., M. F. Contreras, R. Faller, and M. L. Longo. 2012. "Role of Unsaturated Lipid and Erg in Ethanol Tolerance of Model Yeast Biomembranes ." *Biophys. J.* 102: 507–516.

Veatch, S. L., and S. L. Keller. 2002. "Organization in Lipid Membranes Containing Cholesterol." *Phys. Rev. Lett.* 89: 268101.

Vogel, V., and Y. R. Shen. 1991. "Air/liquid interfaces and adsorbed molecular monolayers studied with nonlinear optical techniques." *Annu Rev Mater Sci* 21: 515-534.

Walde, P., and S. Ichikawa. 2001. "Enzymes inside lipid vesicles: Preparation, reactivity and applications." *Biomol. Eng.* 18: 143−177.

Walde, P., H. Umakoshi, P. Stano, and F. Mavelli. 2014. "Emergent properties arising from the assembly of amphiphiles: Artifical vesicle membranes as reaction promoters and regulators." *Chem. Commun.* 50: 10177-10197.

Watanabe, N., Y. Goto, K. Suga, T .K. M. Nyholm, J. P. Slotte, and H. Umakoshi. 2019. "Solvatochromic modeling of Laurdan for multiple polarity analysis of dihydro-sphingomyelin bilayer." *Biphys. J.* 116: 874-883.

Waters, M. J. 2016. "The growth hormone receptor." *Growth hormone & IGF research* 28: 6-10.

Waters, M. J., A. J. Brooks, and Y. Chhabra. 2014. "A new mechanism for growth hormone receptor activation of JAK2, and implications for related cytokine receptors." *JAKSTAT* 3: 29569.

Waters, M. J., H. N. Hoang, D. P. Fairlie, R. A. Pelekanos, and R. J. Brown. 2006. "New insights into growth hormone action." *J. Mol. Endocrinol.* 36: 1-7.

Wolff, J., C. Marques, and F. Thalmann. 2011 . "Thermodynamic approach to phase coexistence in ternary phospholipid- Chol mixtures." *Phys. Rev. Lett.* 106: 128104.

Worcester, L. D., and N. P. Franks. 1976. "Structural analysis of hydrated egg lecithin and Chol bilayers. II. Neutrol diffraction." *J. Mol. Biol.* 100: 359–378.

Wydro, P., S. Knapczyk, and M. Lapczynska. 2011. "Variations in the condensing effect of Chol on saturated versus unsaturated phosphatidylcholines at low and high sterol concentration." *Langmuir* 27: 5433-5444.

Xu, X., and E. London. 2000. "The effect of sterol structure on membrane lipid domains reveals how Chol can induce lipid domain formation." *Biochemistry* 39: 843–849.

Xu, X., R. Bittman, G. Duportail, D. Heissler, C. Vilcheze, and C. London. 2001. "Effect of the structure of natural sterols and sphingolipids on the formation of ordered sphingolipid/sterol domains (rafts)." *J. Biol. Chem.* 276: 33540–33546.

Yeagle, P. L. 1988. "Chol and the cell membrane." In *The biology of cholesterol*, edited by P. L. Yeagle, 121–146. Boca Raton, FL, pp.: CRC Press,Inc.

Yeagle, P. L. 1985. "Chol and the cell membrane." *Biochim. Biophys. Acta.* 822: 267–287.

Yeagle, P. L., W. C. Hutton, C. Huang, and R. B. Martin. 1977. "Phospholipid head-group conformations; intermolecular interactions and Chol effects." *Biochemistry* 16: 4344–4349.

Yoshimoto, M., P. Walde, H. Umakoshi, and R. Kuboi. 1999. "Conformationally changed cytochrome c-mediated fusion of enzyme- and substrate-containing liposomes ." *Biotechnol. Progr.* 15: 689-696.

You, K. M., C. L. Rosenfield, and D. C. Knipple. 2003. "Ethanol tolerance in the yeast Saccharomyces cerevisiae is dependent on cellular oleic acid content." *Appl. Environ. Microbiol.* 69: 1499–1503.

Yuan, C., and L. J. Johnston. 2002. "Phase evolution in cholesterol/DPPC monolayers: Atomic force microscopy and near field scanning optical micros." *Journal of Microscopy* 205: 136-146.

Zohra, F. T., E. H. Chowdhury, S. Tada, T. Hoshiba, and T. Akaike. 2007. "Effective delivery with enhanced translational activity synergistically accelerates mRNA-based transfection." *Biochem. Biophys.* 358: 373-378.

List of Publications

[Papers]

1. Tham Thi Bui, Keishi Suga, Hiroshi Umakoshi, Roles of Sterol Derivatives in Regulating the Properties of Phospholipid Bilayer Systems. *Langmuir*, **2016**, 32, 6176-6184.

2. Tham Thi Bui, Keishi Suga, Hiroshi Umakoshi, Potential Interaction Behavior of Lanosterol and Unsaturated Phosphocholine in Monolayer Membrane, Membrane, *Maku*, **2019**, 44 (4), 199-203

3. Tham Thi Bui, Keishi Suga, Tonya Kuhl, Hiroshi Umakoshi, Melting Temperature Dependent Interactions of Ergosterol with Unsaturated and Saturated Lipids in Model Membranes. *Langmuir*, **2019**, 35(32), 10640-10647.

4. Tham Thi Bui, Keishi Suga, Hiroshi Umakoshi, Ergosterol-Induced Ordered Phase in Ternary Lipid Mixture Systems of Unsaturated and Saturated Phospholipid Membranes, *J. Phys. Chem. B*, **2019**, 123 (29), 6161-6168.

[**Related Papers and Proceedings]**

1. Tham Thi Bui, Yoichiro Hasunuma, Keishi Suga, Takaaki Kubota, Shigeru Deguchi, Hiroshi Umakoshi, Interaction of D-Amino Acids with Lipid Bilayer Membranes Modeling Biomembrane of Deep-Sea Bacteria, in preparation.

2. Tham Thi Bui, Bui Thi Thuy Duong, Quyen Dinh Thi, Nguyen Thi Thao, Dong Van Quyen, Study on the Expression of Bovine Somatotropin (bST) in *Escherichia coli*, *Journal of Genetics and Application*, **2013**, 12, 118-123.

3. Bui Thi Thuy Duong, Tham Thi Bui, Quyen Dinh Thi, Nguyen Thi Thao, Dong Van Quyen, Molecular Cloning, Expression and Purification of Bovine Somatotropin (bST) in Escherichia coli, *Proceedings of National Biotechnology Conference*, **2013** in Hanoi, Vietnam, Vol. 1, p.318-321.

[**International Conference/ Symposium]**

1. Bui Thi Tham, Keishi Suga, Hiroshi Umakoshi, Systematic Characterization of Sterol Molecules in Phospholipid Bilayer Membranes and Its Applications. 3rd International Conference Sustainable Agriculture, Food and Energy, Ho Chi Minh, Vietnam, November (2015) (Poster)

2. Tham Thi Bui, Keishi Suga, Yukihiro Okamoto, Hiroshi Umakoshi, Characterization of Sterol-Incorporated Phospholipid Bilayer Systems and Its Application. The 10th Conference of Aseanian Membrane Society (AMS10), Nara, Japan, July (2016) (Poster)

3. Bui Thi Tham, Keishi Suga, Hiroshi Umakoshi, Investigation of the Roles of Sterol Derivatives in Regulating the Properties of Phospholipid Bilayer Systems. International Seminar on Biophysics and Chemical Biology of Biomembrane and Lipid Bilayers, Osaka, Japan, October (2017) (Poster)

4. Bui Thi Tham, Keishi Suga, Yukihiro Okamoto, Hiroshi Umakoshi, Physicochemical Behaviors of Biology Sterols in Model Cell Membranes. The 11th International Conference on Separation Science and Technology, Busan, Korea November (2017) (Poster)

[Awards]

1. "Best Presentation Award" in Chemical Engineering English Colloquium on 4th March, 2015

2. "Best Poster Presentation Award at AMS10" in The 10th Conference of Aseanian Membrane Society (AMS10) (Nara, Japan, July 2016

3. "Best Poster Presentation Award" in Membrane Symposium 2018 (Kobe, Japan, November 2018

Acknowledgements

The author is deeply grateful to Prof. Dr. Hiroshi Umakoshi (Division of Chemical Engineering, Graduate School of Engineering Science, Osaka University), for his insightful comments, suggestions, and warm encouragement throughout this work. The author is thankful to Prof. Dr. Nobuyuki Matsubayashi and Prof. Dr. Sakai Shinji (Division of Chemical Engineering, Graduate School of Engineering Science, Osaka University) for a number of valuable comments and suggestions during the completion of this thesis. The author would like to express her gratitude to Assist. Prof. Dr. Keishi Suga (Division of Chemical Engineering, Graduate School of Engineering Science, Osaka University) for his enormous encouragements on her research. And the author also would like to express the greatest appreciation to Assoc. Prof. Dr. Yukihiro Okamoto (Division of Chemical Engineering, Graduate School of Engineering Science, Osaka University). The author would like to offer one's special thanks to Ms. Keiko Fukumoto for her kind support during this work.

The author would like to show her greatest appreciation to Prof. Dr. R. Kuboi and Prof. Dr. M. Taya (Honored Professor of Osaka University). The author is thankful to Prof. Dr. K. Jitsukawa, Prof. Dr. Y. Okano, Prof. Dr. M. Nakano, Prof. Dr. T. Hirai, Prof. Dr. N. Nishiyama and all the staff of Division of Chemical Engineering, Graduate School of Engineering Science, Osaka University for their kind cooperation during her research.

The author expresses her sincere thanks to Prof. Dr. L. K. Tonya (Department of Chemical Engineering, University of California, America) for helpful discussions and continuous supports. The author wishes to thank Prof. Dr. B. Higgins (Department of Chemical Engineering and Materials Science, University of California, Davis), Prof. Dr. P. Alexandridis (Department of Chemical Engineering, University at Buffalo), Prof. Dr. Ho-Sup Jung (Department of Mechanical and Aerospace Engineering, Seoul National University) for their comments. The author is grateful for the advice given by Assoc. Prof. Dr. L. Q. Tuan (Nong Lam University), Dr. B. T. Huong (Vietnam Institute of Agricultural Engineering and Post Harvest Technology) and Dr. V. T. Huong (Hanoi National University of Education).

The author is particularly grateful for the assistance given by Y. Hasunuma. Special thanks are given to following colleagues for their experimental collaboration: T. Ishigami, F. Iwasaki, M. Hirose, M. Kiriishi, D. Kondo, Y. Takaya, Y. Kaneko, S. Taguchi, K. Goshima, A. Hamasaki, M. Kota, Y. Tsujimoto, T. Yoshida, B., W. Nozomi, Y. Kishi, K. Akizaki, Y. Higashie, T. Ikeda, R. Matsuba, Y. Mine, Y. Otsuka, Y. Shinozuka, S. Sugisaki, A. Tauchi, D. Wada, J. Han, K. Midogochi, R. Ito, T. Wakita, Y. Ooe, R. Kawakami, R. Kawakami, R. Nishino, K. Yoshida, K. Tanimura, Y. Iimure, K. Kitagawa, Y. Murata, Y. Goto, M. Faried, M. Amau, N. Ikushima, K. Kojima, Y. Seno, R. Ueno, D. Matsui, S. Matsushita, R. Murazawa, M. S. Chern, C. Lishi, C. Tran, A. Ajaikumar, R. Wakerlin, Y.-C. Lai, H. J. Kim, D. Etwaru, B. S. Kan, T. Ozawa, Y. Suzaki, A. Suzuta, K. Hamaguchi, S. Watase, S. Ando and all the member in Bio-Inspired Chemical Engineering Laboratory.

The author would like to express deepest appreciation to her parents Mr. Bui Van Vinh, Mrs. Pham Thi Tuyet, Mr. Nguyen Sy Thao, Mrs. Nguyen Thi Tu, her husband Nguyen Sy Truong, and child Nguyen Minh Ngoc and others persons in her great family about their kind help, support and encourage during her studying period in Japan.

The author gratefully acknowledges the financial support of this work by Japanese Government (MEXT) Scholarship.